SCUOLA DOTTORALE IN GEOLOGIA DELL'AMBIENTE E DELLE RISORSE (SDiGAR)

CORSO DI FORMAZIONE DOTTORALE IN GEOLOGIA DELL'AMBIENTE E GEODINAMICA

CICLO XXVII

THE UPLIFT OF THE ETHIOPIAN PLATEAU

PhD candidate:
Andrea Sembroni _____

Supervisor:
Prof. Claudio Faccenna _____

Co-Supervisor:
Dr. Paola Molin _____

PhD coordinator:
Prof. Claudio Faccenna _____

To my family

“To exist in this vast universe for a speck of time is the great gift of life. Our tiny sliver of time is our gift of life. It is our only life. The universe will go on, indifferent to our brief existence, but while we are here we touch not just part of that vastness, but also the lives around us. Life is the gift each of us has been given. Each life is our own and no one else's. It is precious beyond all counting. It is the greatest value we can have. Cherish it for what it truly is... Your life is yours alone. Rise up and live it.”

[Terry Goodkind]

Index

Chapter 3 – Long term dynamic support of the Ethiopian Swell

Abstract

The topographic configuration of the Earth's surface is the result of the interaction between deep and surface processes. The surface subsides above mantle downwellings and rises up above mantle upwellings forming dynamic topography. Similarly erosion and crustal thickening drive the mean topography to lower and raise respectively because of isostasy. So, in order to reconstruct the topographic evolution of a certain area, it is necessary to distinguish the several components of topography. In this respect, Africa is a perfect natural laboratory to examine the relationships between surface deformation, lithospheric structures and the underlying convecting interior. In particular Ethiopia has long been recognized as an ideal location to study rifting and hot spot tectonism. However, despite all the studies carried out, no consensus exists on several geologic aspects like the timing and pattern of rock uplift, the evolution of the drainage system and the interpretation of deep seismic data.

In this thesis the geologic and geomorphologic features of the Ethiopian Plateau have been analyzed in order to reconstruct the topographic evolution of the area since Oligocene.

The Ethiopian Plateau is located in the northwest of Ethiopia. It is characterized by up to 2 km thick Oligocene continental flood basalts (CFB) related to the Afar plume activity. Such volcanics deposited on an alternation of Mesozoic sandstones and limestones and on a Paleozoic/Precambrian basement. The plateau is bordered by the Main Ethiopian Rift/Afar escarpment to the east and by the Tana escarpment to the west. The drainage system is characterized by the Blue Nile and Tekeze rivers basins.

Here, a multidisciplinary approach has been used combining analytic models, GIS-based analysis, and field work. To characterize the plateau drainage system a quantitative geomorphologic analysis has been performed. The CFB thickness and the amount of the eroded materials have been quantified in order to determine the basalts loading and the erosional unloading. The flexural uplift at the rift and Tana escarpments have been modeled. By subtracting all the isostatic contributions from the present CFB base surface the Oligocene topography has been obtained. Using recent seismic data and crustal models, new residual and dynamic topographies have been elaborated and compared with the pre-CFB one.

The CFB geometry analysis shows a rough CFB base surface and an asymmetric basalts distribution respect to the Rift Valley. The thickest deposits concentrate in the Lake Tana region which represented one of the main basalts source areas.

The morphometric analysis evidences that the Tekeze and Blue Nile drainages have followed divergent pathways of incision. In particular the Tekeze R. seems to be responding in a more or less steady way to a single, early base level fall whereas the Blue Nile R. is responding in an unsteady way to multiple base level falls that may be both external and internal to the plateau in origin.

The regional topographic analysis shows that a dome-shaped feature centered on Addis Ababa is present in both the pre- and post-CFB topography, consistent with the notion that the region has experienced dynamic support since the Oligocene.

Riassunto

La configurazione topografica della superficie terrestre è frutto dell'interazione tra processi superficiali e profondi. In corrispondenza di flussi mantellici discendenti la superficie subisce subsidenza mentre in presenza di flussi mantellici ascendenti si verifica sollevamento. La topografia formata in seguito a tali processi viene definita dinamica. Allo stesso modo l'erosione e l'ispessimento crostale producono rispettivamente l'abbassamento e il sollevamento della topografia media a causa dell'isostasia. Per ricostruire l'evoluzione topografica di una determinata area, è necessario quindi distinguere le diverse componenti della topografia. L'Africa è un laboratorio naturale perfetto per esaminare le relazioni tra la deformazione superficiale, le strutture litosferiche e la convezione mantellica. In particolare l'Etiopia viene considerata da lungo tempo la regione ideale per studiare i processi di rifting e la tettonica legata alla presenza di un punto caldo. Tuttavia, nonostante i numerosi studi effettuati nell'area, sono ancora numerosi gli aspetti geologici dibattuti come ad esempio l'evoluzione temporale e spaziale del sollevamento tettonico, l'evoluzione del drenaggio e l'interpretazione dei dati sismici.

Nella presente tesi sono state analizzate le caratteristiche geologiche e geomorfologiche del plateau etiopico allo scopo di ricostruire l'evoluzione topografica dell'area a partire dall'Oligocene.

Il plateau etiopico si trova nel settore nord-occidentale dell'Etiopia ed è formato da basalti continentali oligocenici (CFB) legati all'attività del plume dell'Afar. Tali vulcaniti si sono depositate su un'alternanza di calcari e arenarie mesozoiche e su un basamento cristallino caratterizzato da sedimenti glaciali paleozoici e rocce metamorfiche precambriche. Il plateau è delimitato ad est dalla scarpata del Rift etiopico e ad ovest dalla scarpata del Tana. Il sistema di drenaggio è costituito dai bacini idrografici dei fiumi Nilo Blu e Tekeze.

Questo lavoro segue un approccio multidisciplinare combinando modelli analitici, analisi in ambiente GIS e indagini di terreno. Per caratterizzare il sistema di drenaggio del plateau è stata realizzata un'analisi geomorfologica quantitativa. Sono stati calcolati gli spessori dei CFB e del materiale eroso allo scopo di determinare i contributi isostatici dovuti al carico dei basalti e allo scarico erosivo. Sono stati modellati i sollevamenti flessurali lungo le scarpate del Rift e del Tana. In seguito, sottraendo tutti i contributi isostatici dalla superficie di base dei CFB, si è ricostruita la topografia oligocenica dell'area di studio. Tale superficie è stata poi confrontata con le attuali topografie residua e dinamica elaborate utilizzando dati sismici e modelli crostali recenti.

L’analisi della geometria dei CFB mostra una superficie di base irregolare ed una distribuzione asimmetrica dei basalti rispetto al Rift etiopico. I depositi più spessi si concentrano nella regione del Lago Tana che rappresenta una delle maggiori aree sorgenti di CFB nell'area.

L’analisi morfometrica evidenzia che i bacini dei fiumi Tekeze e Nilo Blu hanno subito diversi percorsi evolutivi. In particolare il Fiume Tekeze presenta i caratteri morfometrici di un fiume prossimo all'equilibrio e sembra rispondere ad un unico abbassamento del livello di base. Il Fiume Nilo Blu, invece, è in uno stato transiente di disequilibrio e si è evoluto in seguito a numerosi abbassamenti del livello di base causati da fattori sia interni che esterni al plateau.

L’analisi topografica regionale mostra lo stesso andamento a domo centrato nell’area di Addis Ababa sia nella topografia pre- che in quella post-CFB. Tale risultato indica che la regione è soggetta ad un supporto dinamico continuo dall’Oligocene al presente.

Preface

Earth's topography is the result of the competition between deep and surface processes (Molnar and England, 1990; Beaumont et al., 1992; Merritts and Ellis, 1994; Koons, 1995; Avouac and Burov, 1996; Whipple and Tucker, 1999; Molin et al., 2004; Wegmann et al., 2007; Molin et al., 2011; Babault and Van Den Driessche, 2012; Scotti et al., 2013).

The mantle convection drives dynamic upwellings and downwellings in the Earth's surface (Braun, 2010). The mantle flow is driven mostly by the descent of cold tectonic plates during subduction and by the ascent of mantle plumes (Braun, 2010; Allen, 2011). The Earth's surface subsides above mantle downwellings and rises up above mantle upwellings to form the dynamic component of topography (Hager et al., 1985). The link between mantle flow and surface topographic features is not straightforward since it is difficult to isolate the dynamic component of topography from features generated by crustal, subcrustal, and surface processes (Allen, 2011). So to reconstruct the topographic evolution of a certain area, it is necessary to distinguish the several components of topography.

Africa is an perfect natural laboratory to examine relationships between surface deformation, lithospheric structure and the underlying convecting interior (Morgan, 1983; Pérez-Gussinyé, 2009). In particular Ethiopia has long been recognized as an ideal place to study rifting and hot spot tectonism (Ebinger and Casey, 2001; Nyblade and Langston, 2002; Furman et al., 2006; Bastow et al., 2008).

The Ethiopian Plateau

We focused our investigation on the topographic evolution of the Ethiopian Highlands, a highstanding plateau located in the northwestern sector of Ethiopia and bordered on the eastern side by the Main Ethiopian Rift (MER)/Afar escarpment and on the western side by the Tana escarpment. Much of the region lies above 2500 m a.s.l. and comprises extensive areas of nearly flat landscape. It is drained by two major rivers: the Blue Nile and Tekeze rivers.

The area is covered by 1-2 km thick basalts deposited mainly between 30 and 28 Ma (Mohr and Zanettin, 1988; Zumbo et al., 1995; Baker et al., 1996a; Hofmann et al., 1997; Rochette et al., 1998; Pik et al., 2003; Kieffer et al., 2004). These volcanic sequences together with Mesozoic/Paleozoic sediments and metamorphic rocks reach 2 to 5 km of thickness (Mackenzie et al., 2005).

Such area is part of a wide region of anomalously high topography extending from the southeastern sector of the Atlantic Ocean up to the East Africa (Africa Superswell; Nyblade and Robinson, 1994). In fact, much of the African continent stands above 1 km contrasting with the 600 m mean elevation of the other continental areas (Babault and Van Den Driessche, 2012).

Plateau uplift: an unsolved problem

The Ethiopian Plateau has experienced up to ~2 km of rock uplift since ~30 Ma (Pik et al., 2003; Gani et al., 2007). Dainelli (1943) and Beydoun (1960) suggested this uplift to be Upper Eocene in age preceding flood basalts eruption and rifting. Successively, several authors (Mohr, 1967; Baker et al., 1972; McDougall et al., 1975; Merla et al., 1979; Berhe et al., 1987) argued against this theory and hypothesized a more complex history of uplift and volcanism.

Pik et al. (2003), based on thermochronological data, suggested that the elevated plateau physiography existed since the Oligocene (20–30 Ma).

Conversely, a more recent analysis based on the incision of the 1.6 km deep Gorge of the Nile (Gani et al., 2007), argued for a different evolution. They suggested that the uplift of ~2 km occurred episodically in three phases since ca. 29 Ma: a slow and steady uplift rate, between ~29 and ~10 Ma (phase I), that increased at ~10 Ma (phase II) and more dramatically at ~6 Ma (phase III). According to this model, most of rock uplift occurred after 6 Ma, in accordance with Mohr (1967), Baker et al. (1972), McDougall et al. (1975), Almond (1986), Adamson and Williams (1987).

Ismail and Abdelsalam (2012) carried out a quantitative morphometric analysis on the Ethiopian Plateau drainage system. They found out the strong influence of the impinging of Afar plume, of the shield volcanoes build-up event, and of the rift-flank uplift on the western escarpments in the evolution of rivers network.

The influence of uplift on climate

The change in topographic configuration modified and presently influences the circulation of the atmosphere and climate (Manabe and Terpstra, 1974; Ruddiman and Kutzbach, 1989; Molnar and England, 1990; Molnar et al., 1993; Ruddiman and Prell, 1997).

In East Africa rainfall is related to the low tropospheric winds blowing northeasterly during boreal winter and southwesterly during boreal summer (Gatebe et al., 1999). Meridional moisture transport shows that Ethiopian highlands deflect the northeast monsoon flow southward along the Somalian coast during winter and that Kenyan highlands deflect the southeast flow northward during summer (Sepulchre et al., 2006).

By isotopic studies Cerling et al. (1997) have attributed an Upper Miocene (8 to 6 Ma) transition from woodlands to grasslands to atmospheric CO_2 decrease. A later (5 to 3 Ma) spreading of grasslands was attributed to both Indian Ocean sea surface temperature cooling and the onset of glacial-interglacial cycles (Cane and Molnar, 2001; Bonnefille et al., 2004; Bobe and Behrensmeyer, 2004; deMenocal, 2004). Conversely Sepulchre et al. (2006) related these climate changes to uplift events using numerical models.

Mantle plume influence: evidences and open questions

Only a minor part of the total Ethiopian Plateau uplift seems to be related to isostatic processes (Corti, 2009). Several studies demonstrated that East Africa is characterized by a huge dynamic forcing originating in the deeper portion of the mantle (McKenzie and Weiss, 1975; Cox, 1989; Ebinger et al., 1989; Davies, 1998; Ebinger and Sleep, 1998; Ritsema et al., 1999; Gurnis et al., 2000; Şengör, 2001; Behn et al., 2004; Pik et al., 2006; Bastow et al., 2008; Moucha and Forte, 2011; Nyblade, 2011; Bagley and Nyblade, 2013; Faccenna et al., 2013).

Geochemical analysis of rift basalts, volcanic gases and geothermal fluids are consistent with a mantle plume influence (e.g., Hart et al., 1989; Schilling et al., 1992; Marty et al.,1996; Scarsi and Craig, 1996). No consensus exists on the number of mantle upwellings (e.g., Schilling et al., 1992; Ebinger and Sleep, 1998; George et al., 1998; Courtillot et al., 1999; Rogers et al., 2000; Kieffer et al., 2004; Furman et al., 2006; Rogers, 2006; Chang and Van der Lee, 2011). For example, Ebinger and Sleep (1998), suggested that just one large plume impinged the African lithosphere near Turkana at 45 Ma; then the lithosphere base topography funneled buoyant material up to 1000 km from Turkana to the Red Sea. Alternatively, George et al. (1998) and Rogers et al. (2000) proposed the existence of two Cenozoic plumes: one rising beneath southern Ethiopia at 45 Ma and another one impinging the base of the lithosphere beneath the Afar depression. Furman et al. (2006) invoked the idea of multiple plume stems rising from a deeper feature of the mantle (the African Superplume). Faccenna et al. (2013) reconstructed the patterns of mantle convection beneath the Afar–Anatolia–Aegean system evidencing a northward flow of the deep mantle Africa-Afar Plume driven by the Hellenic subduction. The same flow pattern has been observed also by Bagley and Nyblade (2013) and Hansen and Nyblade (2013).

The strong debate on the existence of such continuous hot mantle feature is due essentially to the intrinsic limitations of global tomography studies and on the dependence of seismic velocity on composition, phase and temperature of the mantle (Corti, 2009). Even admitting the existence of

this mantle upwelling, its connection with surface uplift, volcanism and rifting remains poorly defined (Corti, 2009).

Crustal structure

The crust beneath the Ethiopian Plateau has not been modified significantly by the Cenozoic rifting and magmatism (Corti, 2009). Indeed its thickness ranges between ~38 – 40 km (Kebede et al., 1996; Mackenzie et al., 2005; Dugda et al., 2005, 2007; Stuart et al., 2006; Keranen and Klemperer, 2008; Keranen et al., 2009) with a strong north–south decrease occurring at 9°N latitude (Yerer-Tullu volcano-tectonic lineament) where the western shoulder thins rapidly from ~38–40 km to 34–36 km (Dugda et al., 2005; Stuart et al., 2006; Dugda et al., 2007; Keranen and Klemperer, 2008; Keranen et al., 2009). In the Ethiopian plateau (northwest of latitude 9°N) there is a sharp transition to a thinner crust (of ~5 km) below the rift (Corti, 2009).

The Main Ethiopian Rift evolution

Based on geophysical observations, Keranen and Klemperer (2008) suggested that the Ethiopian and Somalian Plateaux correspond to two major Proterozoic basement terranes. Coincidence of the MER with the boundary between the terranes suggests that the location and evolution of the extensional process in the MER was strongly controlled by this ancient lithospheric-scale heterogeneity (Keranen and Klemperer, 2008).

Theoretical modelling (Tommasi and Vauchez, 2001) and studies carried out in other Large Igneous Provinces (Courtillot et al., 1999) demonstrate that the reactivation of the weakness zone occurs at the eastern edge of the upwelling mantle and not above its center.

The MER started to form in the Early Miocene (20–21 Ma) in the southern Ethiopia, following the northward propagation of the Kenya Rift-related deformation (e.g., Bonini et al., 2005). No major extensional deformation apparently affected the Central and Northern MER segments between 21 and 11 Ma (Corti, 2009 and references therein). The Africa – Arabia separation by the Red Sea and Gulf of Aden extensional system was active since about 30 Ma (e.g., Wolfenden et al., 2005). Deformation in the Northern MER started in the Late Miocene at ~11 Ma (Wolfenden et al., 2004). In the Central MER, recent analysis by Bonini et al. (2005) indicated that no major extensional faulting was active in the Late Miocene, as testified by the emplacement at 12 – 8 Ma of extensive basalts currently outcropping on both rift margins. According to this study, extensional deformation in the Central MER started at about 5 – 6 Ma, although WoldeGabriel et al. (1990) suggested an earlier development (8 – 10 Ma) of the boundary faults.

The diachronous development of the different MER segments has been interpreted in terms of different models of rift propagation (see Corti, 2009). The two end-members are Wolfenden et al. (2004) and Bonini et al. (2005). The first suggest an Early Miocene (~18 Ma) initiation of the MER-related deformation in southwestern Ethiopia, and a propagation northwards through the Central and Northern MER into the Afar depression after ~11 Ma. Bonini et al. (2005) argue for a Miocene-Present southwards rift propagation from the Afar depression, with deformation affecting the Northern MER in the Late Miocene, the Central MER in the Pliocene and the Southern MER during the Late Pliocene – Pleistocene. This process was triggered by the clockwise rotation of the Somalian Plate started around 10 Ma (Bonini et al., 2005).

The initial phases of continental rifting in the MER corresponded to the activation of the boundary faults (Corti, 2009). Such fault system developed diachronously along the rift between 11 and 6 Ma and has been active mostly until about 2 Ma (Corti, 2009). During the Early Pleistocene, most of the extension and the volcanic activity shifted from the boundary faults to the central axes of the rift (Ebinger, 2005; Corti, 2009).

Despite the wide literature on the study area, the geologic and geodynamic complexity of the region makes the Ethiopian Plateau evolution matter of debate. More specifically the discussion deals with the pattern and timing of rock uplift, the influence of uplift on climate, the formation and evolution of the rift system, the interpretation of deep seismic data, the interaction between deep and surface processes and, in particular, the evolution of the plateau drainage system.

The present thesis tries to clarify some of these debated topics in order to characterize the landscape evolution of the Ethiopian Plateau. More specifically the work aims to:

- Reconstruct the structure of the Ethiopian Plateau continental flood basalts (CFB) by tracing the CFB base and top surfaces and quantifying the spatial variation in basalts thickness in order to locate the main CFB source area.
- Study the coupling between deep and surface processes by performing a quantitative morphometric analysis on the topography and the river network of the study area.
- Reconstruct the topography evolution of the region by separating and quantifying the isostatic and dynamic contributions to topography.

The thesis includes three chapters. Each chapter deals with a single aim. In particular:

- The first one is about the structure of the Ethiopian Plateau continental flood basalt (CFB).

- The second one focuses on the quantitative morphometric analysis of the Blue Nile and Tekeze rivers basins.

- The third chapter deals with the isostatic and dynamic contributions to topography in the Ethiopian Plateau region.

References

Adamson, D. & Williams, M.A.J. (1987) - "Geological setting of Pliocene rifting and deposition in the Afar Depression of Ethiopia" - Journal of Human Evolution 16, 597–610.

Allen, P.A. (2011) - "Surface impact of mantle processes" - Nature, 4, 498-499.

Almond, D.C. (1986) - "Geological evolution of the Afro-Arabian dome" - Tectonophysics 131, 301–332.

Avouac. J.P. & Burov, E.B. (1996) - "Erosion as a driving mechanism of intracontinental mountain growth" - J. Geophys. Res., 101, 17747-17769.

Babault, J. & Van Den Driessche, J. (2012) - "Plateau uplift, regional warping, and subsidence" - In: Shroder, J. (Editor in Chief), Owen, L.A. (Ed.), Treatise on Geomorphology. Academic Press, San Diego, CA, vol. 5, pp 36.

Bagley, B. & Nyblade, A.A. (2013) - " Seismic anisotropy in eastern Africa, mantle flow, and the African plume" - Geophys. Res. Lett., vol. 40, pp. 1500-1505.

Baker, B.H., Mohr, P.A. & Williams, L.A.J. (1972) - "Geologyof the EasternRift System of Africa" - Geological Society of America Special Paper, vol. 136. 67 pp., Boulder Colorado.

Baker, J., Snee, L. & Menzies, M. (1996a) – "A brief Oligocene period of flood volcanism in Yemen" - Earth and Planetary Science Letters 138, 39–55.

Bastow, I.D., Nyblade, A.A., Stuart, G.W., Rooney, T.O. & Benoit, M.H. (2008) - "Upper mantle seismic structure beneath the Ethiopian hot spot: rifting at the edge of the African low-velocity anomaly" - Geochemistry, Geophysics, Geosystems 9, Q12022. doi:10.1029/2008GC002107.

Beaumont, C., Fullsack, P. & Hamilton, J. (1992) - "Erosional control of active compressional orogens" - In: "Thrust Tectonics" edited by K. R. McClay, pp. 19-31, Chapman and Hall, New York, 1992.

Behn, M.D., C.P. Conrad & P.G. Silver (2004) - "Detection of upper mantle flow associated with the African plume" - EPSL, 224, 259-274.

Berhe, S.M., Desta, B., Nicoletti, M. & Tefera, M. (1987) – "Geology, geochronology and geodynamic implications of the Cenozoic magmatic province in W and SE Ethiopia" - Journal of the Geological Society of London 144, 213–226.

Bobe, R. & Behrensmeyer, A.K. (2004) - "The expansion of grassland ecosystems in Africa in relation to mammalian evolution and the origin of the genus Homo" - Paleogeogr. Paleoclimatol. Paleoecol. 207, 399

Bonnefille, R., Potts, R., Chalie, F., Jolly, D. & Peyron, O. (2004) - "High-resolution vegetation and climate change associated with Pliocene Australopithecus afarensis" - Proc.Natl. Acad. Sci. U.S.A. 101, 12125-12129.

Beydoun, Z.R. (1960) - "Synopsis of the Geology of East Aden Protectorate" - XXI International Geological Congress, Copenhagen 21, 131–149.

Bonini, M., Corti, G., Innocenti, F., & Manetti, P. (2005) – "Evolution of the Main Ethiopian Rift in the frame of Afar and Kenya rifts propagation" - Tectonics, v. 24, doi: 10.1029/2004TC001680.

Braun, J. (2010) - "The many surface expressions of mantle dynamic" - Nature Geoscience 3, 825–833.

Cane, M.A. & Molnar, P. (2001) - "Closing of the Indonesian seaway as a precursor to east African aridification around 3-4 , million years ago" - Nature, 411, 157-162.

Cerling, T.E., Harris, J.M., MacFadden, B.J., Leakey, M.G., Quade, J., Eisenmann V. & Ehleringer, J.R. (1997) - "Global vegetation change through the Miocene/Pliocene boundary" - Nature, 389, 153-158.

Chang, S-J & Van der Lee, S. (2011) - "Mantle plumes and associated flow beneath Arabia and East Africa" - EPSL, 302, 448-454.

Corti, G. (2009) – "Continental rift evolution: From rift initiation to incipient break-up in the Main Ethiopian Rift, East Africa" - Earth-Science Reviews, 96, 1–53.

Courtillot, V., Jaupart, C., Manighetti, I., Tapponnier, P. & Besse, J. (1999) - "On causal links between flood basalts and continental breakup" - EPSL, 166, 177–195.

Cox, K.G. (1989) - "The role of mantle plumes in the development of continental drainage patters" - Nature, 342, 873-877.

Dainelli, G. (1943) - "Geologia dell'Africa Orientale (3 vols. text, 1 vol. maps)" - R. Accad. Ital., Roma.

Davies, G. (1998) - "A channelled plume under Africa" - Nature 395, 743.

deMenocal, P.B. (2004) - "African climate change and faunal evolution during the Pliocene-Pleistocene" - EPSL, vol. 220, pp. 3-24.

Dugda, M.T., Nyblade, A.A., Jordi, J., Langston, C.A., Ammon, C.J. & Simiyu, S. (2005) - "Crustal structure in Ethiopia and Kenya from receiver function analysis: implications for rift development in Eastern Africa" - J. Geophys. Res., 110 (B1), B01303. doi:10.1029/2004JB003065.

Dugda, M., Nyblade, A.A., Julia, J., 2007. "Thin lithosphere beneath the Ethiopian Plateau revealed by a joint inversion of Rayleigh Wave Group velocities and receiver functions" - Journal of Geophysical Research 112. doi:10.1029/2006JB004918.

Ebinger, C. J., T.D. Bechtel, D. W. Forsyth & C. O. Bowin (1989) – "Effective Elastic Thickness beneath the East African and Afar Plateaus and Dynamic compensation for the uplifts" - J. Geophys.Res., 94, 2883-2901.

Ebinger, C. & Sleep, N.H. (1998) – "Cenozoic magmatism in central and east Africa resulting from impact of one large plume" - Nature 395, 788–791.

Ebinger, C.J. & Casey, M. (2001) - "Continental breakup in magmatic provinces: an Ethiopian example" - Geology 29, 527–530.

Ebinger, C. (2005) - "Continental breakup: the East African perspective" - Astronomy and Geophysics 46, 2.16–2.21.

Faccenna, C., Becker, T.W., Jolivet, L. & Keskin, M. (2013) - "Mantle convection in the Middle East: Reconciling Afar upwelling, Arabia indentation and Aegean trench rollback" - EPSL 375, 254-269.

Furman, T., Bryce, J., Rooney, T., Hanan, B., Yurgu, G. & Ayalew, D. (2006) - "Heads and tails: 30 million years of the Afar plume" - In: Yirgu, G., Ebinger, C.J., Maguire, P.K.H. (Eds.), The Afar Volcanic Province within the East African Rift System: Geological Society Special Publication, vol. 259, pp. 95–119.

Gani, N.D., Abdelsalam, M.G. & Gani, M.R. (2007) – "Blue Nile incision on the Ethiopian Plateau: pulsed plateau growth, Pliocene uplift, and hominin evolution" - GSA Today 17, 4–11.

Gatebe, C.K., Tyson, P.D., Annegarn, H., Piketh, S. & Helas, G. (1999) - "A seasonal air transport climatology for Kenya" - J. Geophys. Res., 104, 14237-14244.

George, R., Rogers, N. & Kelley, S. (1998) – "Earliest magmatism in Ethiopia: evidence for two mantle plumes in one flood basalt province" - Geology 26, 923–926.

Gurnis, M., Mitrovica, J.X., Ritsema, J. & van Heijst, H.J. (2000) – "Constraining mantle density structure using geological evidence of surface uplift rates: the case of the African Plume" - Geochemistry, Geophysics, Geosystems 1 1999GC000035.

Hager, B.H., Clayton, R.W., Richards, M.A., Comer, R.P. & Dziewonski, A.M. (1985) - "Lower mantle heterogeneity, dynamic topography and the geoid" - Nature, vol. 313, 541-545.

Hansen, S.E. & Nyblade, A.A. (2013) - "The deep seismic structure of the Ethiopia/Afar hotspot and the African plume" - Geophys. J. Int., doi: 10.1093/gji/ggt116.

Hart, W.K., Woldegabriel, G., Walter, R.C. & Mertzman, S.A. (1989) - "Basaltic volcanism in Ethiopia: constraints on continental rifting and mantle interactions" - J. Geophys. Res., 94, 7731–7748.

Hofmann, C., Courtillot, V., Feraud, G., Rochette, P., Yirgu, G., Ketefo, E. & Pik, R. (1997) – "Timing of the Ethiopian flood basalt event and implications for plume birth and global change" - Nature 389, 838–841.

Ismail, E.H. & Abdelsalam, M.G. (2012) - "Morpho-tectonic analysis of the Tekeze River and the Blue Nile drainage systems on the Northwestern Plateau, Ethiopia" - J. Afric. Erth. Sc., 69, 34-47.

Kebede, F., Vuan, A., Mammo, T., Costa, G. & Panza, G.F. (1996) - "Shear wave velocity structure of Northern and North-eastern Ethiopia" - Acta Geodaetica et Geophysica, 31, 145–159.

Keranen, K. & Klemperer, S.L. (2008) - "Discontinuous and diachronous evolution of the Main Ethiopian Rift: implications for the development of continental rifts" - EPSL, 265, 96–111. doi:10.1016/j.epsl.2007.09.038.

Keranen, K., Klemperer, S.L., Julia, J., Lawrence, J.L. & Nyblade, A. (2009) - "Low lower-crustal velocity across Ethiopia: is the Main Ethiopian Rift a narrow rift in a hot craton?" - Geochemistry, Geophysics, Geosystems 10, Q0AB01. doi:10.1029/2008GC002293.

Kieffer, B., Arndt, N., Lapierre, H., Bastien, F., Bosch, D., Pecher, A., Yirgu, G., Ayalew, D., Weis, D., Jerram, D.A., Keller, F., & Meugniot, C. (2004) – "Flood and shield basalts from Ethiopia: Magmas from the African Superswell" - Journal of Petrology, v. 45, 793–834, doi: 10.1093/petrology/egg112.

Koons, P.O. (1995) - "Modelling the topographic evolution of collisional mountain belts" - Invited paper: Annual Review of Earth and Planetary Sciences, 23, 375-408.

Mackenzie, G.D., Thybo,H. & Maguire, P.K.H. (2005) - "Crustal velocity structure across the Main Ethiopian Rift: results from two-dimensional wide-angle seismic modeling" - Geophysical Journal International 162, 994–1006.

Manabe, S. & Terpstra, T.B. (1974) - "The effects of mountains on the general circulation of the atmosphere as identified by numerical experiments" - J. Atmos. Sci., 31, 3–42.

Marty, B., Pik, R. & Gezahegn, Y. (1996) - "Helium isotopic variations in Ethiopian plume lavas: nature of magmatic sources and limit on lower mantle contribution" - EPSL, 144, 223–237.

McDougall, I., Morton,W.H. & William, M.A.J. (1975) – "Ages and rates of denudation of trap series basalts at the Blue Nile Gorge, Ethiopia" - Nature 254, 207–209.

McKenzie, D.P. & Weiss, N.O. (1975) - "Speculations on the thermal and tectonic history of the Earth" - Geophys. J. R. astr. Soc., 42, 131.

Merla, G., Abbate, E., Canuti, P., Sagri, M. & Tacconi, P. (1979) - "Geological map of Ethiopia and Somalia and comment with a map of major landforms (scale 1:2,000,000)" - Consiglio Nazionale delle Ricerche, Rome. 95.

Merritts, D. & Ellis, M. (1994) - "Introduction to special section on tectonics and topography" - J. Geophys. Res., 99: doi: 10.1029/94JB00810. issn: 0148-0227.

Mohr, P.A. (1967) – "The Ethiopian Rift System" - Bulletin of the Geophysical Observatory of Addis Ababa 11, 1–65.

Mohr, P., & Zanettin, B. (1988) – "The Ethiopian Flood Basalt Province" - In McDougall, J.D., ed., Continental Flood Basalts: Dordrecht, Netherlands, Kluwer Academic Publishers, 63–110.

Molin, P., Pazzaglia, F.J. & Dramis, F. (2004) - "Geomorphic expression of active tectonics in a rapidly deforming forearc, Sila Massif, Calabria, southern Italy" - American Journal of Science 304, 559–589.

Molin, P., Fubelli, G., Nocentini, M., Sperini, S., Ignat, P., Grecu, F. & Dramis, F. (2011) - "Interaction of mantle dynamics, crustal tectonics and surface processes in the topography of the Romanian Carpathians: A geomorphological approach" - Glob. Planet. Change, doi:10.1016/j.gloplacha.2011.05.005.

Molnar, P. & England, P. (1990) – "Late Cenozoic uplift of mountain ranges and global climate change: chicken or egg?" - Nature 346, 29 – 34.

Molnar, P. & England, P. & Martinod, J. (1993) – "Mantle dynamics, uplift of the Tibetan Plateau and the Indian Monsoon" – Reviews of Geophysics, 31, 357-396.

Morgan, P. (1983) - "Constraints on rift thermal processes from heat flow and uplift" - Tectonophysics, 94, 277-298.

Moucha, R. & Forte, A.M. (2011) – "Changes in African topography driven by mantle convection" – Nature Geosc. Let. DOI: 10.1038/NGEO1235.

Nyblade, A.A. & Robinson, S.W. (1994) - "The African superswell" - Geophys. Res. Lett. 21, 765–768.

Nyblade, A.A. & Langston, C.A. (2002) - "Broadband seismic experiments probe the East African rift" - EOS Transaction on American Geophysical Union 83, 405–408.

Nyblade, A.A. (2011) - "The upper-mantle low-velocity anomaly beneath Ethiopia, Kenya, and Tanzania: Constraints on the origin of the African superswell in eastern Africa and plate versus plume models of mantle dynamics" - Geol. Soc. Am., Special Paper 478.

Perez-Gussinye, M., Metois, M., Fernandez, M., Verges, J. & Lowry, A.R. (2009) – "Effective elastic thickness of Africa and its relationship to other prozie for lithospheric structure and surface tectonics" - Earth Planet. Sci. Lett., 287(1-2), 152-167.

Pik, R., Marty, B., Carignan, J. & Lave, J. (2003) – "Stability of Upper Nile drainage network (Ethiopia) deduces from (U–Th)/He thermochronometry: Implication of uplift and erosion of the Afar plume dome" - Earth and Planetary Science Letters, v. 215, 73–88, doi: 10.1016/S0012-821X(03)00457-6.

Pik, R., Marty, B. & Hilton, D.R. (2006) - "How many mantle plumes in Africa? The geochemical point of view" - Chemical Geology 226, 100–114. doi:10.1016/j.chemgeo.2005.09.016.

Ritsema, J., H. J. van Heijst & J. H. Woodhouse (1999) – "Complex shear wave velocity structure imaged beneath Africa and Iceland" - Science, 286, 1925–1928, doi:10.1126/science.286.5446.1925.

Rochette, P., Tamrat, E., Feraud, G., Pik., R., Courtillot, V., Ketefo, E., Coulon, C., Hoffmann, C., Vandamme, D. & Yirgu, G. (1998) - "Magnetostratigraphy and timing of the Oligocene Ethiopian traps" - EPSL, 164, 497-510.

Rogers, N., Macdonald, R., Fitton, J., George, R., Smith, R. & Barreiro, B. (2000) - "Two mantle plumes beneath the East African rift system: Sr, Nd and Pb isotope evidence from Kenya Rift basalts" - EPSL, 176, 387–400.

Rogers, N.W. (2006) - "Basaltic magmatism and the geodynamics of the East African Rift System" - In: Yirgu, G., Ebinger, C.J., Maguire, P.K.H. (Eds.), The Afar Volcanic Province within the East African Rift System: Geological Society Special Publication, vol. 259, pp. 77–93.

Ruddiman, W. F. & Kutzbach, J.E. (1989) - "Forcing of the late Cenozoic northern hemisphere climate by plateau uplift in southeast Asia and the American southwest" - J. Geophys. Res., 94, 18409–18427.

Ruddiman, W.F. & Prell, W.L. (1997) - "Introduction to the Uplift-Climate Connection" - Plenum Press, New York, NY.

Scarsi, P. & Craig, H. (1996) - "Helium isotope ratios in Ethiopian Rift basalts" - EPSL, 144, 505–516.

Schilling, J.G., Kingsley, R.H., Hanan, B.B. & McCully, B.L. (1992) – "Nd–Sr–Pb isotopic variations along the Gulf of Aden: evidence for Afar mantle plume-continental lithosphere interaction" - Journal of Geophysical Research B 97 (7), 10,927–10,966.

Scotti, V.N., Molin, P., Faccenna, C., Soligo, M. & Casas-Sainz, A. (2013) - "The influence of surface and tectonic processes on landscape evolution of the Iberian Chain (Spain): Quantitative geomorphological analysis and geochronology" - Geomorphology, http://dx.doi.org/10.1016/j.geomorph.2013.09.017.

Şengör, A.M.C. (2001) – "Elevation as indicator of mantle-plume activity" - In Ernst, R.E., and Buchan, K.L., eds., Mantle Plumes: Their identification through time: Geological Society of America Special Paper 352, 183–225.

Sepulchre, P., Ramstein, G., Fluteau, F., Schuster, M., Tiercelin, J-J & Brunet, M. (2006) - "Tectonic Uplift and Eastern Africa Aridification" - Science, 313, 1419-1423.

Stuart, G.W., Bastow, I.D. & Ebinger, C.J. (2006) - "Crustal structure of the northern Main Ethiopian Rift from receiver function studies" - In: Yirgu, G., Ebinger, C.J., Maguire, P.K.H. (Eds.), The Afar Volcanic Province within the East African Rift System: Geological Society Special Publication, vol. 259, pp. 253–267.

Tommasi, A. & Vauchez, A. (2001) - "Continental rifting parallel to ancient collisional belts: an effect of the mechanical anisotropy of the lithospheric mantle" - EPSL, 185, 199–210.

Wegmann, K.W., Zurek, B.D., Regalla, C.A., Bilardello, D., Wollenberg, J.L., Kopczynski, S.E., Ziemann, J.M., Haight, S.L., Apgar, J.D., Zhao, C. & Pazzaglia, F.J. (2007) - "Position of the Snake River watershed divide as an indicator of geodynamic processes in the greater Yellowstone region, western North America" - Geosphere 3 (4), 272–281.

WoldeGabriel, G., Aronson, J.L. & Walter, R.C. (1990) - "Geology, geochronology, and rift basin development in the central sector of the Main Ethiopia Rift" - Geological Society of America Bulletin 102, 439–458.

Wolfenden, E., Yirgu, G., Ebinger, C., Deino, A. & Ayalew, D. (2004) – "Evolution of the northern Main Ethiopian rift: Birth of a triple junction" - Earth and Planetary Science Letters, v. 224, 213–228, doi: 10.1016/j.epsl.2004.04.022.

Wolfenden, E., Ebinger, C., Yirgu, G., Renne, P. & Kelley, S.P. (2005) – "Evolution of the southern Red Sea rift: birth of a magmatic margin" - Geological Society of America Bulletin 117, 846–864.

Whipple, K.X. & Tucker, G.E. (1999) - "Dynamics of the stream-power river incision model: implications for height limits of mountain ranges, landscape response timescales, and research needs" - Journal of Geophysical Research, vol. 104, 17661-17674.

Zumbo, V., Feraud, G., Bertrand, H., & Chazot, G. (1995) - "40Ar/39Ar chronology of the Tertiary magmatic activity in Southern Yemen during the early Red Sea-Aden rifting" - J. Volcanol. Geoth. Res. 65, 265–279.

CHAPTER 1*

STRUCTURE OF THE CONTINENTAL FLOOD BASALTS IN THE ETHIOPIAN PLATEAU

1.1 Introduction

Continental flood basalt (CFB) or Trap provinces are the most spectacular examples of volcanic activity on the Earth surface (Bondre et al., 2004).

Geochronological studies (Courtillot et al., 1988; Dickin et al., 1988; Renne et al., 1991;1992; Baker et al., 1996; Duncan et al., 1997; Sinton et al., 1998; Marzoli et al., 1999; Ukstins et al., 2002; Jourdan et al., 2005; Chenet et al., 2007; He et al., 2007; Barry et al., 2010) point to a typical duration of 1 million years for the bulk of CFB eruption. The typical flux is of the order of or larger than 2 km^3yr^{-1} (Courtillot and Renne, 2003). Such activity has been proved to be connected to mantle dynamics by isotope analysis (Campbell and Griffiths, 1990; Ellam et al., 1992; Sharma et al., 1992; Basu et al., 1993; 1995; Chung and Jahn, 1995; Marty et al., 1996; Quin et al., 2011).

Another characteristic of CFB is their extreme lateral extent (Garner, 1996). The Pomona Member of the Saddle Mountains Basalt has a volume >600 km^3 and can be traced for a linear distance of 600 km (Swanson and Wright, 1981).

The magmatic flux during Trap emplacement has the potential to induce global climatic change, through the massive input of ashes and gases in the upper stratosphere. This seems to be the case for the Deccan, Paraná, Central Atlantic and Siberian Traps, which are synchronous with the Cretaceous–Paleogene (K/T), Jurassic–Cretaceous (J-Cr), Triassic-Jurassic (Tr-J) and Permian–Triassic (P/T) boundaries respectively (Rochette et al., 1998). Estimates of the sulphur dioxide output for some of the Miocene Columbia River basalt flows are of the order of 1000 megatons per year, enough to produce conditions similar to those modeled for a nuclear winter (Hon and Pallister, 1995).

The Oligocene Ethiopian-Yemen CFB (Trap series) are located near the Afar triple junction and represent one of the youngest example of a major continental volcanic plateau. Because of their relatively young age and their eruption in a region where plate movements are slow, a complete record from the initial flood volcanic phase through to its shutdown and the onset of continental rifting, and finally the initiation of sea-floor spreading is preserved in the African Horn (Kieffer et al., 2004).

*** This chapter will be submitted as: Sembroni, A., Faccenna, C. and Molin, P. (2015) - "Structure of the Continental Flood Basalts in the Ethiopian Plateau".**

The deposits cover an area of 600000 km^2 and not less than 750000 km^2 before erosion, with a typical thickness varying from 500 to 2000 m (Berhe et al., 1987; Mohr and Zanettin, 1988). The total volume is estimated to be at least 350000 km^3 (Mohr, 1983b; Mohr and Zanettin, 1988) and probably higher than 1200000 km^3 according to Rochette et al. (1998). $^{40}Ar/^{39}Ar$ dating (Zumbo et al., 1995; Baker et al., 1996a; Hofmann et al., 1997; Rochette et al., 1998) indicates that most of the Trap series in Ethiopia and Yemen were extruded 30 Ma over a short time interval, possibly less than 2 Ma. According to the Trap volume calculated by Rochette et al. (1998) this time interval gives an eruption rate of 1 km^3yr^{-1}.

The chemical composition of the Ethiopian CFB supports a magma genesis from a broad region of mantle upwelling, heterogeneous in terms of temperature and composition (Kieffer et al., 2004). However no consensus exists on the number of mantle upwellings (Corti, 2009). Some works have proposed the existence of a single channeled plume (Ebinger and Sleep, 1998) or two starting plumes (George et al., 1998; Rogers, 2006; Montagner et al., 2007; Chang and Van der Lee, 2011) impinging the base of the lithosphere since Eocene time (Ebinger and Sleep, 1998; Şengör, 2001).

The eruption of huge amount of basalts in such short time should have deeply changed the topographic configuration of the area as well as the initial structural and topographic pattern of the area should have influence location of the basalts vents. Understanding the basalts emplacement mode and localizing the main source area are fundamental steps in order to reconstruct the topography evolution of a Trap province. Moreover flood basalt eruptions are intimately associated with the initiation of rifted continental margins (Morgan, 1971; Mohr, 1983b; Richards et al., 1989; Campbell and Griffiths, 1990; Hooper, 1990; Hill, 1991; Griffiths and Campbell, 1991; Courtillot et al., 1999). In this respect Richards et al. (1989) suggest that rifting occurs shortly after Trap emplacement and that lithospheric thinning is not a prerequisite for CFB eruption (active rifting model). In contrast White and McKenzie (1989) assumed that rifts are primarily the result of regional stress distributions related to plate boundary forces and geometry, acting for instance on pre-existing zones of weakness either in the crust, or the mantle part of the lithosphere or both (passive rifting model). For all these reasons the study of Trap provinces and in particular of flood basalts is a powerful tool to understand the geodynamic evolution of a region. However in most of cases localizing the main CFB source area is not straightforward because of the huge thickness of the basalts pile which cover the pre-eruption topography. Despite the number of studies on the provenience, the age and the chemical composition of the Ethiopian Trap, limited efforts have been made to study the CFB geometry. Also the main site of Ethiopian CFB egress is still debated. According to Mohr (1983b) the "expected loci" of the most productive

fissure-feeders for the lavas are aligned along the MER and Afar margins where the crustal warping is maximum. Therefore the CFB eruption preceded the MER initiation and the basalts main source area coincides with the Rift location. However no quantitative data have been produced to justify such statement. Theoretical modelling (Tommasi and Vauchez, 2001) and studies carried out in other Large Igneous Provinces (Courtillot et al., 1999) demonstrated that the reactivation of the weakness zone occurs at the eastern edge of the upwelling mantle and not above its center. According to recent studies (Wolfeden et al., 2004; Bonini et al., 2005), the MER formed between 11 and 5 Ma, more than 20 Ma after the main Trap eruption phase (Zumbo et al., 1995; Baker et al., 1996a; Hofmann et al., 1997; Rochette et al., 1998). Moreover the spatial distribution of flood basalts in the region presents a marked asymmetry about the rift and Afar depression (Mohr, 1983b).

In this work we reconstruct the base and top surfaces of Trap deposits to trace the spatial variation of flood basalts and to quantify the thickness of CFB deposits. This allowed us to localize the main Trap source area and to investigate the relationships basalts-topography and basalts-MER. Our results coupled with literature data permitted us the trace the geologic evolution of the region since Triassic.

1.2 Geological setting

The basement of Ethiopia is characterized by folded and foliated pre-Cambrian rocks overlain by an alternation of sub-horizontal Mesozoic sandstones and limestones (**Figs.1b, 2a-b**). The basement rocks are part of the Arabian–Nubian Shield (northern sector of the East African Orogen) which is formed by collision between east and west Gondwana (Stern, 1994). Collision is marked by north-to east-trending sutures, characterized by low-grade volcano-sedimentary rocks and mafic-ultramafic rocks, sandwiched between medium- to high-grade gneisses and migmatites (Corti, 2009) (**Fig.2a**).

Such deformation was followed by a long period of widespread erosion in the Paleozoic, with the Precambrian orogenic mountain ranges almost completely worn down by denudation (Mohr, 1962).

Since Early Permian extensional deformation associated to Karoo-type rift occurred separating the Horn of Africa from Madagascar-Indian promontory (Guiraud et al., 2005). This episode was followed by the development of several NW–SE striking structural basins associated with the polyphase break-up of Gondwanaland (Blue Nile, Malut and Muglad rifts in Sudan and Anza graben in Southern Ethiopia and Northern Kenya; see **Fig.2b**); during the Mesozoic such

depressions served as depositional basins for continental sandstones and marine limestones (**Plate 1a-b**) (Chorowicz et al., 1998; Mege and Korme, 2004; Gani and Abdelsalam, 2006). These events were followed by local inversions and rift rejuvenation along these NW–SE striking basins up to the Paleogene (Corti, 2009).

During Eocene-Late Oligocene East Africa volcanism started with the eruption of the Ethiopian-Yemen flood basalts (Trap series; **Fig.1b**, **Plate 1c-d**) (Corti, 2009). These eruptions mostly occurred through fissures (**Plate 2c-d**; Mohr and Zanettin, 1988), at places controlled by pre-existing weaknesses inherited from the Precambrian (Mege and Korme, 2004). This phase of extensive eruption was concomitant with the onset of continental rifting in the Red Sea–Gulf of Aden systems by 29 Ma (Wolfenden et al., 2005), but predates the main rifting phases associated with the development of the Main Ethiopian Rift (MER; between 11 Ma [Wolfeden et al., 2004] and 5 Ma [Bonini et al., 2005]). Limited volumes of basalts as old as 45 Ma have been described in southern Ethiopia, in the area between MER and Kenya Rift (Davidson and Rex, 1980; Ebinger et al., 1993; George et al., 1998).

The outpouring of plateau basalts is associated with regional dynamic uplift (Ethiopian and Kenyan domes), attributed to the impinging of hot asthenospheric materials at the base of the lithosphere (Ebinger and Sleep,1998; Rogers, 2006; Yirgu et al., 2006). Immediately after the peak of flood basalt emplacement, a number of large shield volcanoes developed from 30 Ma to about 10 Ma on the surface of the basaltic plateau (Kieffer et al., 2004) (**Fig.1b**). Since late Pliocene to Present, magmatic and tectonic activities moved mainly into the axial sector of the MER and in the Afar depression (Ebinger, 2005; Corti, 2009). In this period the volcanic activity on the plateau was confined mainly in the southern and southeastern sectors of the Lake Tana area. Such activity was characterized by basaltic lava flows coming out from small volcanic cones located immediately south of the lake.

1.3 Topography

The Ethiopian plateau is located at the junction of three rifts: two oceanic rifts, Red Sea and Gulf of Aden, and the East African continental rift (Pik et al., 1998). It stands at a mean elevation of 2500 m a.s.l. with almost flat areas and huge volcanic reliefs which rise 1000-2000 m above the plateau surface (Mt. Ras Dashen 4620 m a.s.l.; Mt. Guna 4231 m a.s.l.; Mt. Abune Yosef 4190 m a.s.l.; Mt. Choke 4100 m a.s.l.; Mt. Guguftu 3975 m a.s.l.) (**Fig.1a**). It is bordered by two huge escarpments: the SSW-NNE trending Tana escarpment to the west and the N-S trending Afar-MER

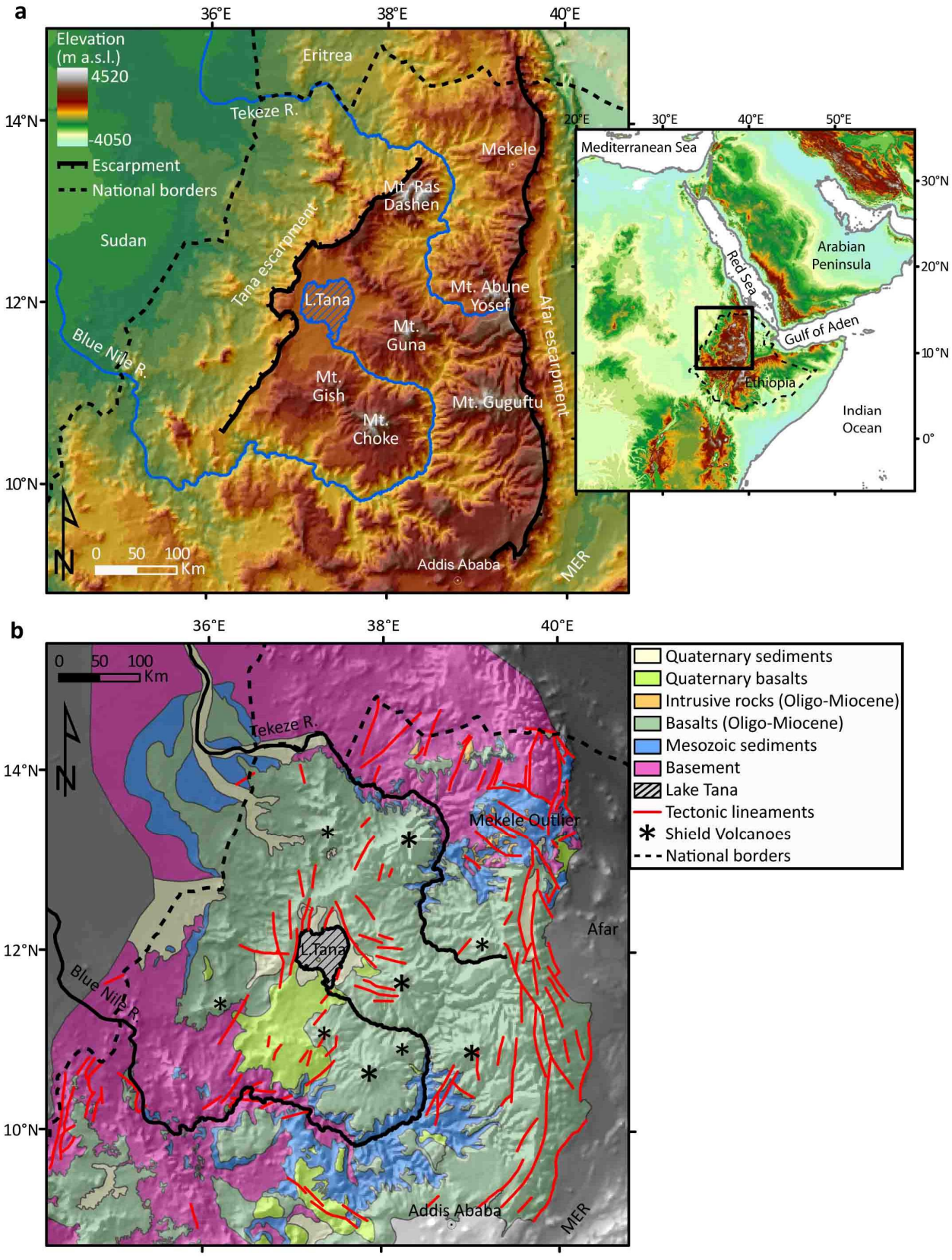

Figure 1 - a) Topography of the Ethiopian Plateau area (ETOPO1 DEM with a resolution of around 2000 m). The black box in the inset indicates the location of the study area and the Ethiopian national boundaries; **b)** geological map of the study area compiled from the 1:2.000.000 (Tefera et al., 1996) and the available 1:250.000 scale maps (Hailu, 1975; Kazmin, 1976; Garland, 1980; Tsige and Hailu, 2007; Chumburo, 2009; Zenebe and Mariam, 2011) of Ethiopia draped over the shaded topography.

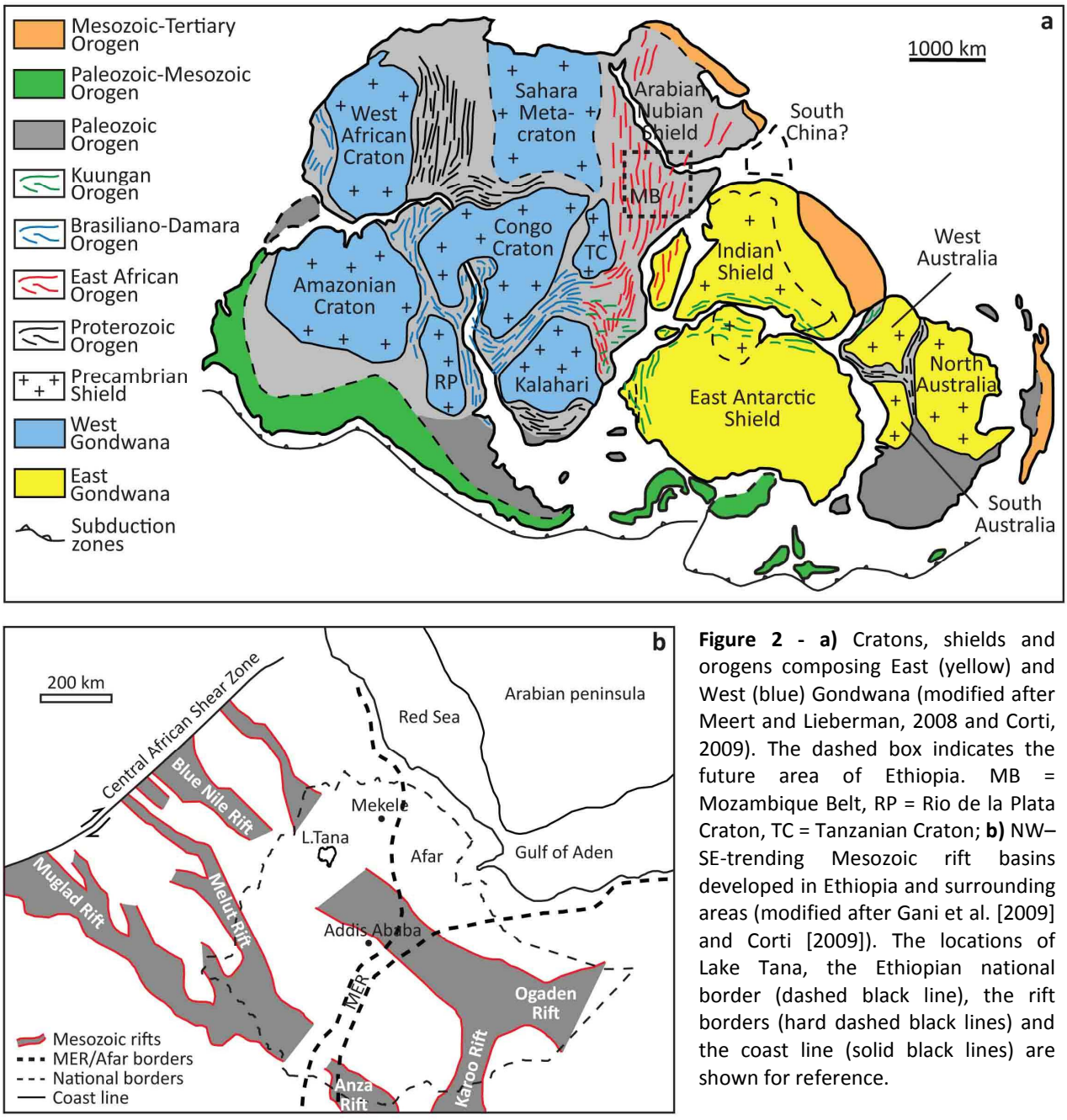

Figure 2 - a) Cratons, shields and orogens composing East (yellow) and West (blue) Gondwana (modified after Meert and Lieberman, 2008 and Corti, 2009). The dashed box indicates the future area of Ethiopia. MB = Mozambique Belt, RP = Rio de la Plata Craton, TC = Tanzanian Craton; **b)** NW–SE-trending Mesozoic rift basins developed in Ethiopia and surrounding areas (modified after Gani et al. [2009] and Corti [2009]). The locations of Lake Tana, the Ethiopian national border (dashed black line), the rift borders (hard dashed black lines) and the coast line (solid black lines) are shown for reference.

escarpment to the east. These huge morphological features separate the high elevated plateau from the Sudan and Afar lowlands (**Fig.1a**).

The Tana escarpment presents a SSW-NNE trend and a total length of about 500 km from the Blue Nile lower course to the Simien Mts (**Fig.1a**). The escarpment takes its name from the Lake Tana located immediately east of it. The lake is thought to result from the damming of a 50-km-long Quaternary basalt flow, which filled the channel of the paleo-Blue Nile River to a possible depth of 100 m (Grabham and Black, 1925; Minucci, 1938b; Jepsen and Athearn, 1961; Mohr, 1962). The Tana basin lies at the convergence of three grabens: the Debre Tabor graben from the east, the Gondar graben from the north-northwest, and the Dengel Ber graben from the south-southwest (Chorowicz et al., 1998) . The grabens are buried in the mid-Tertiary flood basalt pile; the lack of

exposure of the sub-volcanic terrain hides evidence for any earlier structural history (Zanettin, 1993; Chorowicz et al., 1998; Mege and Korme, 2004). The area is characterized by widespread dike and pipe feeders which contributed to the mid-Tertiary flood basalt flows of this sector of the Ethiopian Plateau (Mohr and Zanettin, 1988).

The plateau is carved by two main rivers: the Blue Nile R. and the Tekeze R. which drain respectively from south and north (**Fig.1a**). The present total Nile load is 230±20 x 10^6 t/a (Garzanti et al., 2006). Of such huge amount of detritus, 82±10 x 10^6 t/a are contributed by Atbara R. (Tekeze R.) and 140±20 x 10^6 t/a by the Blue Nile R. (Garzanti et al., 2006). The present erosion rates is estimated to be 0.05 mm/a (Garzanti et al., 2006). Pik et al. (2003), on the basis of partial resetting of apatite helium tracks, argue that the cutting of Blue Nile and Tekeze valleys commenced at 25–29 Ma. This follows uplift associated with eruption of the Afar Plume at 31 Ma and the formation of about 1 km of Ethiopian relief (Şengör 2001). Calculations of volumes eroded in the catchments of these two rivers have been made using the topographic envelope-subenvelope approach described in Molin et al. (2004). Pik et al. (2003) and Gani et al. (2007) have calculated an average erosion of 860 m, broadly in agreement with McDougall et al. (1975). The location of the sink for these volcanogenic sediments is controversial (Macgregor, 2012). The low pyroxene content in pre-Pliocene Nile delta sediments suggests that Ethiopia was not supplying sediment to the Nile delta area in the Miocene (Macgregor, 2012). Salama (1987; 1997) suggests that the Blue Nile basin in Sudan may have acted as a sink capturing Ethiopian-derived sediment and that the Blue Nile R. may have once drained to the Sudan Basin. Bonini et al. (2005) argued for 5 Ma as age for formation of the Ethiopian rift shoulders: this indicates that the majority of erosion should have been during the Plio-Pleistocene, when pyroxenes appeared in Nile R. sediments (Macgregor, 2012).

1.4 Methods

In order to study the geometry of the Ethiopian CFB deposits and the relationships flood basalts-topography and flood basalts-tectonics we analyzed the regional pattern of the topography and the geology of the Ethiopian Plateau area.

We investigated topography at regional scale adopting, as a digital data source, ETOPO1 global relief model (downloaded from http://www.ngdc.noaa.gov/) with a resolution of 1 arc-minute. We extracted, by MatLab topotoolbox (Schwanghart and Kuhn, 2010), four swath profiles choosing a 50 km wide observation window and sampling topography at an interval of 2 km. In order to catch the regional topographic features of the entire high-standing plateau and of the surrounding area,

we extracted the four swath profiles with different orientation (**Fig.3a**): profile 1 crosses the entire Ethiopian plateau following a NNW-SSE direction; profile 2, oriented NW-SE, is perpendicular to the MER; profile 3 trends W-E, transversally to the MER; profile 4, oriented SW-NE, is parallel to the MER and transverse to the Turkana and Afar rift systems.

For each cross section we calculated the trend of the maximum, minimum and mean elevation and the local relief. The maximum topography, obtained connecting peak elevations, displays topography without river incision (envelope surface). The minimum topography corresponds to the general pattern of valley bottom elevations (sub-envelope surface). The mean topography represents the general trend of landscape at regional scale. The local relief is the residual between the maximum and minimum topography and quantifies fluvial incision (Masek et al., 1994; Molin et al., 2004; Scotti et al., 2013).

We peformed the analysis of CFB geometry in an area including the Ethiopian and Somalian plateaux and the Yemen highlands. Such choice is strictly related to the accuracy of the source geological data. In fact the stratigraphic contacts in the plateau area have been mapped by 1:250.000 scale geological maps (Hailu, 1975; Kazmin, 1976; Garland, 1980; Tsige and Hailu, 2007; Chumburo, 2009; Zenebe and Mariam, 2011). On the contrary the Ethiopia-Sudan border area northwest of the plateau is covered just by the 1:2.000.000 scale geological map of Ethiopia (Tefera et al., 1996). For this reason, in order to reduce the interpolation error, we chose not to use data with too low accuracy, limiting the analysis only in the plateau area.

We assembled and operated all the data in GIS using ETOPO1 DEM as digital data source (http://www.ngdc.noaa.gov/). In particular we traced the flood basalts base mapping the contact with the sedimentary basement and interpolating points by a nearest-neighbor triangulation algorithm. Moreover in order to verify possible correlation between the Trap base surface configuration and tectonics we mapped tectonic lineaments and dikes in the Lake Tana region by applying a high-pass filter on the present topography (ETOPO1 DEM) and by using previous study structural data (Chorowicz et al., 1998; Mege and Korme, 2004). We reconstructed the flood basalts top surface by basaltic plateau remnants. They appear all over Ethiopia and Yemen highlands between an elevation of 2400 and 2600 m a.s.l. and consist of flat or gently sloping (1-2°) surfaces bounded by steep slopes. Using geological maps and a DEM analysis, we selected all the remnants and interpolated them by a nearest-neighbor triangulation algorithm. Then by subtracting the Trap base surface from the top one, we elaborated the Trap thickness map. To check to possible role of the Trap thickness in the present topographic setting, we elaborated an erosion map. It consists in quantifying the thickness of the eroded material in the plateau by

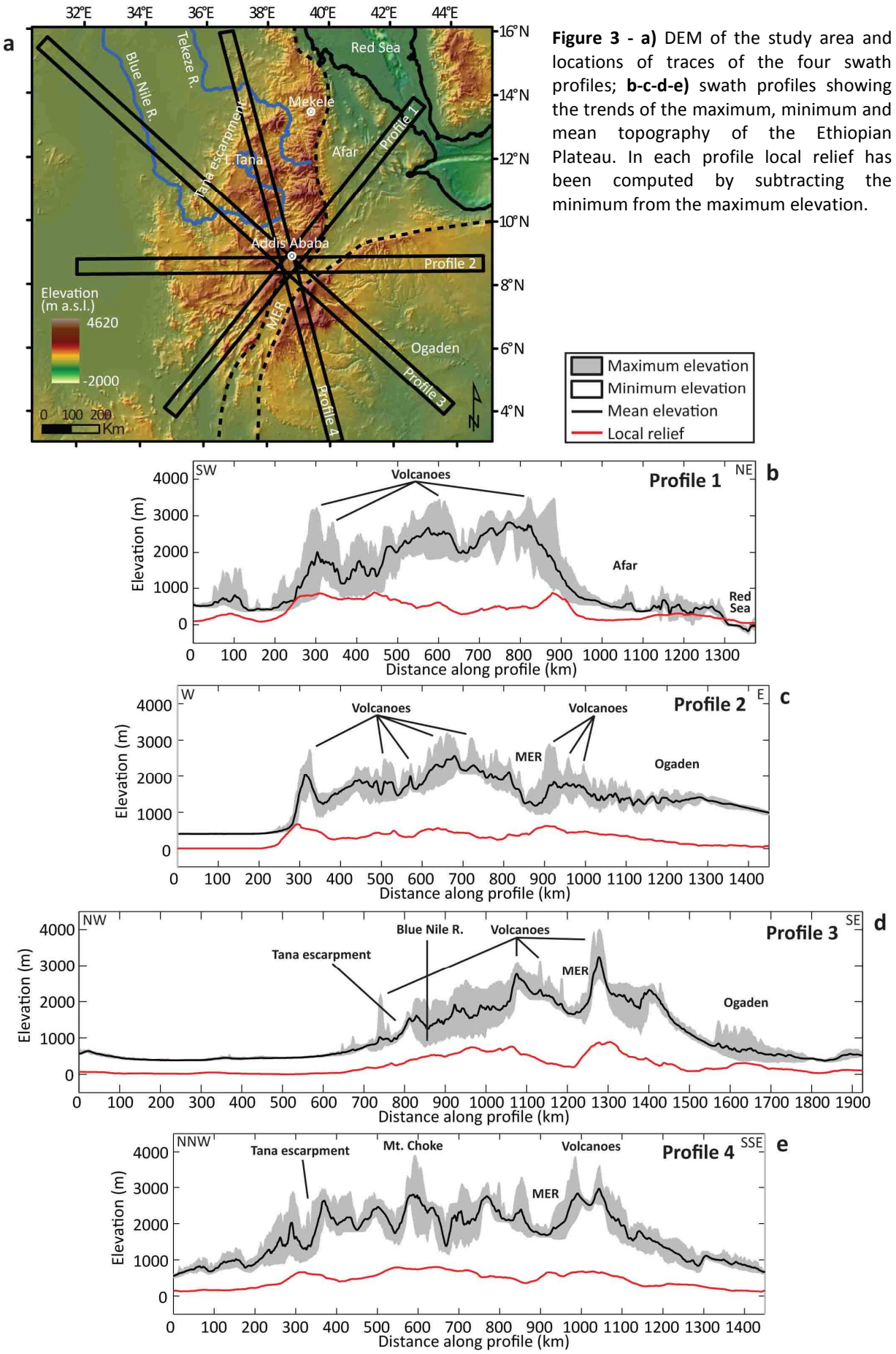

Figure 3 - a) DEM of the study area and locations of traces of the four swath profiles; **b-c-d-e)** swath profiles showing the trends of the maximum, minimum and mean topography of the Ethiopian Plateau. In each profile local relief has been computed by subtracting the minimum from the maximum elevation.

calculating the average difference in elevation between the present topography (DEM) and the reconstructed Trap top surface ("geophysical relief" - Small and Anderson, 1998). It allows to investigate the erosion pattern and its possible relation with trap thickness.

To investigate the relationship between the Trap geometry and the underlying basement we also elaborated two geologic sections

1.5 Results

All the swath profiles show a dome-shaped topography (**Fig.3**). The dome has a maximum elevation of ~2500 m, corresponding to the Addis Ababa area, and a diameter between 1100 and 1400 km with the maximum elongation axis trending SW-NE. All around the dome the topography dramatically drops ~500 m. The high peaks in the profiles correspond with volcanoes rising from the plateau up to 4500 m (**Fig.3**). The general dome shape is interrupted by the MER which is located directly east of the apex of the dome. Throughout the dome local relief is mostly constant at ~500 m, even where the principal drainage basins (Blue Nile, Tekeze and Omo basins) are located (**Fig.3**). This flat pattern indicates a very low spatial variation in fluvial incision in the whole study area. The highest values (up to 900 m) concentrate on the plateau margins where the drainage systems are capturing the inner part which, in turn, appears to be less affected by erosion (the local relief decreases down to 200 m) (**Fig.3**).

The Trap base surface shows a rough topography ranging from 450 to 2750 m (**Fig.4b**). The highest sectors are the Mekele and Addis Ababa areas. These two topographic highes are separated by a wide depression oriented NNW-SSE and extending from Desse to Lake Tana (Desse-Tana Depression). Such feature presents an irregular, almost triangular shape: the width ranges from 200 to 400 km, while its depth increases from 600 m to 1000 m to the NW. The presence of this depression under the Trap deposits is also evidenced by geological sections (**Figs.4e**) and by gravimetric investigation for oil extraction (W. St. John, Unpublished report, 1994). The lineaments analysis shows a strong correlation between the Dessie-Tana Depression and the principal tectonic structures occurring in the Lake Tana area (**Fig.4c**). In particular the depression trend coincides mostly with the Debre Tabor graben one (**Fig.4c**). In the western part of the Trap base map (**Fig.4b**) a 200 km long and 50 km wide depression trending NW-SE is partially coincident with the present lower course of Blue Nile R.

The Trap top surface presents an average altitude of 2500 m (**Fig.5b**). The lowest elevations are located all around the Ethiopian plateau reaching the minimum (2000 m) in the Mekele area.High

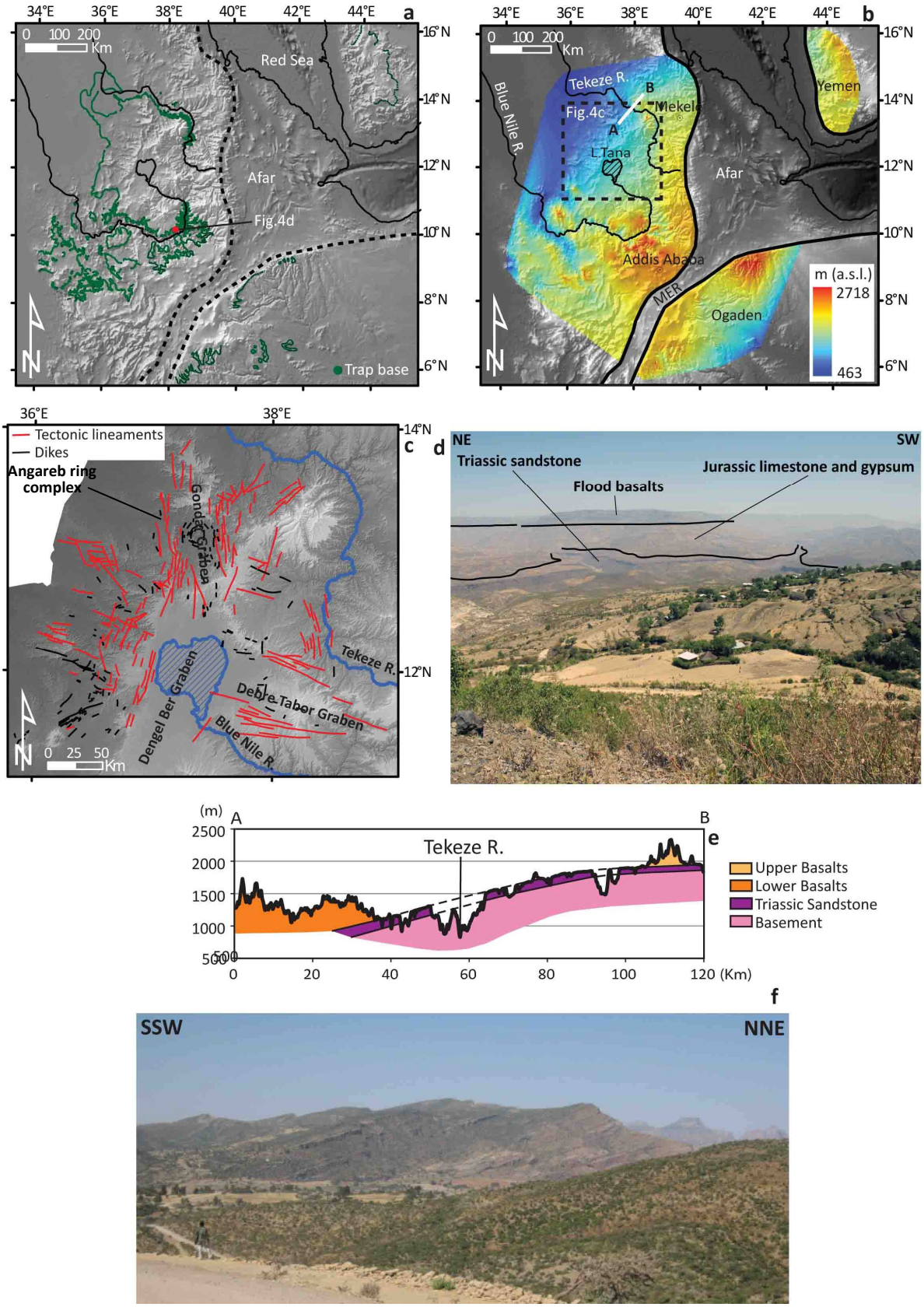

Figure 4 - a) Map of the stratigraphic contacts basement/flood basalts and Mesozoic sediments/flood basalts. The red point indicates the location of Fig.4d; **b)** map of the CFB base surface. The dashed black box indicates the location of Fig.4c; **c)** map of lineaments in the Lake Tana region. The locations of the main graben structures coincide with the wide depression found in Fig.4b; **d)** panoramic view of the Blue Nile valley. The black lines indicate the stratigraphic contacts between the main lithologies; **e)** geological section across the Tekeze R. located at the northernmost edge of the depression (profile A-B in Fig.4b). Note that the Triassic Sandstones gently dip toward SW; **f)** panoramic view of the Triassic Sandstone immediately north-west of Mekele. The strata dip to the SW, as evidenced in Fig.4d.

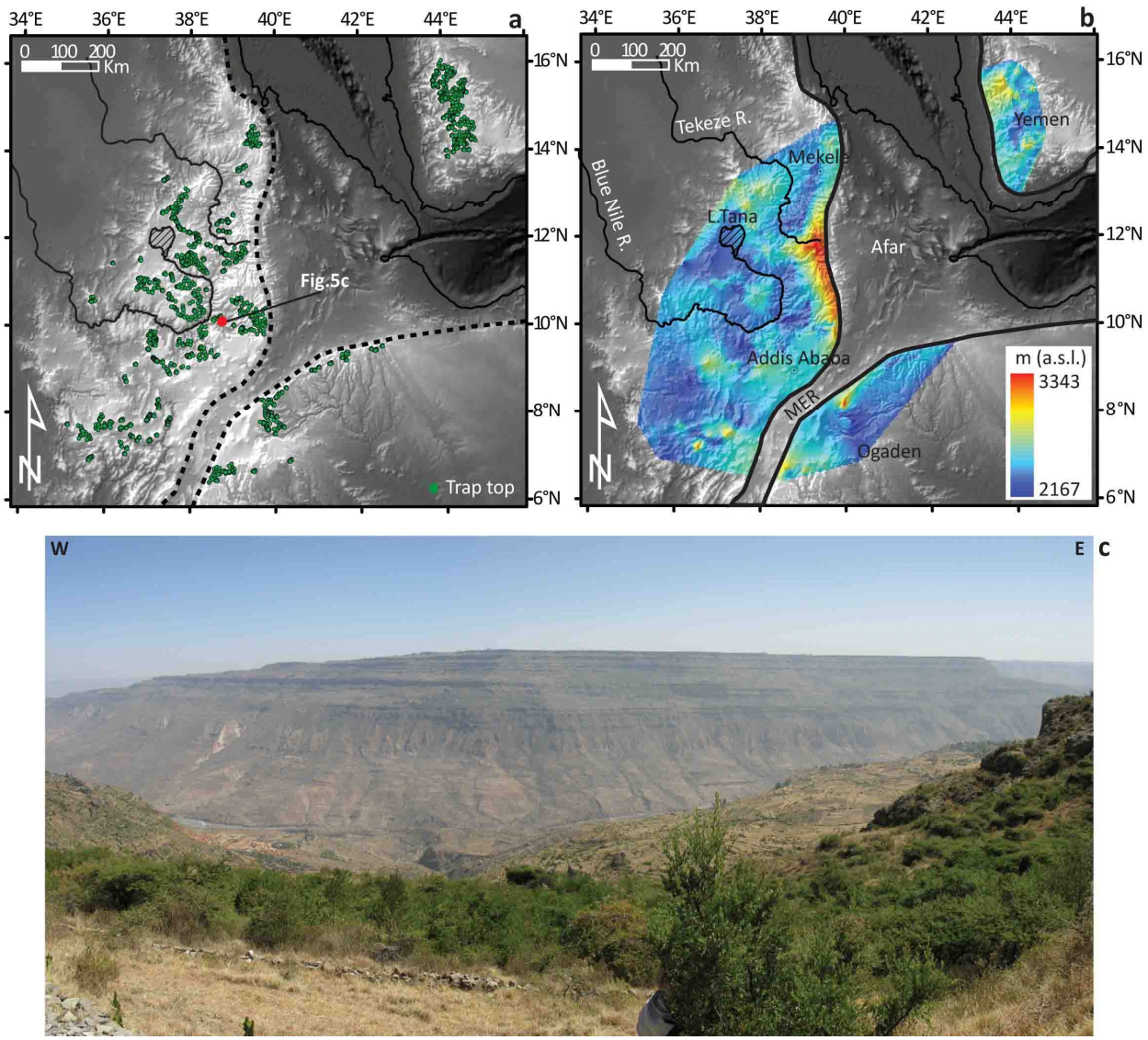

Figure 5 - **a)** Location map of the plateau remnants used to reconstruct the flood basalts top surface. The red point indicates the location of Fig.5c; **b)** map of the CFB top surface; **c)** plateau remnant along the Jema R. valley immediately northwest of Addis Ababa.

elevations of the Trap top surface (between 2700 and 2850 m) are concentrated under the volcanoes which preserved the original basalts thickness from erosion. The highest elevations are along the eastern portion of the Ethiopian Plateau. Here the flexural uplift of the rift shoulder deformed the basalts starting from the Late Miocene (Weissel et al., 1995; Wolfeden et al., 2004; Bonini et al., 2005) (see chapter 3 of this thesis). The same high values are registered in the Yemen region. According to Dadarich et al. (2003) this is due to the combined effect of the flexural uplift of Red Sea shoulders and of the dynamically supported tilting of the Arabian plate eastward.

The Trap thickness map shows an asymmetrical distribution with respect to the Afar depression and to the rift valley (**Fig.6a**). Most of the entire volume forms the Ethiopian plateau and concentrates around Lake Tana. Thick deposits (1500-1800 m) fill the Desse-Tana Depression and are located in correspondence of the lower Blue Nile R. valley.

The erosion map (Fig.6b) shows that the highest amount of erosion concentrates along the Tana escarpment (1500-2000 m) and the main fluvial trunks with particularly high values in the lower and medium Blue Nile basin (1250-1750 m). The lowest values (0-250 m) concentrate in the inner portion of the plateau.

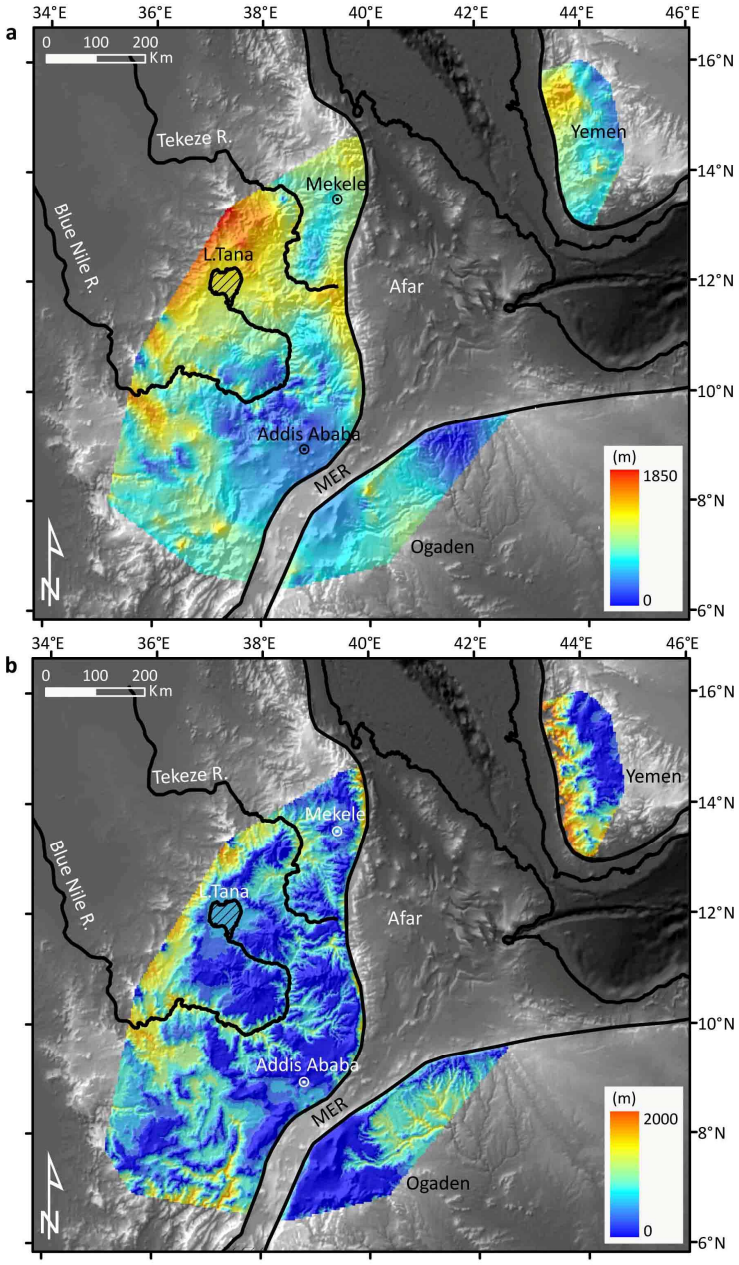

Figure 6 - a) Flood basalts thickness map obtained by subtracting the basalt's base surface from the basalts top one (see text for further explanation); **b)** erosion map resulted from the subtraction of basalts top surface from the present topography (ETOPO1 DEM database). For further explanation see the text.

In the geological maps of northwestern Ethiopia (scales 1:250.000 - [Hailu, 1975; Kazmin, 1976; Garland, 1980; Tsige and Hailu, 2007; Chumburo, 2009; Zenebe and Mariam, 2011]) Trap are separated into two main units: lower and upper basalts. Geological sections (Fig.7) cutting across the dome show that the lower basalts filled the Desse-Tana Depression (average thickness of 1000 m) while the upper basalts simply flowed onto the lower ones reaching the originally more elevated zones of northern Ethiopia and Eritrea (basalt thickness between 250 and 500 m; Fig.7b).

The lower basalts constitute the bulk of the Ethiopian Plateau while the upper basalts seem to be related to more local volcanic episodes. The geological sections show also a dome-shaped deformation of the basement rocks (Fig.7c).

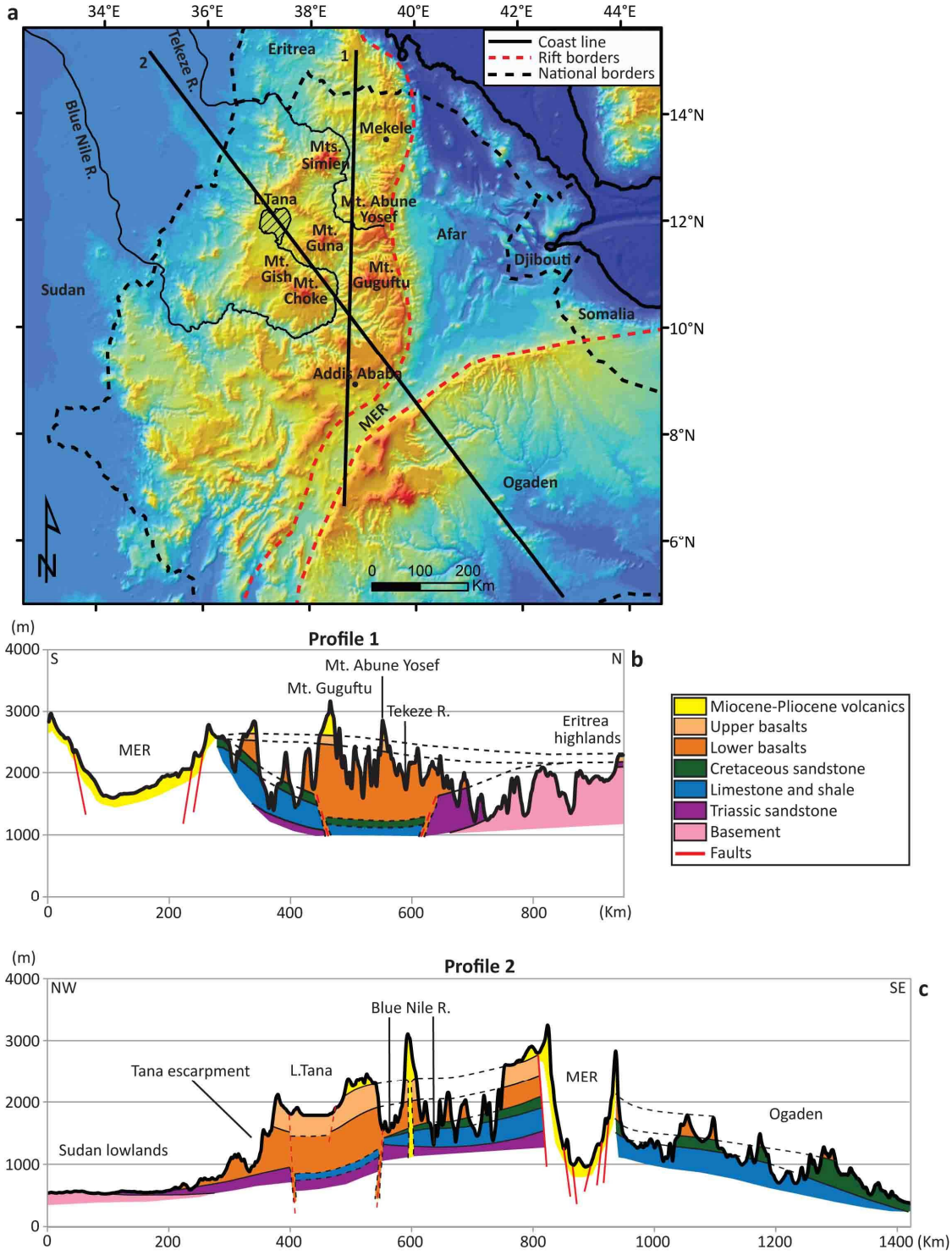

Figure 7 - a) DEM of the Ethiopian Plateau and surrounding areas (ETOPO1 DEM database). The straight solid black lines indicate the location of the two geologic sections (Figs.7b-c); **b-c)** geologic sections of the Ethiopian Plateau and surrounding areas compiled using the geological maps of Ethiopia (scales 1:2.000.000 [Kazmin, 1972; Tefera et al., 1996] and 1:250.000 [Hailu, 1975; Kazmin, 1976; Garland, 1980; Tsige and Hailu, 2007; Chumburo, 2009; Zenebe and Mariam, 2011]) and Sudan (scale 1:2.000.000 [G.M.R.D., 1981]).

1.6 Discussion

The topographic configuration of the Ethiopian Plateau is the result of two main geological processes: the impinging of hot astenospheric material at the base of the lithosphere and the outpouring of CFB. The first one produced a dome-shaped topography as evidenced by the swath profiles (**Fig.3**). The dome shows a maximum mean elevation of ~2100 m in correspondence with the Addis Ababa area. The same configuration is also evidenced by the geologic sections (**Fig.7**) where the basement rocks are uplifted and warped. Swath profiles and geologic sections indicate a net uplift of ~1500 km with respect to the Sudan and Ogaden lowlands (~600 m a.s.l.). The deposition of the CFB caused an increase in elevation over the whole area between 30 and 28 Ma ago (Zumbo et al., 1995; Baker et al., 1996a; Hofmann et al., 1997; Rochette et al., 1998). Indeed the basalts cover completely concealed the pre-Trap topography as well as the evidence of the main effusion points. The study of CFB geometry provides us with important clues on the Trap outpouring process and, in particular, on the main basalts source area.

The Trap base surface presents topographic lows and highs (**Fig.4b**). In particular a huge depression separates the Mekele and Addis Ababa highs and extends to the west (Desse-Tana Depression). On the other hand the Trap top surface has an average elevation of 2500 m with an almost flat pattern (**Fig.5b**), suggesting that the Trap emplacement leveled the pre-existing topography. On this flat topography mostly underlaid by basalts, erosion is very low, so that the plateau is preserved despite its elevation above sea level (**Fig. 6b**).

The Trap thickness map and the geologic profiles (**Figs.6-7**) show an asymmetrical distribution of CFB with respect to Afar depression and to the rift valley. Indeed only few and thin CFB deposits (< 500 m) outcrop in the Ogaden basin while the most of the entire volume forms the Ethiopian Plateau (**Fig.7b**). The thickest deposits concentrate around the Lake Tana (up to 1800 m) and along the Desse-Tana Depression (**Fig.4b**) This area of maximum thickness partially influences the present erosion of the plateau. The Blue Nile and Tekeze rivers carve around it, incising mostly where the CFB thickness is lower (**Fig. 6**). Moreover, along the Tana escarpment, the thick CFB should partially prevent the rivers to integrate into the plateau (**Fig. 6**).

The area of maximum CFB thickness, the Desse-Tana Depression, is coincident with the tectonic lineaments around the Lake Tana (**Fig. 4c**), that have the same orientation of the Mesozoic Blue Nile - Ogaden rift system structures affecting the sedimentary basement (Chorowicz et al., 1998; Mege and Korme, 2004; Gani et al., 2008). Moreover, the Desse-Tana Depression is characterized by a number of basaltic dike swarms concentrated mainly southwest and north of Lake Tana (Jepsen and Athearn, 1963a; Mohr, 1971; Mohr, 1983b; Hahn et al., 1977; Chorowicz et al., 1998;

Mege and Korme, 2004) (Fig.4c). In the first area two major NE-SW and NW-SE trending dike swarms, 30.5 Ma in age, have been described (Jepsen and Athearn, 1963a; Chorowicz et al., 1998; Mege and Korme, 2004). Both dyke swarms seem to follow the NE-SW trending shear zone, inherited from the Precambrian, and the Mesozoic Blue Nile - Ogaden rift system oriented NW-SE (Mege and Korme, 2004; see Fig.2b). Such features may have been preferential zones of dyke intrusion (Mege and Korme, 2004). The northern sector of the Lake Tana region is characterized by the Angareb ring complex (Mohr, 1971; Hahn et al., 1977; see Fig.4c). The igneous complex intruded the lower section of the Trap Series and presents almost vertical basaltic ring dikes, very similar in composition to the upper flood basalts, and widespread silicic tuff breccia deposits (Hahn et al., 1977). Such feature outcrops inside the Gondar graben (see Fig.4c) and represented one of the most active Trap eruption centre (Hahn et al., 1977).

Geophysical data suggest that large volumes of magmatic material have been added to the crust under the Ethiopian Plateau and along the rift segments (Keranen et al., 2004; Wolfenden et al., 2004; Dugda et al., 2005; Kendall et al., 2005; Mackenzie et al., 2005). In particular these studies indicate the highest crustal thickness values in corrispondence of the Lake Tana and Addis Ababa regions (Tiberi et al., 2005; Bastow et al., 2008). Seismic refraction and receiver function data west of 40°E (i.e. below the Ethiopian Plateau) show a 7.4–7.7 kms^{-1} layer at ~30 km depth, interpreted as 15 km thick mafic underplate probably accreted during the flood basalt event (Mackenzie et al. 2005).

All these evidences suggest that the area corresponding with the buried Dessie-Tana Depression should be at least one of main source areas of the Ethiopia-Yemen flood basalts. The depressed configuration of the Lake Tana region probably is related to the reactivation of Mesozoic lineaments by magma intrusion (see Fig.7c). Moreover the huge basalts load deposited all over the area caused an additional subsidence of up to 1600 m (see chapter 3 of this thesis) accomodated through the same Mesozoic faults. Subsidence is evident along the southwestern side of the Tana basin, where Chorowicz et al. (1998) observed a 20 km-wide zone of curvilinear faults with associated tilted fault-blocks. Moreover in the western, northern and eastern sectors of the basin, the Trap deposits gently dip toward the centre of the lake (Chorowicz et al., 1998)

The fast emission of huge amount of basalts filled valleys and depressions all over the area and flattened the topography (Fig.7b). The “lower basalts” filled the Desse-Tana Depression arriving up to the Sudan lowlands. Successively the “upper basalts”, associated mainly to the eruption activity of the new-formed volcanoes (Mt. Choke, Mt. Guguftu, and Mt. Guna; Kieffer et al., 2004), flowed onto the lower ones reaching the northernmost sector of Ethiopia and Eritrea.

1.6.1 New insights in the geological evolution of the Ethiopian Plateau

The study of the Ethiopian CFB structure permitted us to better understand the Trap outpouring process and in particular the influence of pre-eruption topography on the deposition of basalts.

The obtained results allow to integrate the data from the previous works (Mohr, 1962; Mohr, 1971; Hahn et al., 1977; Mohr, 1983b; Berhe et al, 1987; Ebinger and Sleep, 1998, Şengör, 2001; Wolfeden et al., 2004; Bonini et al., 2005; Gani et al., 2007; Gani et al., 2008; Corti, 2009) and to delineate a more detailed geological evolution of the Ethiopian Plateau area .

According to literature (Ebinger and Sleep, 1998; Şengör, 2001), the Afar Plume reached the base of the African lithosphere during the Middle Eocene. Through time, such process produced a domal uplift of about 1.5 km centered in the Addis Ababa area (**Figs.3, 7**). This event deformed the pre-impingment landscape characterized by NW-SE narrow rift basins related to the Gondwana break up rifting phase (**Figs.2b-8a**; Gani et al., 2008; Corti, 2009). Segments of such structures still characterize the present topography of the Lake Tana region (**Fig.4c**). The rift basins terminate sharply to the northwest against the NE-trending Central African Shear Zone, which is considered to be a major dextral strike-slip shear zone (**Figs.2b-8a**; McHargue et al. 1992; Binks and Fairhead 1992). The start of domal uplift predates or is concomitant with the first flood basalts eruption in southern Ethiopia and northern Kenya (**Fig.8b**; Davidson and Rex, 1980; Ebinger et al., 1993; George et al., 1998).

Between Late Eocene and Early Oligocene (**Figs.8c**) volcanism started in the northern sector of the N-S trending Kenya rift followed by faulting and extension after few million years (Morley et al. 1992; Smith, 1994; Ebinger et al. 2000). Traces of such tectonic event have been found also in Ethiopia (Hahn et al., 1977; Berhe et al, 1987). Indeed, in the same time, the N-S trending Omo and Tana rifts formed in the southwestern and northwestern regions respectively. More in details, the Tana rift appears separated into two branches: the Dengel Ber and the Gondar grabens (Fig.4c). According to Berhe et al (1987), the Omo and Tana rifts could be interpreted as evidence of a proto rift west of the present day rift system.

During the Late Oligocene (**Fig.8d;** Zumbo et al., 1995; Baker et al., 1996a; Hofmann et al., 1997; Rochette et al., 1998) a huge extrusion of 500–2000 m thick flood basalts (lower basalts) covered the area increasing the topography. The majority of the basaltic magma came out from the Lake Tana area characterized by the intersection between Precambrian shear zones and Mesozoic normal faults (**Figs.6a, 7**). The eruption event is testified by the presence of extended dike swarms dated at ~30 Ma (Mohr, 1971; Hahn et al., 1977; Mege and Korme, 2004). The spatial distrubution of CFB thickness (**Fig.6a**) inherited from the Oligocene main eruption event (**Fig.8d**) conditioned

the erosion pattern of the Ethiopian Plateau drainage system (**Fig.6b**). In particular the huge basalts pile in the Lake Tana area slowed down erosion along the Tana escarpment and forced the Blue Nile and Tekeze rivers to work around it where the Trap thickness is lower (<500 m; see **Fig.6a**). Around 29 Ma the onset of continental rifting in the Red Sea–Gulf of Aden systems took place (Wolfenden et al., 2005). Immediately after the Trap event huge shield volcanoes rose up from the new formed Ethiopian Plateau (Simien and Abune Yosef Mts.; see **Fig.8d**).

In the Early Miocene (**Fig.9a**) the stress regime in northern and central Africa changed dramatically from NE–SW to NW–SE. The Tana graben, which structures were preferential pathways for Trap eruption, was covered and partially sealed. The tectonic activity progressively affected southern Ethiopia where the southern portion of MER started to spread following the northward propagation of the Kenya Rift-related deformation (e.g., Bonini et al., 2005).

In the same time a new flood basalt eruption occurred (**Fig.9a**). Such event was related mainly to the activity of new volcanoes formed on the Ethiopian Plateau (Mt.Choke, Mt.Gish, Mt.Guguftu; Kieffer et al., 2004). The new basalts (upper basalts) flowed onto the lower ones reaching the Eritrean highlands to the north (**Fig.7b, 9a**).

No major extension affected the Central and Northern MER segments between 21 and 11 Ma (Corti, 2009 and references therein). Deformation in the Northern MER started in the Late Miocene at ~11 Ma (**Fig.9b**; Wolfenden et al., 2004) in coincidence of the formation of Guna volcano. In the Late Miocene (5-6 Ma) the extension started in the Central MER (**Fig.9c;** Bonini et al., 2005; 8-10 Ma, WoldeGabriel et al., 1990). During the Pliocene (**Fig.9d**) the extension affected the southern MER: such southward rift propagation was triggered by the clockwise rotation of the Somalian Plate started around 10 Ma (Bonini et al., 2005). Contemporary, a large volume of basalts erupted in the central and southern portion of the MER covering part of the Addis Ababa region (Tefera et al., 1996). Minor magmatic activity has been registered also in the Axum-Adua area (Hagos et al., 2010). During the Early Pleistocene (**Fig.10**), most of the extension and the volcanic activity shifted from the boundary faults to the central axes of the rift (Ebinger, 2005; Corti, 2009). A number of volcanoes formed all over Ethiopia, in particular along the rift axis. The Lake Tana area is characterized in this period by a local volcanic activity (Grabham and Black, 1925; Minucci, 1938b; Jepsen and Athearn, 1961).

More than one direction of extension affected the Ethiopian Plateau and the surrounding area in the Quaternary up to Present (**Fig.10**) (Gani et al., 2008; Corti, 2009).

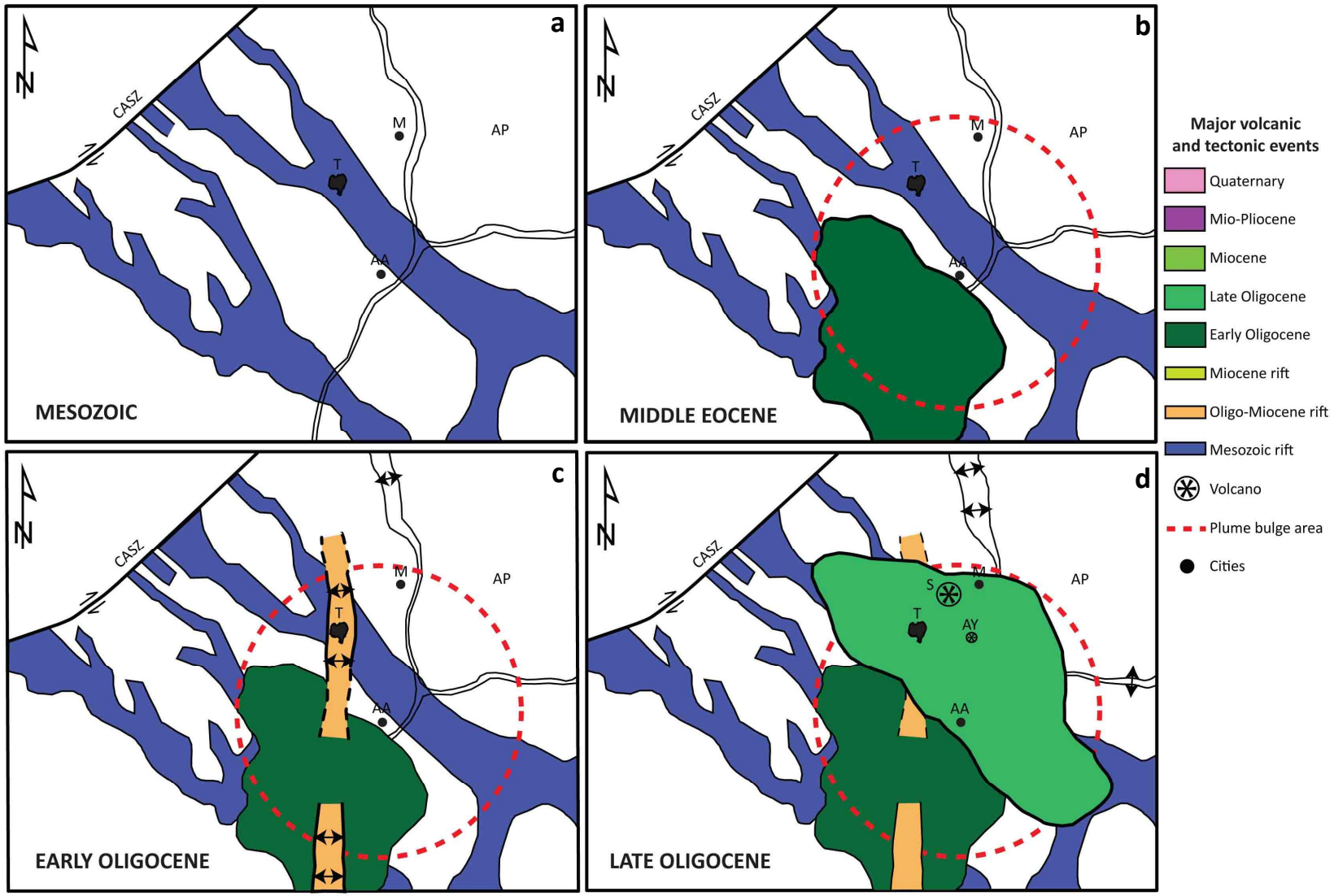

Figure 8 – Paleogeographic reconstruction of the Ethiopian Plateau and surrounding areas in the Mesozoic (**a**), Middle Eocene (**b**), Early Oligocene (**c**), and Late Oligocene (**d**). Central African Shear Zone (CASZ), Arabian Peninsula (AP), Lake Tana (T), Simient Mt. (S), Mt. Abune Yosef (AY), Mekele (M), Addis Ababa (AA). The locations of Lake Tana, Mekele and Addis Ababa are shown for references.

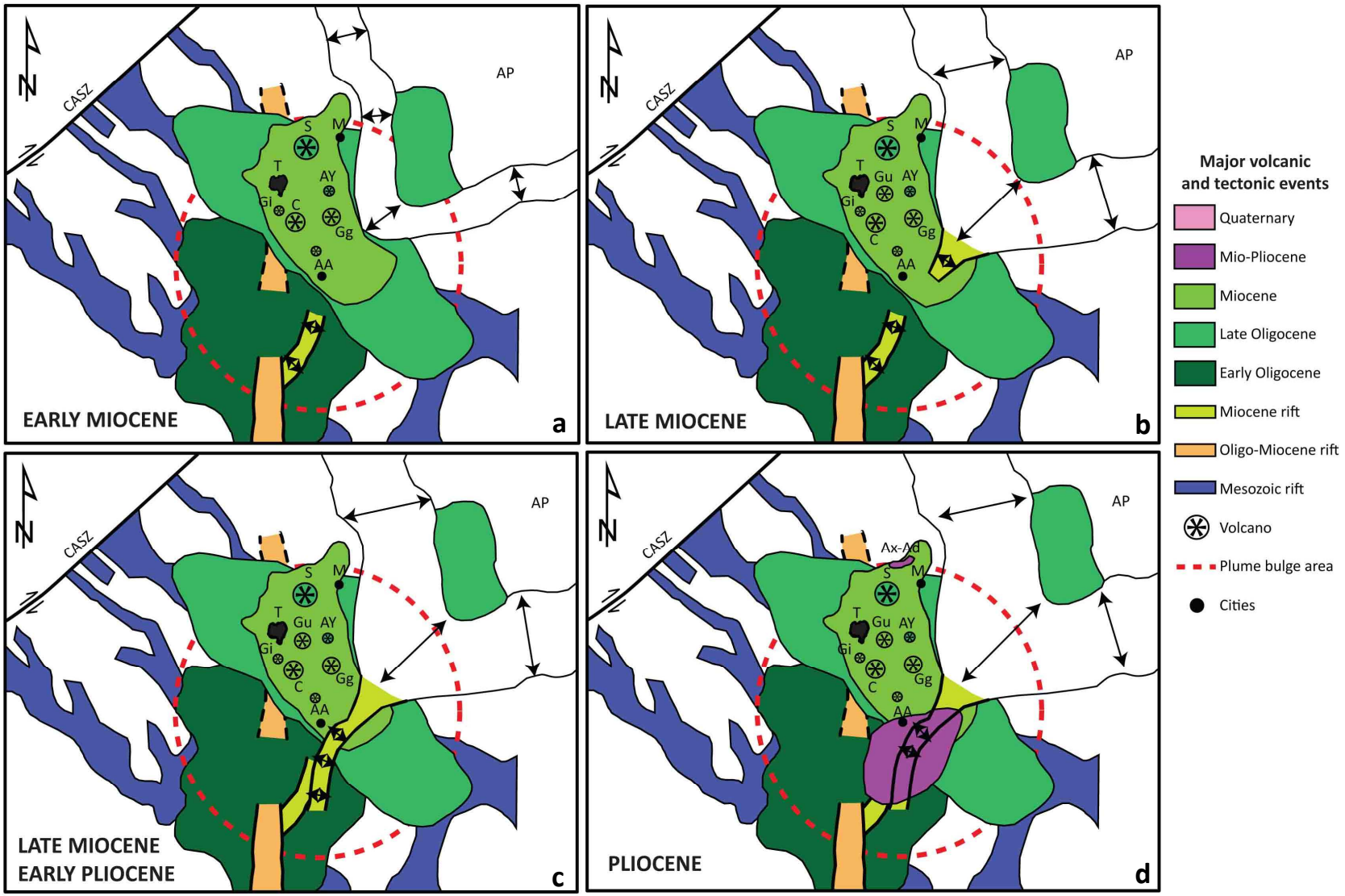

Figure 9 - Paleogeographic reconstruction of the Ethiopian Plateau and surrounding areas in the Early Miocene (**a**), Late Miocene (**b**), Late Miocene – Early Pliocene (**c**), and Pliocene (**d**). Central African Shear Zone (CASZ), Arabian Peninsula (AP), Lake Tana (T), Simient Mt. (S), Mt. Abune Yosef (AY), Mt. Choke (C), Mt. Guguftu (Gg), Mt. Gish (Gi), Mt. Guna (Gu), Axum-Adua plugs (Ax-Ad), Mekele (M), Addis Ababa (AA). The locations of Lake Tana, Mekele and Addis Ababa are shown for references.

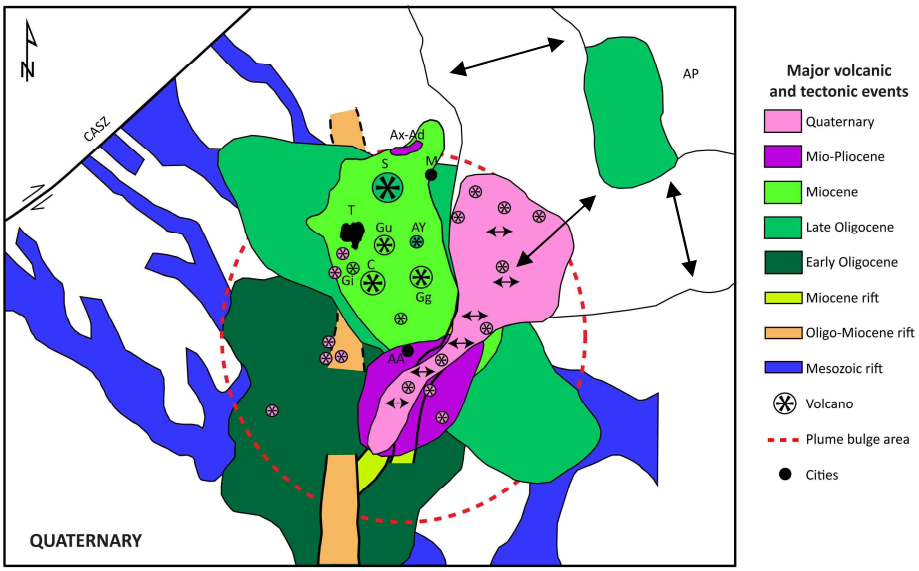

Figure 10 - Paleogeographic reconstruction of the Ethiopian Plateau and surrounding areas in the Quaternary. Central African Shear Zone (CASZ), Arabian Peninsula (AP), Lake Tana (T), Simient Mt. (S), Mt. Abune Yosef (AY), Mt. Choke (C), Mt. Guguftu (Gg), Mt. Gish (Gi), Mt. Guna (Gu), Axum-Adua plugs (Ax-Ad), Mekele (M), Addis Ababa (AA). The locations of Lake Tana, Mekele and Addis Ababa are shown for references.

1.7 Conclusions

The Ethiopian Plateau is composed maily by a huge CFB pile deposited between 30 and 28 Ma (Zumbo et al., 1995; Baker et al., 1996a; Hofmann et al., 1997; Rochette et al., 1998). The deposits cover an area of 600000 km^2 with a typical thickness varying from 500 to 2000 m (Berhe et al., 1987; Mohr and Zanettin, 1988). The chemical composition of the Ethiopian CFB supports a magma genesis from a broad region of mantle upwelling, heterogeneous in terms of temperature and composition (Kieffer et al., 2004).

The outpouring of such huge amount of basalts in such short time deeply changes the topographic configuration of the area. Indeed most of the Ethiopian Plateau topography is related to the uplift caused by the impinging of Afar Plume and to the deposition of CFB. For these reasons studying the structure of CFB it is a powerfull tool to understand the geodynamic evolution of the region.

In this study we investigated the Ethiopian Plateau topographic pattern and the geometry of CFB by reconstructing the base and top surfaces and quantifying the spatial variation in Trap thickness. A summary of the results includes the following:

- The present topographic configuration shows a dome-shaped topography centered in the Addis Ababa area with a maximum mean elevation of ~2100 m a.s.l. (**Fig.3**). Such configuration is related to the impinging of hot astenospheric material at the base of East Africa lithosphere (Middle Eocene according to Ebinger and Sleep [1998] and Şengör [2001]). The same pattern is also

showed by the geologic sections (**Figs.7b-c**) which evidence a strong deformation of the sedimentary basement. The net domal uplift calculated with respect to the Sudan lowlands and Ogaden basin (~600 m a.s.l.) in both cases is ~1500 m.

- The Trap base surface is characterized by a rough relief with a wide depression extending from Lake Tana to MER and lying between the Addis Ababa and Mekele topographic highs (Desse-Tana Depression; **Fig.4b**). This depression is tectonic in origin, being coincident with Mesozoic rift structures (**Figs.4c, 8**). Moreover a minor depression is located along the downstream course of the present Blue Nile R. (**Fig.4b**).

- The emplacement of basalt flows smoothed the original rough topography generating the present plateau. The spatial variation in Trap thickness drove the Blue Nile and Tekeze rivers to turn around the Desse-Tana Depression where the maximum amount of basalts accumulate (see **Fig.6b**).

- The CFB thickness map and the geologic sections (**Figs.6a-7c**) show an asymmetric distribution of CFB with respect to the Rift Valley. The thickest deposits (1500-2000 m) are concentrated along the Desse-Tana Depression. This evidence together with the widespread presence of Oligocene dike swarms outcropping all over the region suggests that the Desse-Tana Depression is one of the main Trap source areas.

- The geologic sections (**Fig.7**) show that lower basalts flowed into the main depressions, flattening the topography of the area. Successively, the upper basalts deposited on the lower ones and flowed up to the Eritrea highlands. The resulting Trap top surfaces presents a mean elevation of 2500 m a.s.l. (**Fig.5b**).

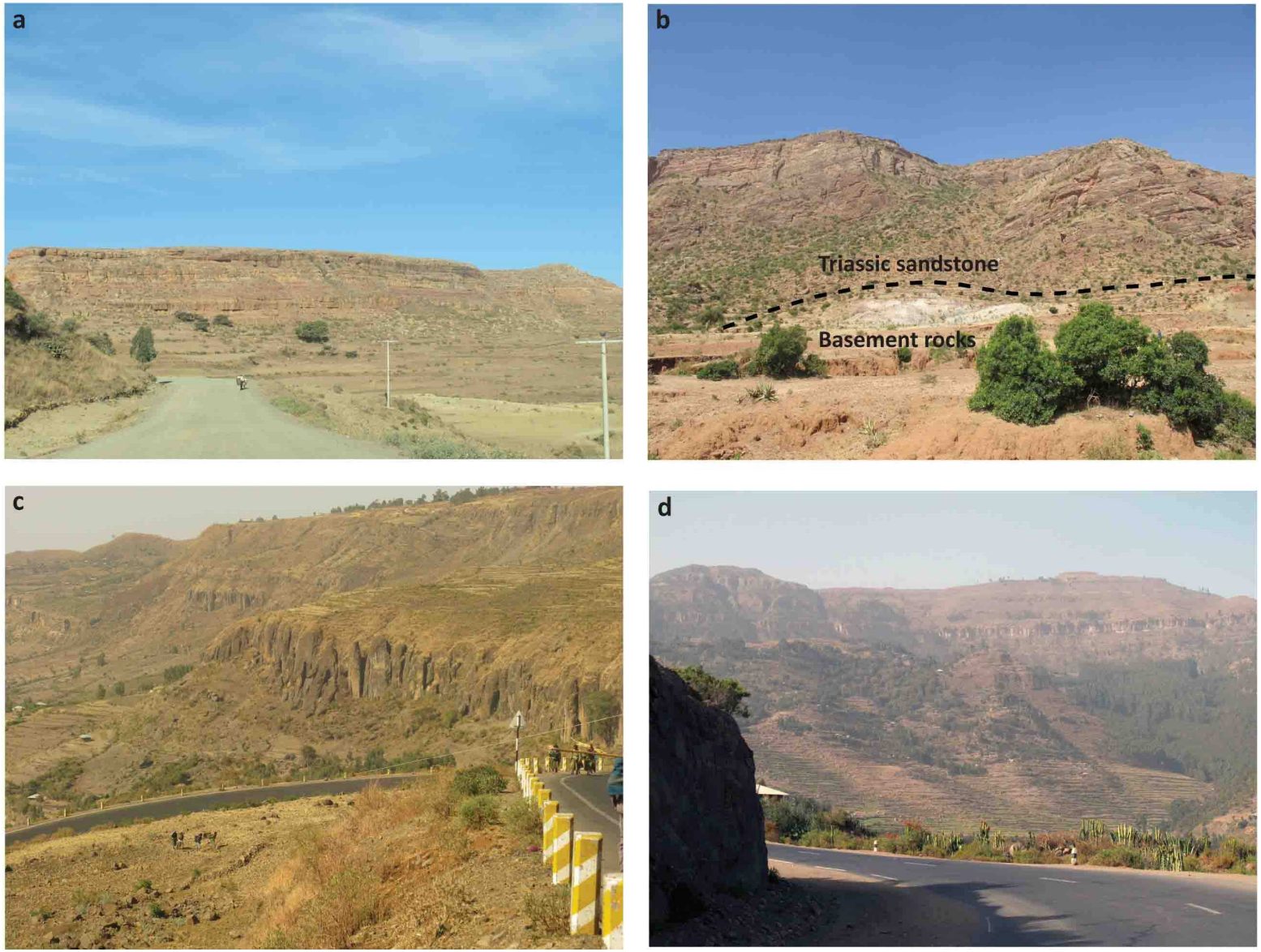

Plate 1 - a) Tabular limestones outcropping near the city of Mekele; **b)** unconformal contact between Triassic sandstone and Paleozoic basement rocks (glacial sediments) outcropping in the valley north of Wukro; **(c) CFB** outcropping in the Blue Nile R. Valley**; (d)** CFB near the Woldiya village, along the road Dese-Kobo.

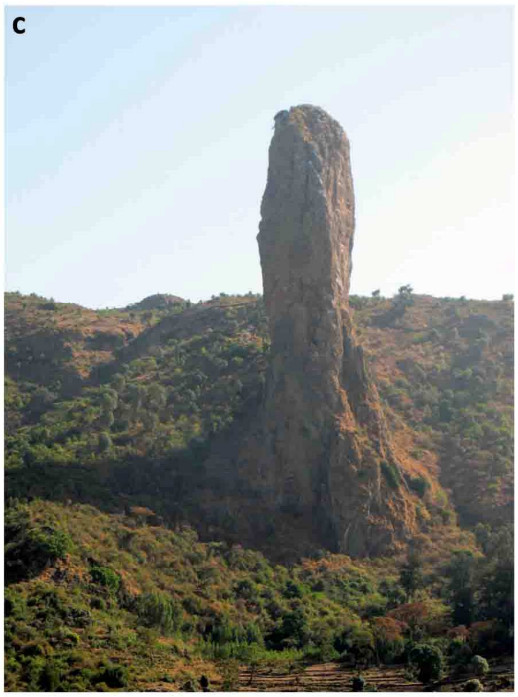

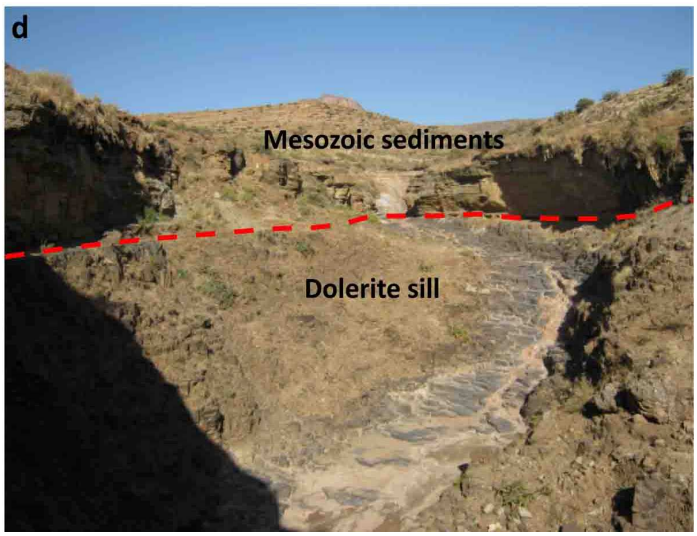

Plate 2 - a) Panoramic view of the axial sector of the Central MER; **b)** minor border fault along the Afar escarpment east of the Mekele outlier; **c)** basaltic dike outcropping immediately east of the Lake Tana; **d)** dolerite sill intruded into Mesozoic sediments near the city of Antalo (Mekele outlier).

References

Baker, J., Snee, L. and Menzies, M. (1996a) – “A brief Oligocene period of flood volcanism in Yemen” – EPSL, 138, 39–55.

Barry, T.L., Self, S., Kelley, S.P., Reidel, S., Hooper, P. and Widdowson, M. (2010) - "New $^{40}Ar/^{39}Ar$ dating of the Grande Ronde lavas, Columbia River Basalts, USA: Implications for duration of flood basalt eruption episodes" - Lithos, vol. 118, pp. 213-222.

Bastow, I.D., Nyblade, A.A., Stuart, G.W., Rooney, T.O. and Benoit, M.H. (2008) - "Upper mantle seismic structure beneath the Ethiopian hot spot: rifting at the edge of the African low-velocity anomaly" - Geochemistry, Geophysics, Geosystems 9, Q12022. doi:10.1029/2008GC002107.

Basu, A.R., Renne, P.R., DasGupta, D.K., Teichmann, F. and Poreda, R.J. (1993) - "Early and Late Alkali Igneous Pulses and a High-3He Plume Origin for the Deccan Flood Basalts" - Science, vol. 261, pp. 902-906.

Basu, A.R., Poreda, R.J., Renne, P.R., Teichmann, F., Vasiliev, Y.R., Sobolev, N.V. and Turrin, B.D. (1995) - "High-^{3}He Plume Origin and Temporal-Spatial Evolution of the Siberian Flood Basalts" - Science, vol. 269, pp. 822-825.

Berhe, S.M., Desta, B., Nicoletti, M. and Tefera, M. (1987) – “Geology, geochronology and geodynamic implications of the Cenozoic magmatic province in W and SE Ethiopia” - Journal of the Geological Society of London 144, 213–226.

Binks RM and Fairhead JD. (1992) – “A plate tectonic setting of Mesozoic rifts of West and Central Africa” – Tectonophysics, 213, 141–151.

Bondre, N.R., Duraiswami, R.A. and Dole, G. (2004) - "A brief comparison of lava flows from the Deccan Volcanic Province and the Columbia-Oregon Plateau Flood Basalts: Implications for models of flood basalt emplacement" - Proc. Indian Acad. Sci., 113, n°4, pp. 809-817.

Bonini, M., Corti, G., Innocenti, F., and Manetti, P. (2005) – “Evolution of the Main Ethiopian Rift in the frame of Afar and Kenya rifts propagation” - Tectonics, v. 24, doi: 10.1029/2004TC001680.

Bosellini, A., Russo, A., Fantozzi, P.L., Assefa, G. and Solomon, T. (1997) – “The Mesozoic succession of the Mekele outlier (Tigre Province, Ethiopia)” - Memorie Scienze Geologiche 49, 95-l 16.

Burov, E.B. and Diament, M. (1995) – “The effective elastic thickness (Te) of continental lithosphere: What does it really mean?” – J. Geophis. Res., vol.100, pp.3905-3927.

Campbell, I.H. and Griffiths, R.W. (1990) - "Implications of mantle plume structure for the evolution of flood basalts" - EPSL, 99, 79-93.

Chang, S.J. and Van der Lee, S. (2011) – “Mantle plumes and associated flow beneath Arabia and East Africa” - Earth and Planetary Science Letters, 302, 448–454.

Chenet, A.L., Quidelleur, X., Fluteau, F., Courtillot, V. and Bajpai, S. (2007) - "$^{40}K/^{40}Ar$ dating of the Main Deccan large igneous province: Further evidence of KTB age and short duration" - EPSL, vol. 263, pp. 1-15.

Chery, J., Vilotte, J.P. and Daignieres, M. (1991) – “Thermomechanical evolution of a thinned continental lithosphere under compression: Implications for Pyrenees, J. Geophys. Res., 96, 43854412.

Chorowicz, J., Collet, B., Bonavia, F.F., Mohr, P., Parrot, J.-F. and Korme, T. (1998) - "The Tana basin, Ethiopia: intraplateau uplift, rifting and subsidence" - Tectonophysics 295, 351–367.

Chumburo, F. (2009) – "Geological Map of Debre Markos sheet (NC 37-6)" – EIGS.

Chung, S.L. and Jahn B.M. (1995) - "Plume-lithosphere interaction in generation of the Emeishan flood basalts at the Permian-Triassic boundary" - Geology, v. 23, pp. 889-892.

Corti, G. (2009) – "Continental rift evolution: From rift initiation to incipient break-up in the Main Ethiopian Rift, East Africa" - Earth-Science Reviews, 96, 1–53.

Courtillot, V., Feraud, G., Maluski, H., Vandamme, D., Moreau, M.G. and Besse, J. (1988) - "Deccan flood basalts and the Cretaceous/Tertiary boundary" - Nature, vol. 333, pp. 843-846.

Courtillot, V., Jaupart, C., Manighetti, I., Tapponnier, P. and Besse, J. (1999) - "On causal links between flood basalts and continental breakup" - EPSL, 166, 177–195.

Courtillot, V.E. and Renne, P.R. (2003) - "On the ages of flood basalt events" - Comptes Rendus Geoscience, vol. 335, 113–140.

Daradich, A., J. X. Mitrovica, R. N. Pysklywec, S. D. Willett and A. M. Forte (2003) – "Mantle flow, dynamic topography, and rift-flank uplift of Arabia" - Geology, 31, 901–904, doi:10.1130/G19661.1.

Davidson, A. and Rex, D.C. (1980) – "Age of volcanism and rifting in south-western Ethiopia" - Nature 283, 654–658.

Dickin, A.P. (1988) - "The North Atlantic Tertiary Province" - In: "Continental Flood Basalts" - J.D. MAcdougall (ed), Kluwer Academic Publishers, London, p.111.

Dugda, M., Nyblade, A., Julia, J., Langston, C.A., Ammon, C. and Simiyu, S. (2005) - "Crustal structure in Ethiopia and Kenya from receiver function analyses: Implication for rift development in eastern Africa" - J. geophys. Res., 110, B01303, doi:10.1029/2004JB003065.

Duncan, R.A., Hooper, P.R., Rehacek, J., Marsh, J.S. and Duncan, A.R. (1997) - "The timing and duration of the Karoo igneous event, southern Gondwana" - J. Geoph. Res., vol. 102, pp. 18127-18138.

Ebinger, C.J., Yemane, T.,WoldeGabriel, G., Aronson, J.L. and Walter, R.C. (1993) – "Late Eocene-Recent volcanism and faulting in the southern main Ethiopian rift" - Journal of the Geological Society of London 150, 99–108.

Ebinger, C. and Sleep, N.H. (1998) – "Cenozoic magmatism in central and east Africa resulting from impact of one large plume" - Nature 395, 788–791.

Ebinger, C. J., Yemane, T., Harding, D. J., Tesfaye, S., Keley, S. and Rex, D. C. (2000) – "Rift detection, migration, and propagation: Linkage of the Ethiopian and Eastern Rifts, Africa" - Buletin of the Geological Society of America 112, 163-176.

Ebinger, C. (2005) - "Continental breakup: the East African perspective" - Astronomy and Geophysics 46, 2.16–2.21.

Ellam, R.M., Carlson, R.W. and Shirey, S.B. (1992) - "Evidence from Re-Os isotopes for plume-lithosphere mixing in Karoo flood basalt genesis" - Nature, vol. 359, pp.718-721.

Forsyth, D. W. (1985) –"Subsurface loading and estimates of the flexural rigidity of continental lithosphere" -J. Geophys. Res.,90(B14),12623–12632, doi:10.1029/JB090iB14p12623.

Gani, N.D. and Abdelsalam, M.G. (2006) - "Remote sensing analysis of the Gorge of the Nile, Ethiopia with emphasis on Dejen–Gohatsion region" - Journal of African Earth Sciences, v. 44, p. 135–150, doi: 10.1016/j.jafrearsci.2005.

Gani, N.D., Abdelsalam, M.G. and Gani, M.R. (2007) – "Blue Nile incision on the Ethiopian Plateau: pulsed plateau growth, Pliocene uplift, and hominin evolution" - GSA Today 17, 4–11.

Gani, N.D.S., Abdelsalam, M.G., Gera, S. and Gani, M.R. (2008) – "Stratigraphic and structural evolution of the Blue Nile Basin, Northwestern Ethiopian Plateau" - Geological Journal 44, 30–56.

Garland, C.R. (1980) – "Geology of the Adigrat Area" - Ministry of Mines, Addis Ababa Memoir No.1, 51.

Garner, P. (1996) - "Continental Flood Basalts indicate a pre-Mesozoic Flood/post-Flood Boundary" - CENTech. J., vol. 10, pp. 114-127.

Garzanti, E., Andò, S., Vezzoli, G., Megid, A.A.A. and El Kammar, A. (2006) - "Petrology of Nile River sands (Ethiopia and Sudan): Sediment budgets and erosion patterns" - EPSL, 252, 327-341.

George, R., Rogers, N. and Kelley, S. (1998) – "Earliest magmatism in Ethiopia: evidence for two mantle plumes in one flood basalt province" - Geology 26, 923–926.

Grabham, G.W. and Black, R.P. (1925) - "Report of the Mission to Lake Tana 1920–21" - Government Press, Cairo.

Griffiths, R.W. and Campbell, I.H. (1991) - "Interaction of mantle plume heads with the Earth's surface and onset of small-scale convection" - J. Geophys. Res. 96, 18295–18310.

Guiraud, R., Bosworth, W., Thierry, J. & Delplanque, A. (2005) - "Phanerozoic geological evolution of Northern and Central Africa: An overview" - J. of African Earth Science, 43, 83-143.

Hagos, M., Koeberl, C., Kabeto, K. and Koller, F. (2010) – "Geochemical characteristics of the alkaline basalts and the phonolite-trachyte plugs of the Axum area, northern Ethiopia" – Austrian Journal of Earth Sciences, 103, 153-170.

Hahn, G.A., Raynolds, R.G.H., Wood, R.A. (1977) – "The geology of the Angarebring dike complex, north-western Ethiopia" - Bull. Volcanol. 40, 1-10.

Hailu, T. (1975) - "Geological Map of Adiarkay Sheet (ND 37 -10) 1:250,000" - EIGS.

He, B., Xu, Y.G., Huang, X.L., Luo, Z.Y., Shi, Y.R., Yang, Q.J. and Yu, S.Y. (2007) - "Age and duration of the Emeishan flood volcanism, SW China: Geochemistry and SHRIMP zircon U–Pb dating of silicic ignimbrites, post-volcanic Xuanwei Formation and clay tuff at the Chaotian section" - EPSL, vol. 255, pp. 306-323.

Hill, R.I. (1991) - "Starting plumes and continental breakup" - EPSL, 104, 398–416.

Hofmann, C., Courtillot, V., Feraud, G., Rochette, P., Yirgu, G., Ketefo, E. and Pik, R. (1997) – “Timing of the Ethiopian flood basalt event and implications for plume birth and global change” - Nature 389, 838–841.

Hon, K. and Pallister, J. (1995) - "Wrestling with restless calderas and fighting floods of lava" - Nature, 376, 554-555.

Hooper, P.R. (1990) - "The timing of crustal extension and the eruption of continental flood basalts" - Nature, 345, 246–249.Jepsen, D.H. and Athearn, M.J. (1961) - "A general geological map of the Blue Nile River basin, Ethiopia (1:1,000,000)" - Dep. Water Resources, Addis Ababa.

Jepsen, D.H. and Athearn, M.J. (1961) - "A general geological map of the Blue Nile River basin, Ethiopia (1 : 1,000,000)" - Dep. Water Resources, Addis Ababa.

Jourdan, F., Feraud, G., Bertrand, H., Kampunzu, A.B., Tshoso, G., Watkeys, M.K. and Le Gall., B. (2005) - " Karoo large igneous province: Brevity, origin, and relation to mass extinction questioned by new $^{40}Ar/^{39}Ar$ age data" - Geology, vol. 33, pp. 745-748.

Kazmin, V. (1972) - "Geological map of Ethiopia, scale 1.2.000.000" - Imperial Ethiopian Government, Ministry of Mines.

Kazmin, V. (1976) – “Geological Map of Adigrat Sheet (ND 37 -7), 1:250,000” - EIGS.

Kendall, J.-M., Stuart, G., Ebinger, C., Bastow, I. and Keir, D. (2005) - "Magma-assisted rifting in Ethiopia" - Nature, 433, 146–148.

Keranen, K., Klemperer, S., Gloaguen, R. and EAGLEWorking Group, (2004) - "Three-dimensional seismic imaging of a protoridge axis in the Main Ethiopian rift" - Geology, 32, 949—952.

Kieffer, B., Arndt, N., Lapierre, H., Bastien, F., Bosch, D., Pecher, A., Yirgu, G., Ayalew, D., Weis, D., Jerram, D.A., Keller, F., and Meugniot, C. (2004) – “Flood and shield basalts from Ethiopia: Magmas from the African Superswell” - Journal of Petrology, v. 45, 793–834.

Louvat, P. and Allegre, C.J. (1997) - "Present denudation rates on the island of Reunion determined by river geochemistry: Basalt weathering and mass budget between chemical and mechanical erosions" - Geochimica et Cosmochimica Acta, Vol. 61, No. 17, pp. 3645-3669.

Macgregor, D.S. (2012) - "The development of the Nile drainage system: integration of onshore and offshore evidence" - Petr. Geosc., vol. 18, pp. 417-431.

Mackenzie, G.D., Thybo, H. and Maguire, P.K.H. (2005) - "Crustal velocity structure across the Main Ethiopian Rift: Results from two-dimensional wideangle seismic modelling" - Geophys. J. Int., 162, 994–1006.

Makris, J. and Ginzburg, A. (1987) – “The Afar Depression: Transition between continental rifting and sea-floor spreading” - Tectonophysics 141, 199-214.

Marzoli, A., Renne, P.R., Piccirillo, E.M., Ernesto, M., Bellieni, G. and De Min, A. (1999) - "Extensive 200-Million-Year-Old Continental Flood Basalts of the Central Atlantic Magmatic Province" - Science, vol. 284, pp. 616-618.

Marty, B., Pik, R. and Gezahegn, Y. (1996) - "Helium isotopic variations in Ethiopian plume lavas: nature of magmatic sources and limit on lower mantle contribution" - EPSL, 144, 223–237.

Masek, J., Isacks, B., Gubbels, T. and Fielding, E. (1994) - "Erosion and tectonics at the margins of continental plateau" - J. Geophys. Res. 99 (B7), 13941–13956.

McDougall, I., Morton,W.H. and William, M.A.J. (1975) – "Ages and rates of denudation of trap series basalts at the Blue Nile Gorge, Ethiopia" - Nature 254, 207–209.

McHargue T, Heidrick T and Livingstone J. (1992) – "Tectonostratigraphic development of the interior Sudan rifts, Central Africa" - In Geodynamics of Rifting, Volume II. Case History Studies on Rifts: North and South America and Africa, Ziegler PA (ed.) - Tectonophysics 213, 187–202.

McKenzie, D., and D. Fairhead (1997) – "Estimates of the effective elastic thickness of the continental lithosphere from Bouguer and free air gravity anomalies" - J. Geophys. Res., 102(B12),27523–27552, doi:10.1029/97JB02481.

Meert, J.G. and Lieberman, B.S. (2008) – "The Neoproterozoic assembly of Gondwana and its relationship to the Ediacaran–Cambrian radiation" - Gondwana Research 14, 5–21.

Mege, D. and Korme, T. (2004) - "Dyke swarm emplacement in the Ethiopian Large Igneous Province: not only a matter of stress" - Journal of Volcanology and Geothermal Research 132, 283–310.

Minucci, E. (1938b) - "Ricerche geologiche nella regione del Tana" - In: Missione di Studio al Lago Tana. R. Accad. Ital. 1, 19–36.

Mohr, P. (1962) – "The geology of Ethiopia" - Addis Ababa: Addis Ababa University Press.

Mohr, P. (1971) – "Ethiopian Tertiary Dyke Swarms" - Smithson. Astrophys. Obs. Spec. Rep., 339, 53 pp.

Mohr, P. (1983b) - "Ethiopian flood basalt province" - Nature, vol. 303, pp. 577-584.

Mohr, P., and Zanettin, B. (1988) – "The Ethiopian Flood Basalt Province" - In McDougall, J.D., ed., Continental Flood Basalts: Dordrecht, Netherlands, Kluwer Academic Publishers, 63–110.

Molin, P., Pazzaglia, F.J. and Dramis, F. (2004) - "Geomorphic expression of active tectonics in a rapidly deforming forearc, Sila Massif, Calabria, southern Italy" - American Journal of Science 304, 559–589.

Montagner, J.P., Marty, B., Stutzmann, E., Sicilia, D., Cara, M., Pik, R., Leveque, J.-J., Roult, G., Beucler, E., and Debayle, E. (2007) – "Mantle upwellings and convective instabilities revealed by seismic tomography and helium isotope geochemistry beneath eastern Africa" - Geophysical Research Letters, v. 34, p. L21303, doi:10.1029/2007GL031098.

Morandini, G. (1938) - "Ricerche fisiche sul Lago Tana" - In: "Missione di Studio al Lago Tana", R. Accad. Ital. 1, 57–76.

Morgan, W.J. (1971) - "Convection plumes in the lower mantle" - Nature, 230, 42–43.

Morley, C. K., Westcott, W. A., Stone, D. M., Harper, R. M., Wigger, S. T. and Karanja, F. M. (1992) – "Tectonic evolution of the northern Kenya Rift" - Journal of the Geological Society, London 149, 333-348.

Nemeth, K., Martin, U. and Csillag, G. (2003) - "Calculation of Erosion Rates Based on Remnants of Monogenetic Alkaline Basaltic Volcanoes in the Bakony–Balaton Highland Volcanic Field (Western Hungary) of Mio/Pliocene Age" - Geolines, 15.

Ni, S., Tan, E., Gurnis, M. and Helmberger, D. (2002) – "Sharp sides to the African plume" - Science 296, 1850-1852.

Perez-Gussinye, M., Metois, M., Fernandez, M., Verges, J. and Lowry, A.R. (2009) – "Effective elastic thickness of Africa and its relationship to other prozie for lithospheric structure and surface tectonics" - Earth Planet. Sci. Lett., 287(1-2), 152-167.

Petit, C. and C. Ebinger (2000) – "Flexure and mechanical behavior of cratonic lithosphere: Gravity models of the East African and Baikal rifts" - J. Geophys. Res., 105(B8), 19151–19162, doi:10.1029/2000JB900101.

Pik, R., Deniel, C., Coulon, C., Yirgu, G., Hofmann, C. and Ayalew, D. (1998) – "The Northwest Ethiopian plateau flood basalts: classification and spatial distribution of magma types" - Journal of Volcanology and Geothermal Research 81, 91–111.

Pik, R., Marty, B., Carignan, J. and Lave, J. (2003) – "Stability of Upper Nile drainage network (Ethiopia) deduces from (U–Th)/He thermochronometry: Implication of uplift and erosion of the Afar plume dome" - Earth and Planetary Science Letters, v. 215, 73–88, doi: 10.1016/S0012-821X(03)00457-6.

Quin, K., Su, B., Sakyi, P.A., Tang, D., Li, X., Sun, H., Xiao, Q. and Liu, P. (2011) - "Sims zircon U-Pb geochronology and Sr-Nd isotopes of Ni-Cu-bearing mafic-ultramafic intrusions in eastern Tianshan and Beishan in correlation with flood basalts in Tarim basin (NW China): constraints on a ca.280 ma mantle plume" - A. J. Sci., vol. 311, pp. 237-260.

Renne, P.R. and Basu, A.R. (1991) - "Rapid eruption of the Siberian Traps flood basalts at the Permo-Triassic boundary" - Science, 253: 176-179.

Renne, P. R., Ernesto, M., Pacca, I. G., Coe, R. S., Glen, J. M., Prévot, M. and Perrin, M. (1992) - "The age of the Paraná flood volcanism, rifting of Gondwanaland, and the Jurassic–Cretaceous boundary" - Science 258:975–979.

Richards, M.A, Duncan, R.A. and Courtillot, V (1989) - "Flood basalts and hot spot tracks: Plume heads and tails" - Science, 246, 103–107.

Ritsema, J. and van Heijst, H. (2000) – "New seismic model of the upper mantle beneath Africa" - Geology 28, 63-66.

Rochette, P., Tamrat, E., Feraud, G., Pik., R., Courtillot, V., Ketefo, E., Coulon, C., Hoffmann, C., Vandamme, D. and Yirgu, G. (1998) - "Magnetostratigraphy and timing of the Oligocene Ethiopian traps" - EPSL, 164, 497-510.

Rogers, N.W. (2006) – "Basaltic magmatism and the geodynamics of the East African Rift System" - In: Yirgu, G., Ebinger, C.J., Maguire, P.K.H. (Eds.) "The Afar Volcanic Province within the East African Rift System" - Geological Society Special Publication, vol. 259, pp. 77–93.

Salama, R.B. (1987) - "The evolution of the River Nile. The buried saline rift lakes in Sudan I. Bahr El Arab Rift, the Sudd buried saline lake" - Journal of African Earth Sciences, 6(6), 899–913.

Salama, R.B. (1997) - "Rift Basins of the Sudan" - In: Selley, R.C. (ed.) "Sedimentary Basins of the World", Vol. 3, African Basins. Elsevier, Amsterdam, 105–147.

Schwanghart, W. and Kuhn, N.J. (2010) - "TopoToolbox: A set of Matlab functions for topographic analysis" - Environmental Modelling and Software, vol. 25(6), pp. 770-781.

Scotti, V.N., Molin, P., Faccenna, C., Soligo, M. & Casas-Sainz, A. (2013) - "The influence of surface and tectonic processes on landscape evolution of the Iberian Chain (Spain): Quantitative geomorphological analysis and geochronology" - Geomorphology, http://dx.doi.org/10.1016/j.geomorph.2013.09.017.

Şengör, A.M.C. (2001) – "Elevation as indicator of mantle-plume activity" - In Ernst, R.E., and Buchan, K.L., eds., Mantle Plumes: Their identification through time: Geological Society of America Special Paper 352, 183–225.

Sharma, M., Basu, A.R. and Nesterenko, G.V. (1992) - "Temporal Sr-, Nd- and Pb-isotopic variations in the Siberian flood basalts: Implications for the plume-source characteristics" - EPSL, 113, 365-381.

Sims, K.W.W., Ackert Jr, R.P., Ramos, F.C., Sohn, R.A., Murrell, M.T. and DePaolo, D.J. (2007) - "Determining eruption ages and erosion rates of Quaternary basaltic volcanism from combined U-series disequilibria and cosmogenic exposure ages" - Geology, vol. 35, n°5, pp. 471-474.

Sinton, C.W., Duncan, R.A., Storey, M.; Lewis, J.; Estrada, J.J. (1998) - "An oceanic flood basalt province within the Caribbean plate" - EPSL, 155(3-4), 221-235.

Small, E.E. and Anderson, R.S. (1998) - "Pleistocene relief production in Laramide mountain ranges, western United States" - Geology, vol. 26, n°2, pp.123-126.

Smith, M. (1994) – "Stratigraphic and structural constraints on mechanisms of active rifting in the Gregory Rift, Kenya" - Tectonophysics 236, 3-22.

Stern, R.J. (1994) - "Arc assembly and continental collision in the Neoproterozoic East African orogen" - Annual Review of Earth and Planetary Sciences 22, 319–351.

Swanson, D.A. and Wright, T.L. (1981) - "The regional approach to studying the Columbia River Basalt Group" - In: "Deccan Volcanism and Related Basalt Provinces in Other Parts of the World", K.V. Subbaro and R.N. Sukheswala (eds), Geological Society of India Memoir 3, Bangalore, p.74.

Tefera, M, Cherenet, T and Haro, W (1996) – "Geological map of Ethiopia (1:2,000,000)" - Ethiopian Institute of Geological Survey, Addis Ababa, Ethiopia.

Tiberi, C., Ebinger, C., Ballu, V., Stuart, G. and Befekadu O. (2005) - "Inverse models of gravity data from the Red Sea-Aden-East African rifts triple junction zone" - Geophys. J. Int., 163, 775-787.

Tommasi, A. and Vauchez, A. (2001) - "Continental rifting parallel to ancient collisional belts: an effect of the mechanical anisotropy of the lithospheric mantle" - EPSL, 185, 199–210.

Tsige, L. and Hailu, E. (2007) – "Geological Map of Bure" – EIGS.

Ukstins, I.A., Renne, P.R., Wolfenden, E., Baker, J., Ayalew, D. and Menzies, M. (2002) – "Matching conjugate volcanic rifted margins: 40Ar39Ar chrono-stratigraphy of pre and syn-rift bimodal flood volcanism in Ethiopia and Yemen" - Earth and Planetary Sciences Letters 198, 289–306.

USCGS (United States Coast and Geodetic Survey) (1963) - "1957–1961 Ethiopia Geodetic Survey, Blue Nile River Basin" - Washington, DC, 563 pp.

Weissel, J., Malinverno, A. and Harding, D. (1995) – “Erosional development of the Ethiopian Plateau of Northeast Africa from fractal analysis of topography” - In: Barton, C.C., Pointe, P.R. (Eds.) “Fractals in Petroleum Geology and Earth Processes” - Plenum Press, New York, pp. 127–142.

White, R.S. and McKenzie, D. (1989) - "Magmatism at rift zones: The generation of volcanic continental margins and flood basalts" - J. Geophys. Res., 94, 7685–7729.

WoldeGabriel, G., Aronson, J.L. and Walter, R.C. (1990) – “Geology, geochronology, and rift basin development in the central sector of the Main Ethiopia Rift” - Geological Society of America Bulletin 102, 439–458.

Wolfenden, E., Yirgu, G., Ebinger, C., Deino, A. and Ayalew, D. (2004) – “Evolution of the northern Main Ethiopian rift: Birth of a triple junction” - Earth and Planetary Science Letters, v. 224, 213–228, doi: 10.1016/j.epsl.2004.04.022.

Wolfenden, E., Ebinger, C., Yirgu, G., Renne, P. and Kelley, S.P. (2005) – “Evolution of the southern Red Sea rift: birth of a magmatic margin” - Geological Society of America Bulletin 117, 846–864.

Yirgu, G., Ayele, A. and Ayalew, D. (2006) - "Recent seismovolcanic crisis in northern Afar, Ethiopia" - EOS, Trans. Am. geophys. Un., 87, 325–336.

Zanettin, B. (1993) - "On the evolution of the Ethiopian volcanic province" - In: "Geology and Mineral Resources of Somalia and Surrounding Regions", Abbate, E. et al. (Eds.). Ist. Agron. Oltremare, Firenze, Relaz. Monogr. Agrar. Subtrop. Trop., Nuova Ser. 113, 279–310.

Zenebe, B. and Mariam, D.H. (2011) – “Geological Map of Yifag area” – EIGS.

Zumbo, V., Feraud, G., Bertrand, H., and Chazot, G. (1995) - "40Ar/39Ar chronology of the Tertiary magmatic activity in Southern Yemen during the early Red Sea-Aden rifting" - J. Volcanol. Geoth. Res. 65, 265–279.

CHAPTER 2*

THE INFLUENCE OF DEEP AND SURFACE PROCESSES ON THE EVOLUTION OF DRAINAGE SYSTEMS: THE EXAMPLE OF THE ETHIOPIAN PLATEAU

2.1 Introduction

Topography is the result of the complex interaction of deep and surface processes. This leaves a unique mark on the landscape and, in particular, on some topographic parameters mostly deduced from river network analysis such as local relief, drainage pattern, hypsometry, river longitudinal profiles, channel concavity and steepness, channel slope-basin area relationship (e.g., Wells et al., 1988; Pazzaglia et al., 1998; Wegmann and Pazzaglia, 2002; Tomkin et al., 2003; Molin et al., 2004; Lock et al., 2006; Wobus et al., 2006; Wegmann et al., 2007; Roy et al., 2009; Molin et al., 2011; Scotti et al., 2013). For this reason such parameters can be used to quantitatively characterize the feedback between crustal tectonics, mantle dynamics, and geomorphology (Molin et al., 2011).

Ethiopia is one of the best places to study the effects of mantle dynamics and surface processes on landscape evolution. The northwestern sector of Ethiopia is characterized by a huge basaltic plateau (Ethiopian Plateau or Highlands) which is part of the African Superswell, a wide region of anomalously high topography related to the rise of the Afar plume (Lithgow-Bertelloni and Silver, 1998; Davies, 1998; Ebinger and Sleep, 1998; George et al., 1998, Ritsema et al., 1999; Gurnis et al., 2000; Şengör, 2001; Nyblade, 2011; Faccenna et al., 2013).

Many works attempted to date the dynamic uplift due to the impingement of the plume at the base of the lithosphere. Early ones (Dainelli, 1943; Beydoun, 1960) proposed this uplift to be Upper Eocene in age and to precede both the flood basalt event and the main rifting episodes. Successively, many authors (Mohr, 1967; Baker et al., 1972; McDougall et al., 1975; Merla et al., 1979; Behre et al., 1987) suggested for a complex Tertiary history of uplift and volcanism.

Pik et al. (2003), based on thermochronological analysis on the Blue Nile drainage network, argued that erosion initiated in the Blue Nile canyon as early as 25–29 Ma and that the elevated plateau physiography existed since the Oligocene (20–30 Ma).

*** This chapter will be submitted as: Sembroni, A., Molin, P., Pazzaglia, F.J., Faccenna, C. and Giachetta, E. (2015) - "The influence of deep and surface processes on the evolution of drainage systems: the example of the Ethiopian Plateau".**

A more recent study on the incision of the 1.6-km-deep Gorge of the Nile (Gani et al., 2007) suggests that the uplift of ~2 km occurred episodically in three different phases since 29 Ma: a slow and steady uplift between 29 and 10 Ma (phase I), an increased uplift at 10 Ma (phase II) and a further dramatic uplift at 6 Ma (phase III).

Ismail and Abdelsalam (2012) carried out a quantitative analysis on Ethiopian Plateau drainage system finding that the evolution of these drainage systems was influenced by three tectonic and geological events: (1) the uplift of the plateau caused by the rising of the Afar plume at 30 Ma; (2) the shield volcanoes build-up event at 22 Ma; (3) the rift-flank uplift on the western escarpments of the Afar Depression and the MER.

Despite these works several questions are still open. Poor efforts have been made in understanding the influence of mantle dynamic on the evolution of topography and drainage system in this area. No convergence exists on the Ethiopian Plateau dynamic topography model. The most comprehensive study of topography evolution comes from Gani et al. (2007). However in such work the response of fluvial systems to uplift is not fully investigated. In this respect we analyzed the Blue Nile and Tekeze basins which drain respectively the southern and northern portions of the plateau. In particular we investigated the general topographic features (filtered topography, swath profiles, local relief) and the river network (rivers longitudinal profiles and hypsometric curves). Moreover, in order to model steady vs unsteady base level fall and to test the central hypothesis of the Gani et al. (2007) paper, a knickpoint celerity model has been performed. The results permitted us to develop a conceptual model for the long-term evolution of the Ethiopian Plateau drainage system since Oligocene unraveling the influence of tectonics on the main rivers courses.

2.2 Geological setting

Northwestern Ethiopia is characterized by a folded and foliated basement rocks which are part of the Arabian-Nubian Shield (Stern, 1994). This basement is overlain by a thick sub-horizontal alternation of continental (sandstones) and marine sediments (limestones and shales) deposited between Triassic and Cretaceous and separated by regional unconformity (**Fig.11b**) (Blanford, 1869; Dainelli and Marinelli, 1912; Dainelli, 1943; Merla and Minucci, 1938; Levitte, 1970, Dow et al., 1971; Beyth, 1972a, b; Merla et al., 1979; Bosellini et al., 1997).

In the Eocene and Late Oligocene the area was affected by intense magmatic activity which led to the emplacement of continental flood basalts (Trap series). In the Eocene (45 Ma) the activity was

mostly centered in southern Ethiopia (Davidson and Rex, 1980; Ebinger et al., 1993; George et al., 1998) but successively it moves more to the north. In Oligocene and Early Miocene (Baker et al., 1996a; Hofman et al., 1997; Pik et al., 1998; Ukstins et al., 2002; Coulié et al., 2003) the so-called Ethiopian-Yemen flood basalt covered a total area of at least 600000 km^2 with a thickness varying from 500 to 1500m (Mohr and Zanettin, 1988). In particular the southern and central sectors of the Ethiopian Plateau (Blue Nile R. basin) present basalts thickness ranging from 500 m (medium and lower portions of Blue Nile R. basin) up to 2000 (Lake Tana region). On the other hand the northern sector (Tekeze R. basin) is characterized by a lower basalts thickness values (mostly less than 1000 m).

The trap eruption was concomitant with the onset of the Red Sea-Gulf of Aden continental rift systems (29 Ma; Wolfenden et al., 2005), but predates the development of the Main Ethiopian Rift (MER, Middle-Late Miocene; Wolfeden et al., 2004; Bonini et al., 2005). The Ethiopian flood basalts have been attributed to melting associated with the activity of one (Afar plume) or two (Afar and East African or Kenyan plumes) mantle plumes impinging the base of the continental lithosphere (e.g., Ebinger and Sleep, 1998; George et al., 1998).

The outpouring of the Oligocene Trap basalts was interrupted by a period of quiescence (29-27 Ma) marked by the deposition of continental sediments (intertrappean beds) (Abbate et al., 2014). They outcrop all over the Ethiopian Plateau and consist of fluvio-lacustrine deposits a few tens of meters thick (Abbate et al., 2014).

Immediately after the peak of flood basalt emplacement, several shield volcanoes developed from 30 Ma to about 10 Ma (Kieffer et al., 2004) rising 1000–2000 m above the top of the basaltic plateau (Mohr and Zanettin, 1988; Kieffer et al., 2004).

Since late Pliocene magmatic and tectonic activities moved mainly into the axial sector of the MER and in the Afar depression even though, in Quaternary time, some volcanic episodes occurred on the plateau (south of the Lake Tana; see **Fig.11b**) forming small tuff cones and basaltic lava flows (Chorowicz et al., 1994; Bonini et al., 1997; Wolfenden et al., 2004; Ebinger, 2005; Kendall et al., 2005; Corti, 2008; Corti, 2009).

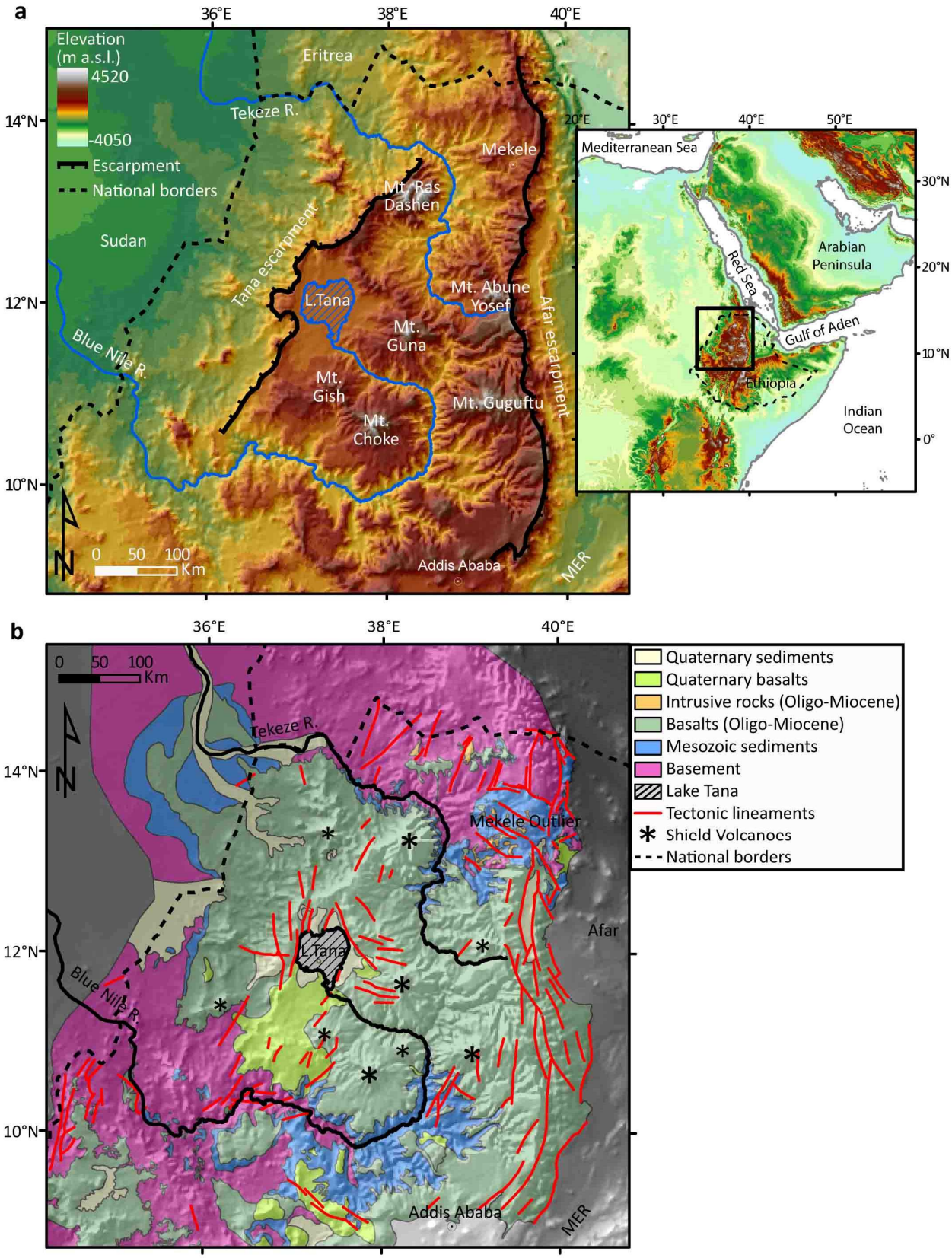

Figure 11 - a) Topography of the Ethiopian Plateau area (ETOPO1 DEM with a resolution of around 2000 m). The black box in the inset indicates the location of the study area and the Ethiopian national boundaries; **b)** geological map of the study area compiled from the 1:2.000.000 (Tefera et al., 1996) and the available 1:250.000 scale maps (Hailu, 1975; Kazmin, 1976; Garland, 1980; Tsige and Hailu, 2007; Chumburo, 2009; Zenebe and Mariam, 2011) of Ethiopia draped over the shaded topography.

2.3 Geomorphology

The Ethiopian Highlands are mostly characterized by a flat or gently rolling topography standing at an elevation of more than 2500 m a.s.l. (**Fig.12a**). Locally, huge shield volcanoes rise 1000-2000 m above the average plateau elevation (Mt. Ras Dashen 4550 m a.s.l. (**Fig.12b**); Mt. Guna 4231 m a.s.l.; Mt. Abune Yosef 4190 m a.s.l.; Mt. Choke 4100 m a.s.l.; Mt. Guguftu 3975 m a.s.l.; see **Fig.11a**).

The fluvial incision is limited except where the main rivers (like Blue Nile, Tekeze rivers) formed valleys up to 1500 m deep and 70 km wide flowing from the plateau (2500 m a.s.l.) to the Sudan lowlands (500 m a.s.l.). Here extensive areas of fan deposits represent significant long-term sediment sinks (Woodward et al., 2007). Such large volume of sediment deposition along the main course of the Nile caused, during the Late Pleistocene, the formation of a lake (Lawson, 1927; Ball, 1939; Salama, 1987; Williams et al., 2003; Barrows et al., 2014) as far north as 15°N, with a length of 650 km, a maximum width of 80 km, a maximum depth of ~12 m, and an area of 45,000 km^2 (Barrows et al., 2014).

The general flat morphology of the Ethiopian Highlands is strongly related to the underlying geological setting (**Fig.11b**). Regional subhorizontal unconformities characterize the Precambrian basement and Mesozoic rocks whereas the Mesozoic marine deposits and Tertiary flood basalts present almost flat top surfaces (**Figs.13c-d**).

The Ethiopian plateau is bordered by two huge escarpments: the rift western margin to the east and the Tana escarpment to the west (**Fig.11a**). While the rift escarpment is due mainly to the border faults displacements and to the flexural uplift caused by the tectonic activity of the rift system (Weissel et al., 1995), the Lake Tana escarpment appears to be only the result of erosional escarpment retreat into the plateau, in response to a base level determined by the Nile axial valley (Grabham and Black, 1925; Minucci, 1938b; Dainelli, 1943; Comucci, 1950; Jepsen and Athearn, 1961; Mohr, 1967; Hahn et al., 1977; Chorowicz et al., 1998; Gani et al., 2008).

The Blue Nile R. has a total length of 1,450 km (from the Lake Tana to the confluence with the White Nile), 800 km of which are in Ethiopia. It flows from the Lake Tana, with a NW-SE direction, than it turns around the Mt. Choke assuming a WNW-ESE trend. Before the junction with Didessa R. the trend is NE-SW becoming SE-NW in the Sudan lowlands.

a

b

Figure 12 - a) Panoramic view of the plateau landscape; **b)** Mt. Ras Dashen (4520 m a.s.l.) (Simien National Park).

Lake Tana formed since volcanic activity blocked the outlet of a number of rivers in the early Pliocene ~5 million years ago (Mohr, 1962). In the Pleistocene, this basin, before the present connection with the Blue Nile R., was alternatively open and closed because of climate variations (Lamb et al., 2007) and widespread volcanic activity (Grabham and Black, 1925; Minucci, 1938b; Jepsen and Athearn, 1961).

The Tekeze R. is 608 km long and originates from the eastern side of Mt. Abune Yosef, an Oligocene volcano located at the rift shoulder, northeastern sector of the Ethiopian plateau. It flows from its source to the W, then it turns around the Ras Dashen volcano (Simien Mts.) assuming a S-N direction and reaches the Sudan lowlands with an ESE-WNW trend.

2.4 Methods and Results

To study the influence of surface and deep processes in the evolution of the Ethiopian Plateau hydrography, we performed a morphometric analysis on topographic features and river network. In particular the study area covers the medium-high sector of Blue Nile R. and Tekeze R. basins. The first one extends from the Lake Tana to the junction with Didessa R. (**Fig.13a**). The drainage basin has an area of 89000 km^2 and an elevation ranging between 4261 m (Guna volcano) and 650 m (Didessa R. junction); the mean elevation is 1796 m. The Tekeze R. basin sector includes the area between the Tekeze R. source (Mt. Abune Yosef) and the Ethiopia-Sudan border (**Fig.13b**); the drainage area is 69000 km^2 with an elevation ranging between 760 m (Sudan border) and 4517 m (Simien Mts.); the mean elevation is 1915 m.

2.4.1 Topography analysis

The main data source for the analysis of the study area topography is ETOPO1 global elevation model (www.ngdc.noaa.gov), which has a resolution of 1 arc-minute (~2 km). More in detail we produced maps of the local relief to investigate the spatial distribution of incision (**Figs.13e-f**), extracted three swath profiles cutting across different portions of the study area to show the variation of the regional topographic pattern (**Fig.14**), and elaborated a map of the topography smoothed at a long wavelength to capture regional features not directly evident from the raw DEM (**Fig.15**).

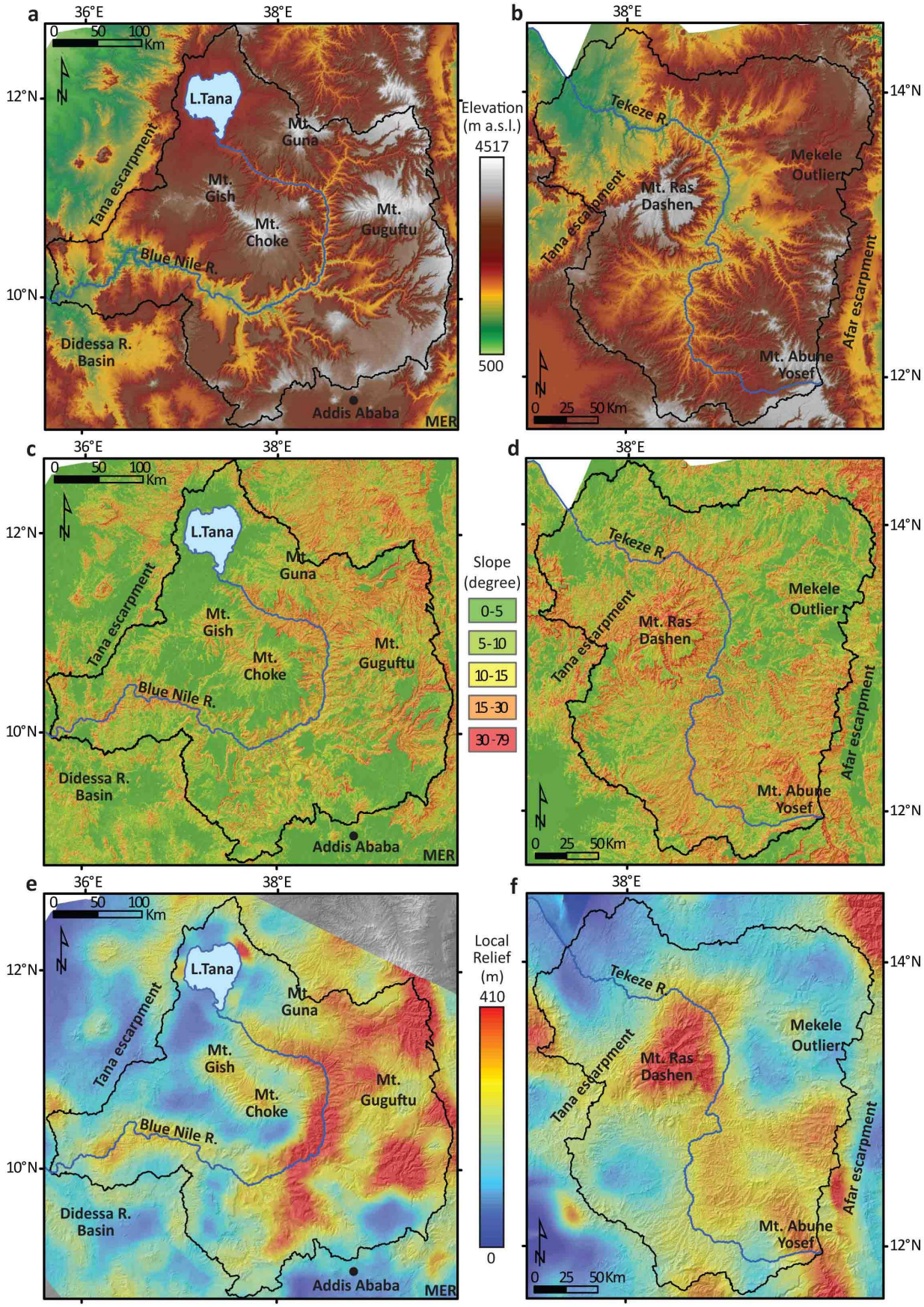
a
b
c
d
e
f
36°E
38°E
12°N
10°N
14°N
0 50 100 Km
0 25 50 Km
L.Tana
Mt. Guna
Mt. Gish
Mt. Choke
Mt. Guguftu
Tana escarpment
Blue Nile R.
Didessa R. Basin
Addis Ababa
MER
Tekeze R.
Mekele Outlier
Mt. Ras Dashen
Afar escarpment
Mt. Abune Yosef
Elevation (m a.s.l.)
4517
500
Slope (degree)
0-5
5-10
10-15
15-30
30-79
Local Relief (m)
410
0

Figure 13 - a-b) Topography of the Blue Nile R. and Tekeze R. basins (SRTM DEM database); **c**) slope map of the Blue Nile R. basin (SRTM DEM database). The slope pattern evidences the flat areas (plateau remnants) around the major volcanic edifices and bounded by valley flanks and escarpments; **d**) slope map of the Tekeze R. basin (SRTM DEM database). The plateau remnants are located all along the divide between Blue Nile R. and Tekeze R. basins. An exception is the Mekele Outlier characterized by an almost flat topography caused by tabular mesozoic sediments (Beyth, 1972a, b; Bosellini et al., 1997); **e-f**) local relief maps of the Blue Nile R. and Tekeze R. basins (see text for explanation). The values at the edges of both maps are overestimated because of the interpolation method. Note that the scales of Blue Nile R. and Tekeze R. basins are different.

2.4.1.1 Local relief distribution in the Ethiopian plateau

In order to have a general overview of the spatial variation in fluvial incision in the Ethiopian Plateau, we elaborated the maps of local relief of Blue Nile R. and Tekeze R. basins (**Figs.13e-f**). We produced them by subtracting arithmetically a subenevelope surface (that describes the general pattern of valley bottoms elevations) from an envelope surface (that connects peak elevations) (Molin et al., 2004). We obtained these surfaces by smoothing the maximum and minimum topography of the SRTM 90 m-pixel-size DEM by a 20 km-wide circular moving window. We chose the value of 20 km since it is the average of the main valley spacing. This allowed us to remove small valleys which would generate a noisy map that misses to show the regional-scale features.

In the local relief map of the Blue Nile R. basin (**Fig.13e**), the highest values of local relief are located in eastern half corresponding with the Blue Nile R. valley and with those portions of the plateau more deeply incised by the Blue Nile R. tributaries. Also the rift margin escarpment is characterized by high values. Medium/high local relief is located in correspondence with the Mt. Choke and Mt. Gish volcanoes, with the lower valley of Blue Nile R., where highly fractured and bended basement rocks crop out, and with the Lake Tana escarpment.

Low values (<150 m) of local relief mostly characterize the plateau around Mt. Choke and Mt. Gish volcanoes, close to Lake Tana, and the southern sector of the Blue Nile R. basin.

The local relief map of Tekeze R. basin (**Fig.13f**) has the highest values located in correspondence with the Simiens Mts. and with the southern rift margin escarpment. High/medium values are in the south-eastern sector of the basin, where Mt. Abune Yosef rises from remnants of the plateau. Values of local relief < 150 m are located in the south-western portion of the basin, in the most downstream portion and in correspondence with the so-called Mekele outlier. Here fractured sub-horizontal Mesozoic sediments intruded by dolerite sills and dikes crop out (**Figs.11b, 13f**).

2.4.1.2 Swath profiles

Swath profiles permit to view the pattern of maximum, minimum and mean topography of a landscape into a single plot (Isacks, 1992; Molin et al., 2004; Ponza et al., 2010). So, in order to study and quantify the general topographic trend of the Ethiopian Highlands we extracted by MatLab topotoolbox (Schwanghart and Kuhn, 2010) three swath profiles from the ETOPO1 DEM (**Fig.14**). Its ~2 km pixel-size is an acceptable resolution for such regional scale analysis. To produce the swath, we sampled topography every 2 km following observation windows 50 km-wide and with a varying length according to the area to be represented (**Fig.3a**).

Profile 1 (**Fig.14b**) is oriented W-E and crosses the lower and medium portions of the Tekeze R. basin up to the Afar depression; profile 2 (**Fig.14c**), trending W-E, extends from the Lake Tana escarpment to the Afar depression western margin passing through the Lake Tana basin and the most upstream part of the Tekeze basin; profile 3 (**Fig.14d**) is oriented NW-SE and cuts across the lower and medium sectors of the Blue Nile basinup to the Ogaden basin.

The three swath profiles describe the topography of Blue Nile and Tekeze basins, evidencing the main features of the plateau.

Profile 1 describes the northern portion of the Tekeze basin. Here the maximum topography is characterized by plateau remnants (up to 2000 m) to the west, by the northernmost portion of the Simien Mts. and by the the Afar escarpment that almost reaches 3000 m of elevation. The mean and minimum topographies indicate a regularly decreasing regional slope from the rift margin to the western lowlands. Just the westernmost remnants of the plateau disrupt the trend.

Profile 2 shows the high-standing plateau bordered by the Tana and the rift escarpments. While the last is determined mainly by the tectonic activity of the Afar-MER rift system, the Tana escarpment development and retreat is mainly bounded by the fluvial erosion occurring at the Ethiopia-Sudan border where the drainage system carved hundreds of meters of flood basalts (Grabham and Black, 1925; Minucci, 1938b; Dainelli, 1943; Camucci, 1950; Jepsen and Athearn, 1961; Mohr, 1967; Hahn et al., 1977; Chorowicz et al., 1998; Gani et al., 2008).

Profile 3 cuts across the Blue Nile basin showing a very dissected topography with deep valleys and high volcanoes. The deepest (more than 1000 m) gorges correspond with the Blue Nile R. valley. The maximum topography pattern evidences the flat areas of the Ethiopian plateau standing at ~2500 m a.s.l. From this surface many volcanoes rises up to more than 3000 m. To the west, the Tana escarpment borders the highlands, whereas to the east the MER margin abruptly

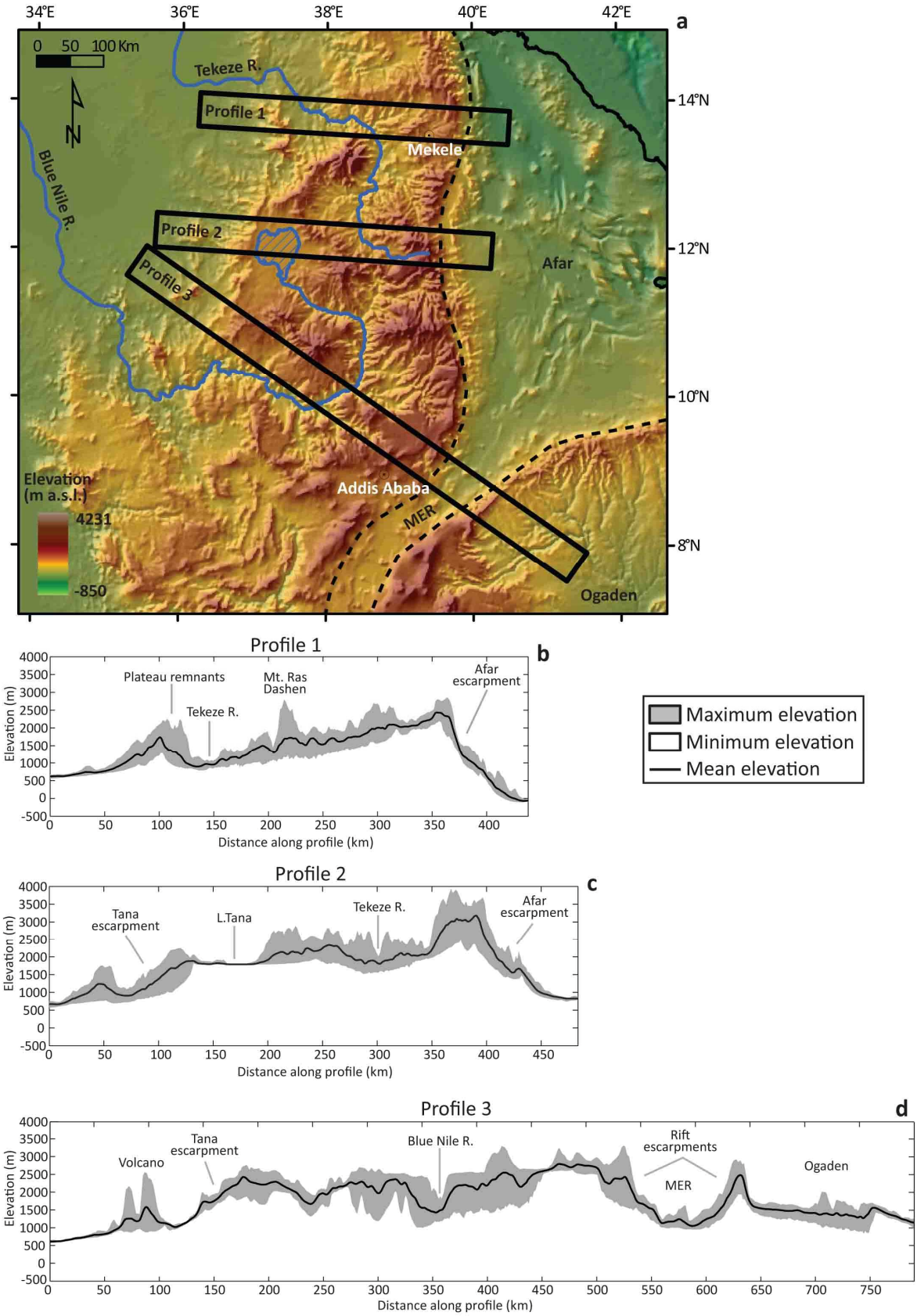

Figure 14 - a) ETOPO1 DEM of the study area and locations of the three swath profiles; **b-c-d**) swath profiles showing the trends of the maximum, minimum and mean topography of the Ethiopian Plateau.

interrupts the plateau. Beyond the eastern rift margin, topography decreases progressively to the SE.

Both profiles 2 and 3 describe the dome-shaped topography of the Ethiopian highlands: the elevation decreases from a maximum of 300-3500 m to a minimum of 600-700 m along both sides. In profile 2 the dome is interrupted and broken by the Afar depression.

2.4.1.3 Filtered topography

To investigate the signal of the plume in the present topography of Ethiopia, we elaborated a map showing the regional topography without the high frequency features related to local tectonics (**Fig.15**). We smoothed the raw elevation data in frequency domain by a low pass filter to attenuate all local scale topographic signals possibly connected with shallow tectonic processes and isolate the regional one related to subcustal processes. Similar methods were previously used in areas such as Yellowstone and the Colorado Plateau (Wegmann et al., 2007; Roy et al., 2009) or such as Apennines and Carpathians (D'Agostino and McKenzie, 1999; Molin et al., 2004; Faccenna et al., 2011; Molin et al., 2011) to isolate mantle-related topographic features. Since the size of these topographic signal is dependent on intensity, scale and depth of the mantle processes that generate it (Braun, 2010), it is important to choose an appropriate filter wavelength (Molin et al., 2011).

Considering the topographic pattern of Ethiopia, we used a circular low-pass filter with a wavelength of 250 km to eliminate the signals of the large shield volcanoes, of the MER/Afar depressions and of wide valleys such as Blue Nile and Tekeze rivers ones.

The resulting map (**Fig.15**) shows a large dome-shape topography centered in the Addis Ababa region. The elevation ranges between 0 m a.s.l. (in the Sudanese and Somalian plains) and 1500 m a.s.l. in the Addis Ababa topographic high. Several tomographic studies in the same area demonstrated the presence of a huge low velocity anomaly interpreted as upwelling of hot astenospheric material from the core-mantle boundary (Afar plume) (Lithgow-Bertelloni and Silver, 1998; Davies, 1998; Ebinger and Sleep, 1998; Ritsema et al., 1999; Gurnis et al., 2000; Nyblade et al., 2000; Ritsema and van Heijst, 2000; Montagner et al., 2007; Bastow et al., 2008; 2011; Mucha and Forte, 2011; Nyblade, 2011; Faccenna et al., 2013; Hansen and Nyblade, 2013).

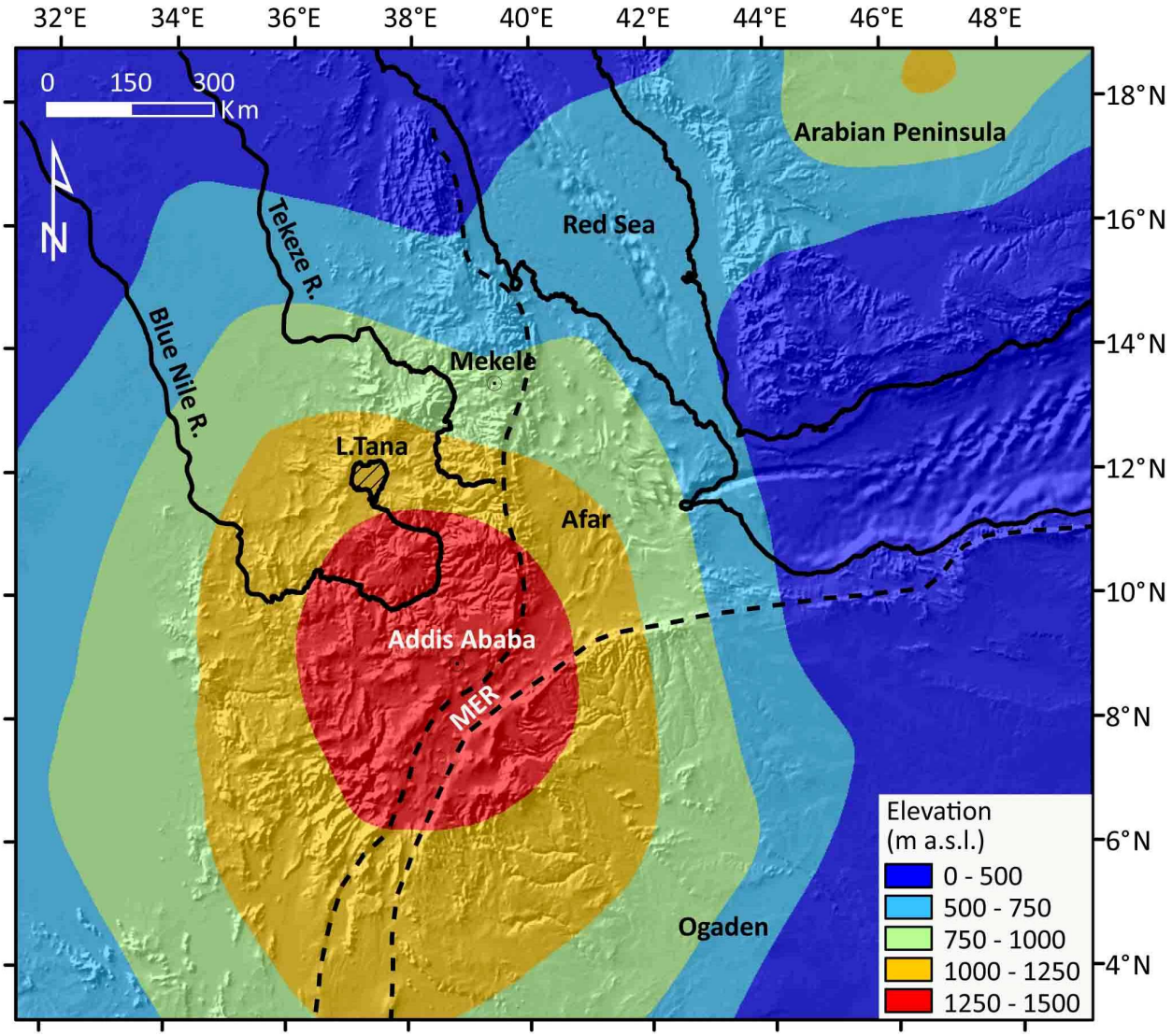

Figure 15 - Topography of the study area filtered at a wave length of 200 km. The locations of the Lake Tana, the rift borders (dashed black lines) and the coast line (solid black lines) are shown for reference.

2.4.2 Drainage network analysis

2.4.2.1 Hypsometry

The hypsometric curve represents the relative amount of the basin area below (or above) a given height (Strahler, 1952) and measures the percentage of landscape that has been fully integrated into the fluvial system and lowered to base level. Hurtez et al. (1999) used it as an indicator for the relative dominance of fluvial erosion or hillslope processes in landscape evolution. Hypsometry is sensitive to various forcing factors, which are scale-dependent, such as tectonics, lithology and climate (Hurtrez et al., 1999; Chen et al., 2003).

For the Ethiopian Plateau we analyzed the whole Blue Nile R. and Tekeze R. basins (**Figs.16a, 17a**) and 37 subbasins (18 in the Blue Nile R. basin [**Fig.16**] and 19 in the Tekeze R. one [**Fig.17**]). We

extracted the hypsometric curves from SRTM 90 m pixel size DEM by using the MatLab topotoolbox (Schwanghart and Kuhn, 2010). We also calculated the hypsometric integral (HI) as the area below the hypsometric curve. Its value varies from 0 to 1. Convex-up hypsometric curves (high HI values) are typically related to low relief uplands uplifted by tectonic, where fluvial incision and hillslope processes dominate (Hurtrez et al., 1999). S-shaped curves (concave upwards at high elevations and concave downwards at low elevations) characterize landscapes where fluvial erosion is both vertical and lateral and hillslope processes widely affect valley flanks. Concave-up shapes (low values of HI) are typical of landscapes characterized by wide valleys generated by rivers eroding laterally (Weissel et al., 1994; Moglen and Bras, 1995; Willgoose and Hancock, 1998; Hurtrez et al., 1999; Keller and Pinter, 2002; Huang and Niemann, 2006; Scotti et al., 2013).

2.4.2.1.1 Blue Nile basin

The Blue Nile R. basin geology is characterized mainly by Trap basalts and post-Trap volcanic deposits in the upper-medium portion. Mesozoic sediments and basement rocks outcrop along the medium and lower portion of the Blue Nile valley.

The hypsometric curve of the Blue Nile basin (**Fig.16a**) has a quite regular S shape (HI = 0.41) with a straight segment in the middle part disrupted by a small plateau around 0,7 of relative area.

The downstream right portion of Blue Nile basin is characterized mainly by flood basalts and Choke-Gish volcanoes products. Rivers draining Gish and Choke Mts. (15-16-17-18) show hypsometric curves with a concave part at high elevation corresponding with the plateau and the volcanoes that rise from it. The portion displaying the lower elevation of the basins, i.e. the sector of the basins located along the Blue Nile valley flank, is irregular (**Fig.16d**). HI ranges between 0.38 and 0.51 (**Table 1**).

The hypsometric curves of the rivers that flow across the Quaternary lava flows south of the Lake Tana (13-14) are almost straight, just slightly convex upward and steeper at lower elevation. HI values range between 0.38 and 0.56 (**Table 1**).

The downstream left portion of the Blue Nile basin has a varied geology since the Blue Nile R. and many of its tributaries incised into the basalts down to Mesozoic sediments and the basement. The basins 5-6-7-8-9-10 are mainly underlay by Trap basalts and Miocene-Pliocene volcanic deposits which overlay Mesozoic sediments that usually outcrop close to the confluence with the Blue Nile R.

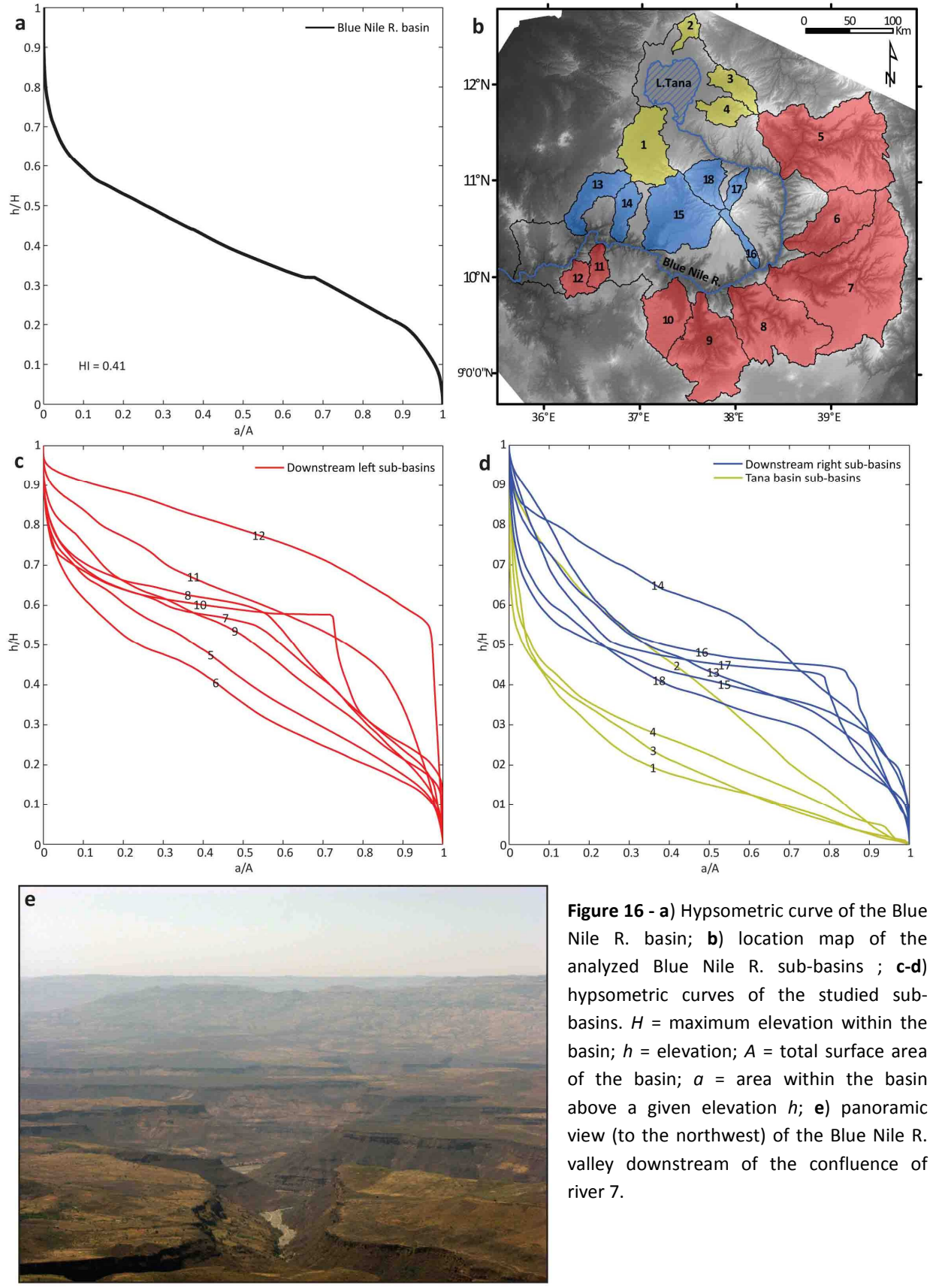

Figure 16 - a) Hypsometric curve of the Blue Nile R. basin; **b**) location map of the analyzed Blue Nile R. sub-basins ; **c-d**) hypsometric curves of the studied sub-basins. *H* = maximum elevation within the basin; *h* = elevation; *A* = total surface area of the basin; *a* = area within the basin above a given elevation *h*; **e**) panoramic view (to the northwest) of the Blue Nile R. valley downstream of the confluence of river 7.

The easternmost basins (5, 6, 7) have their headwaters on the rift shoulder. Basins 5 and 6 show similar hypsometric curve shape: an almost straight segment with a slight convexity in its middle

part. In the basin 7 curve this convexity is stronger so that the upper portion becomes concave (**Fig.16d**). This concave portion is coincident with the highstanding plateau. HI values range between 0.37 and 0.49 (**Table 1**).

The hypsometric curves of the rivers draining the southernmost sector (8-9-10) are similar to the previous ones (Fig. 6d): basins 8 and 10 curves show again an upstream concavity corresponding with the plateau. HI ranges between 0.49 and 0.53 (**Table 1**).

The lower basin is mainly characterized by the outcrop of basement rocks with some few basaltic remnants. Hypsometric curves (basins 11 and 12) show a convex upward shape with a very steep final segment (**Fig.16d**). HI values are 0.60 and 0.76 respectively (**Table 1**).

The inflows (basins 1-2-3-4) of Lake Tana basin have very concave hypsometric curves (**Fig.16d**) characterized by low values (from 0.18 to 0.24) of HI (**Table 1**). The only exception is basin 2 that has an almost straight curve (HI=0.38).

Table 1 - Hypsometric integrals of the analyzed Blue Nile R. sub-basins.

	TANA BASIN				DOWNSTREAM LEFT								DOWNSTREAM RIGHT					
SUB-BASINS	1	2	3	4	5	6	7	8	9	11	10	12	13	14	15	16	17	18
HI	0.18	0.38	0.20	0.24	0.42	0.37	0.50	0.52	0.49	0.60	0.53	0.76	0.45	0.56	0.42	0.51	0.46	0.38

2.4.2.1.2 Tekeze R. basin

The Tekeze basin geology mirrors the Blue Nile basin. The upper-medium part is characterized by Trap basalts and Simien - Abune Yosef volcanic deposits while the middle and lower portions are composed mainly by Mesozoic sediments and basement rocks with few Trap remnants.

The hypsometric curve of the whole basin has a regular S-shape (**Fig.17a**). HI value is 0.33.

The downstream left geology is characterized by flood basalts and Ras Dashen, Guna and Abune Yosef volcanoes deposits.

The curves of the downstream tributaries (8-9-10-11) show a very concave trend (**Fig.17c**) with low values of HI (0.24-0.27) (**Table 2**).

The curves of rivers draining the volcanoes reliefs of Guna and Simien Mts. (1-2-5-6-7) has almost straight curves with some irregularities in correspondence with plateau remnants at the bottom of volcanic edifices (**Fig.17c**). HI values range between 0.34 and 0.42 (**Table 2**).

The rivers located at the Tana - Tekeze divide (basins 3-4) present a general S shape. In particular curve 3 has an almost perfect S shape while curve 4 shows an upper convex part (**Fig.17c**).

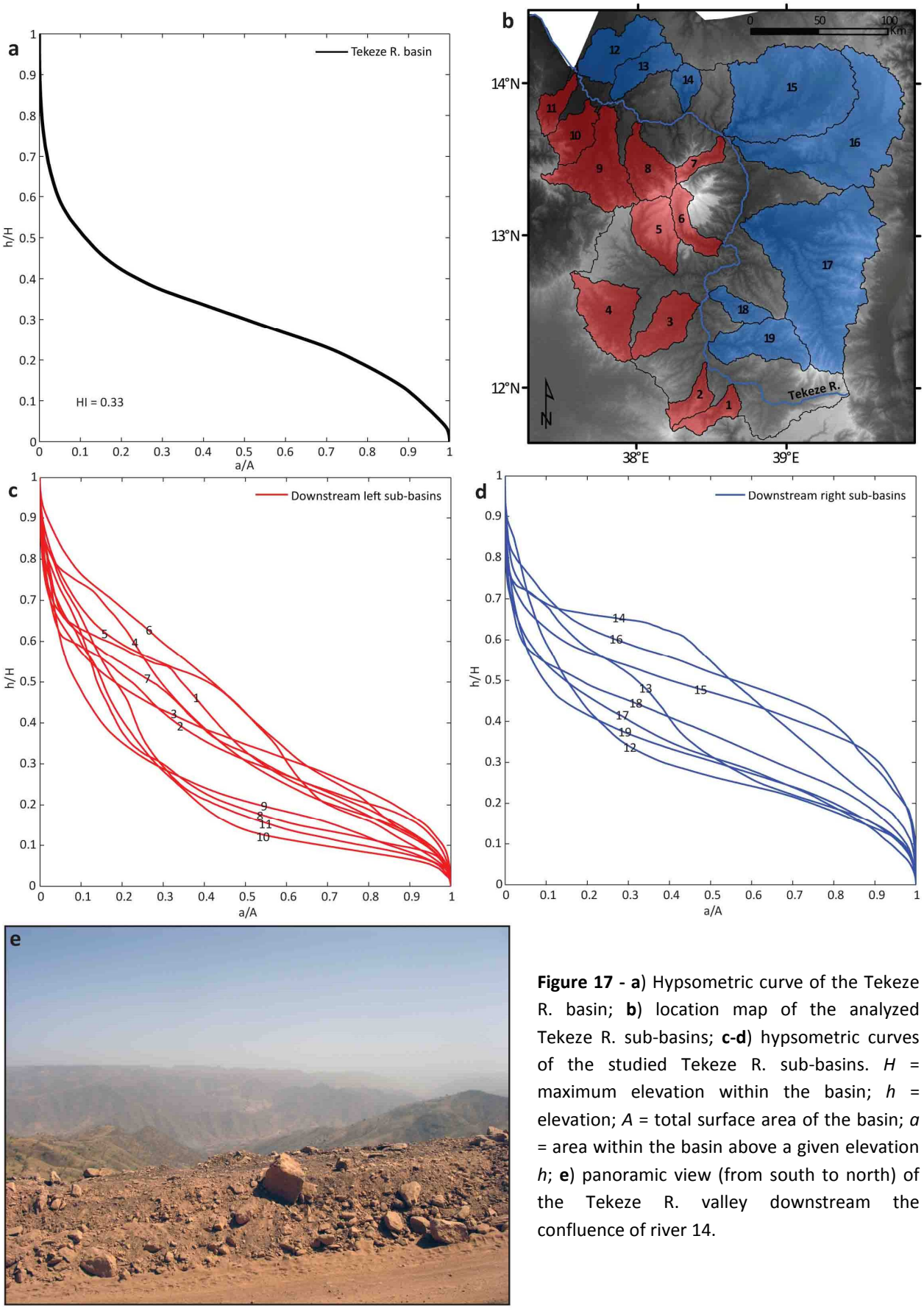

Figure 17 - a) Hypsometric curve of the Tekeze R. basin; **b**) location map of the analyzed Tekeze R. sub-basins; **c-d**) hypsometric curves of the studied Tekeze R. sub-basins. *H* = maximum elevation within the basin; *h* = elevation; *A* = total surface area of the basin; *a* = area within the basin above a given elevation *h*; **e**) panoramic view (from south to north) of the Tekeze R. valley downstream the confluence of river 14.

The hypsometric curves of the rivers on the downstream right are more regular despite the less homogeneous geologic configuration (**Fig.17d**). Indeed this portion of the basin is underlain by Trap in the very upper part, by Mesozoic sediment in the middle and by basement rocks in the lower part.

In the lower portion of the Tekeze R. basin, basin 12 has a very concave curve (HI=0.31), whereas basins 13 (HI=0.37) and 14 (HI=0.49) have a very irregular shape characterized by a convexity in their middle part (**Fig.17d; Table 2**). Their concave upper portion correspond with remnants of the plateau.

Basins 15 and 16, located in the NE sector and draining the so-called Mekele outlier, have a S-shape curve (**Fig.17d**) with relatively high value of HI (0.51 and 0.47) (**Table 2**) and with a steep final step.

The hypsometric curves of rivers draining the medium-high downstream right portion of Tekeze basin (17-18-19) have an almost perfect S-shape with small irregularities in the highest elevation part (**Fig.17d**) with HI ranging between 0.32-0.36 (**Table2**).

Table 2 - Hypsometric integrals of the analyzed Tekeze R. sub-basins.

	DOWNSTREAM LEFT											DOWNSTREAM RIGHT							
SUB-BASINS	1	2	3	4	5	6	7	8	9	10	11	12	13	14	15	16	17	18	19
HI	0.37	0.34	0.36	0.38	0.41	0.42	0.36	0.26	0.25	0.24	0.27	0.31	0.37	0.49	0.47	0.51	0.33	0.36	0.32

2.4.2.2 Stream longitudinal profiles

Steady state river channels have a smoothly concave-up shape quantified by the following power law relationship (Hack, 1957; Flint, 1974):

$$S = k_s A^{-\theta} \qquad (1)$$

where S is the slope, A is the drainage area, k_s is the steepness index, and θ is the concavity index (Hack, 1957; Flint, 1974). The steepness index has been shown to have a linear relationship with the uplift rate (e.g., Snyder et al., 2000; Kirby and Whipple, 2001; Wobus et al., 2006; Kirby et al., 2007). Moreover, under steady-state conditions, the θ value is expected to fall in a range between 0.4 and 0.6, normally ~0.45 (Tarboton et al., 1989; Whipple and Tucker, 1999; Snyder et al., 2000; Kirby and Whipple, 2001; Lague and Davy, 2003; Whipple, 2004; Wobus et al., 2006; Whipple et

al., 2007). Such effects can be modeled when the bedrock channel erosional process is assumed to be detachment-limited and proportional to stream power,

$$E = KA^m S^n \qquad (2)$$

where E is the rate of bedrock erosion, K is a dimensional resistance to erosion (whose dimensions are dependent on the values of m and n) that combines the effects of lithology, climate, and sediment load, A is drainage area, S is channel slope, and m and n are positive non-dimensional constants that reflect basin hydrology, hydraulic geometry, and erosion process (Berlin and Anderson, 2007).

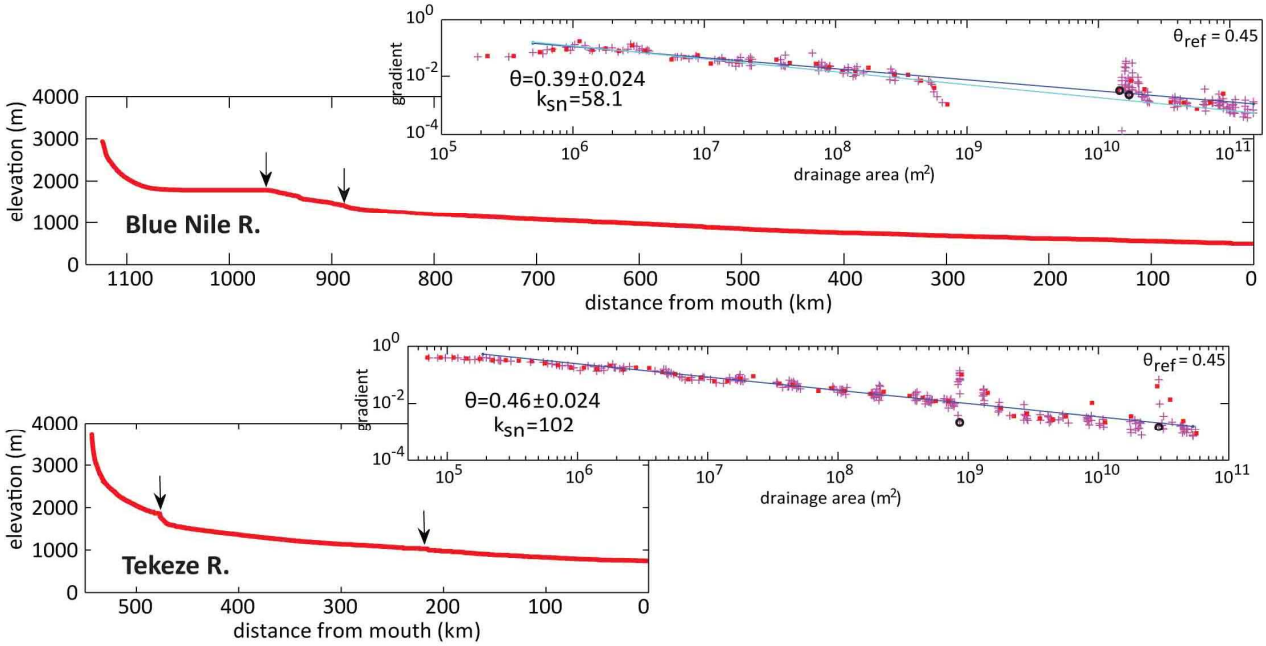

Figure 18 - Longitudinal profiles of Blue Nile and Tekeze rivers. Each plot consists of two diagrams: elevation vs. distance (longitudinal profile) and log gradient vs. log drainage area. The black arrows indicate the locations of the major knickpoints. The dark blue and cyan lines are the profiles predicted by the regressed channel concavity θ and by the specified reference concavity θ_{ref} = 0.45, respectively. Red squares are log-bin averages of the slope-area data (Wobus et al., 2007).

Adopting the SRTM DEM as digital data source, we investigated the Blue Nile R. and Tekeze R. basins analyzing the two main river courses (**Fig.18**) and 63 tributaries (34 in the Blue Nile R. basin [**Fig.19**] and 29 in the Tekeze R. one [**Fig.20**]). For each river we performed a quantitative morphometric analysis by using the Stream Profiler tool (http://www.geomorphtools.org) developed by Whipple et al. (2007). We extracted river longitudinal profiles and calculated the concavity (θ) and steepness (k_{sn}) indices (**Tables 3, 4**). Such indices represent respectively the slope

and y-intercept of the regression line drawn in the gradient vs drainage area in log-log plots (Fig.18). Since θ and k_s are autocorrelated, we normalized the steepness index by a reference concavity θ_{ref} = 0.45 (e.g. Wobus et al., 2006). This permitted us to compare river longitudinal profiles despite of drainage area differences.

2.4.2.2.1 Blue Nile R. basin

The Blue Nile longitudinal profile is concave-up, but its shape is very irregular and composed of three segments separated by two main knickpoints. The uppermost one is concave and includes Lake Tana. Downstream it is bounded by a knickpoint (at about 1800 m a.s.l.) corresponding with Tis Issat waterfalls (45 m high). The second segment is almost straight and bounded by a knickpoint at about 1500 m a.s.l. The lowermost part of the river profile is characterized by minor knickpoints (Fig.18a).

Rivers	θ	θ error	ksn
1	0.44	0.045	64.1
2	0.32	0.087	91.6
3	0.51	0.069	99.6
4	0.38	0.033	102
5	0.44	0.023	96.4
6	0.46	0.11	120
7	0.43	0.021	72.2
8	0.49	0.031	161
9	0.37	0.041	135
10	0.38	0.041	92.2
11	0.43	0.02	76.7
12	0.44	0.037	103
13	0.41	0.03	83.8
14	0.4	0.063	103
15	0.38	0.16	103
16	0.16	0.12	66.5
17	0.25	0.14	103
18	0.24	0.2	105
19	0.36	0.092	115
20	0.31	0.046	109
21	0.09	0.076	51.4
22	0.022	0.088	79.7
23	-0.36	0.14	94.5
24	0.29	0.046	71.1
25	0.16	0.052	66.2
26	0.26	0.04	88.3
27	0.28	0.047	109
28	0.19	0.056	113
29	0.13	0.072	109
30	0.38	0.047	143
31	0.18	0.075	123
32	0.26	0.045	99.9
33	0.52	0.065	53.1
34	0.42	0.052	43.6

Table 3 - Concavity and steepness indices of the studied Blue Nile R. tributaries.

The θ values of the Blue Nile R. tributaries (Fig. 8) range between 0.1 and 0.6 with a mean value of 0.36 (Table 3). Most of the values is lower than the reference concavity (θ_{ref} = 0.45) traditionally referred to an equilibrium profile (Tarboton et al., 1989; Snyder et al., 2000; Kirby and Whipple, 2001; Lague and Davy, 2003; Whipple, 2004; Wobus et al., 2006; Whipple et al., 2007). In general, the θ values decrease from north to south, i.e. from the upper to the lower portion of the basin (Fig.19b).

The values of k_{sn} range between 40 and 160 (Table 3). The higher values (>110) mostly correspond with rivers draining the Choke (27-28-29-30-31) and Guguftu (8-9) volcanoes (Fig.18). Excluding these values related to the higher elevation of river sources, the mean value of 100 is referred to the other tributaries.

In order to find correlation or groups among the data we plotted θ vs k_{sn} (Fig.19d). Although this plot is apparently

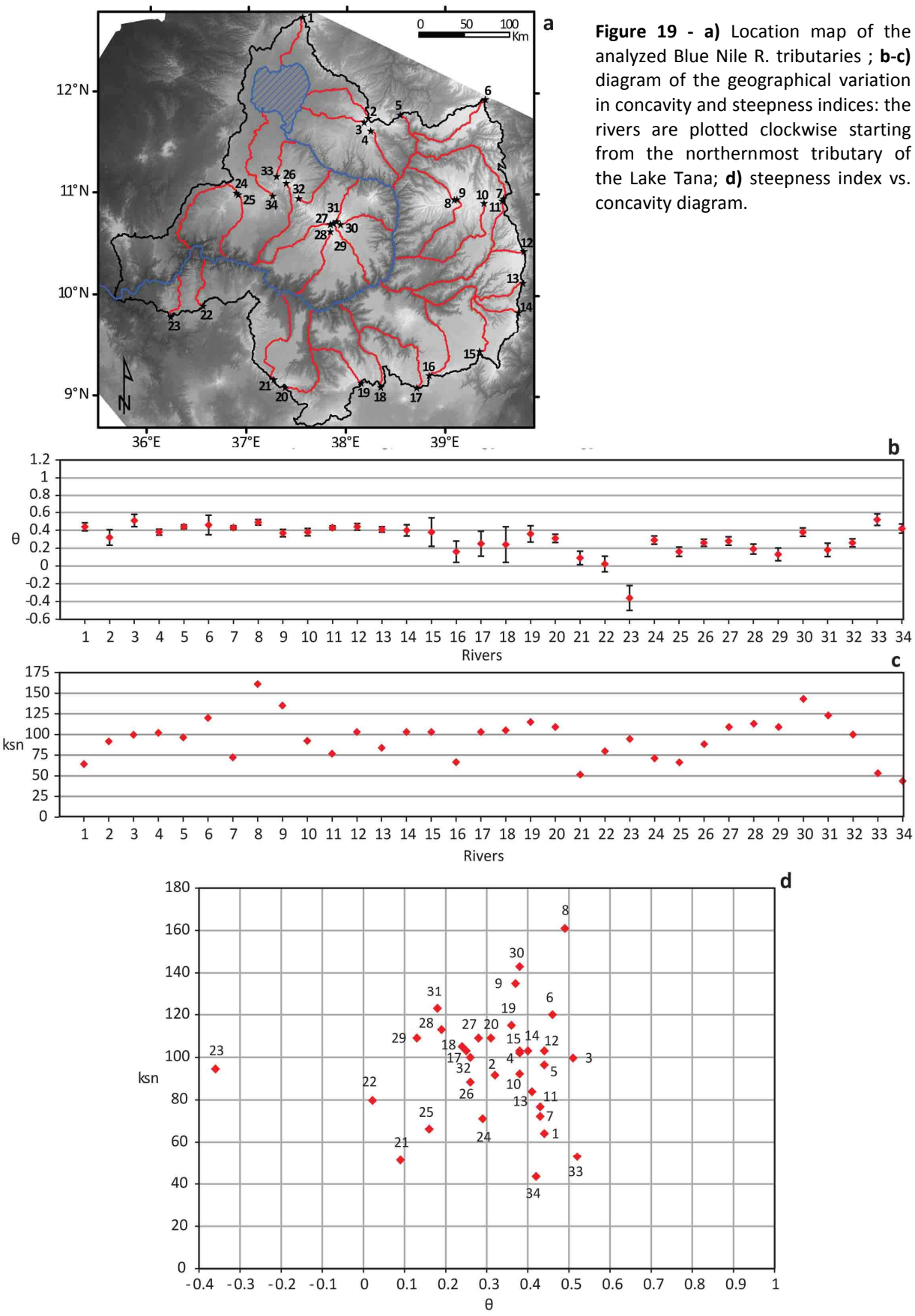

Figure 19 - a) Location map of the analyzed Blue Nile R. tributaries ; **b-c)** diagram of the geographical variation in concavity and steepness indices: the rivers are plotted clockwise starting from the northernmost tributary of the Lake Tana; **d)** steepness index vs. concavity diagram.

chaotic, it shows how the data are grouped according to their location in the basin.

Rivers draining volcanic reliefs (2-3-4-8-9-10-27-28-29-30-31) show the highest k_{sn} values (>88) and a wide θ range (0.13 – 0.52).

Lake Tana inflows (1-2-3-34) have low k_{sn} values (43.6 - 99.6) and θ close to the reference value (0.32<θ<0.52).

Rivers draining the rift shoulder (12-13-14-15) have medium-high k_{sn} values (70-120) and θ very close to θ_{ref} (0.38-0.46).

In the Addis Ababa region rivers 16-17-18-19 have values of concavity ranging between 0.16-0.36 and values k_{sn} that are higher than 65. All these rivers rise from the high basaltic plateau remnants (~2500 m a.s.l.) and have the junctions with Blue Nile R. in the Mesozoic sediments with a drop in elevation of more than 1000 m.

Rivers flowing on Quaternary lava flow (24-25) show very low k_{sn} and θ values (ks≈70, 0.15<θ<0.3).

The downstream tributaries of Blue Nile R. (21-22-23) have k_{sn} values ≤95 and the lowest θ values (<0,1) of the whole Blue Nile R. basin.

2.4.2.2.2 Tekeze R. basin

The Tekeze R. longitudinal profile shows a concave-up shape characterized by two major knickpoints. The one downstream is immediately upstream the Tekeze dam, whose construction finished in 2009. The upstream knickpoint, located at an elevation of 1900 m a.s.l., separates the river profile into two segments: the upstream reach is concave-up whereas the downstream one is almost straight. The values of the concavity index (θ = 0.46 ± 0.024) is very close to the reference value (θ_{ref} = 0.45). The steepness index (k_{sn}) is 102 (**Fig.18b**).

We calculated also the concavity and steepness indices of the Tekeze R. tributaries (**Table 4**; **Fig.20**). In the downstream left of the lower basin, rivers 14-15-16 drain the northern continuation of Tana escarpment where basalts are the dominant outcropping rock-type. The difference in elevation between the Tekeze R. as base level and the heads of the tributaries is ~1500 m. The ranges of θ and k_{sn} are 0.62-0.70 and 83.4-105 (**Table 4**) These values of both indices are traditionally referred to bedrock channels draining an homogeneous bedrock experiencing uniform (or close to uniform) rock uplift (Whipple, 2004).

In the downstream right of the lower basin, rivers 17-18-19 flow mainly on Triassic sandstones which unconformally overlie the metamorphic basement. Here the topography is smoother than

the left side one with a maximum difference in elevation between tributaries heads and Tekeze R. of ~500 m. The θ and k_{sn} ranges are 0.31-0.41 and 39.7-62.3 respectively.

The profile concavity (0.33-0.51; **Table 4**) of the rivers draining the principal volcanoes (Simien Mts., rivers 10-11-12-12; Mt. Guna, rivers 1-2; Mt. Abune Yosef, rivers 27-28-29) are close to the θ_{ref}. The values of their k_{sn} are higher than 100 (**Table 4**).

In the eastern sector of Tekeze basin, rivers 23-24-25-26 drain the rift shoulder. Their values of θ are relatively low (0.15-0.27) whereas k_{sn} ranges between 48.5 and 98.1 (**Table 4**).

The southwestern sector of the basin is characterized only by the outcrop of thick flood basalts. Rivers 3-4-5-6-7-8-9 rise from plateau remnants and the high and narrow Tana-Tekeze divide. The profiles of rivers 6-7-8-9 draining the most elevated part of the divide present θ and k_{sn} ranges similar to the ones of Lake Tana inflows ($0.47<\theta<0.58$; $60.1<k_{sn}<84$). More to the southeast along the divide the profiles of rivers 3-4-5 show very low values of both concavity and steepness indices ($0.15<\theta<0.26$; $48.2<k_{sn}<68.7$; **Table 4**).

Rivers	θ	θ error	ksn
1	0.33	0.055	117
2	0.39	0.093	109
3	0.15	0.035	68.7
4	0.26	0.027	65.3
5	0.16	0.056	48.2
6	0.58	0.096	60.1
7	0.47	0.034	63.3
8	0.54	0.046	78
9	0.51	0.075	84
10	0.5	0.018	148
11	0.33	0.046	156
12	0.38	0.02	170
13	0.46	0.024	172
14	0.62	0.026	105
15	0.67	0.023	83.4
16	0.7	0.076	91.9
17	0.41	0.03	39.7
18	0.34	0.086	61.3
19	0.31	0.077	62.3
20	0.12	0.075	59.2
21	0.39	0.026	67.8
22	0.39	0.038	66.8
23	0.19	0.095	48.5
24	0.27	0.065	88.9
25	0.2	0.084	98.1
26	0.15	0.07	63.5
27	0.49	0.02	121
28	0.51	0.029	81.2
29	0.51	0.02	110

Table 4 - Concavity and steepness indices of the studied Tekeze R. tributaries.

The plot θ vs k_{sn} (**Fig.20d**) permits to identify groups of rivers that drain the upper, medium and lower portions of the Tekeze R. basin and the Simien Mts.

The rivers that drain the upper portion of the basin have values of concavity ($0.35<\theta<0.55$) close to the values of 0.45, traditionally referred to an equilibrium profile (Tarboton et al., 1989; Whipple and Tucker, 1999; Snyder et al., 2000; Kirby and Whipple, 2001; Lague and Davy, 2003; Whipple, 2004; Wobus et al., 2006; Whipple et al., 2007), and steepness index ranging between 60 and 120. In the middle portion, rivers, that drain the uplifting rift shoulder, have in general low values of concavity ($0.1<\theta<0.3$) and steepness indices between 50 and 100. An exception is the group of rivers draining the Simien Mts. and the underlying plateau: they are more concave ($0.38<\theta<0.5$) and steeper ($148< k_{sn}<172$) (**Table 4**). On the downstream right rivers draining the Mesozoic sediments (sandstone, limestone, shale) of the Mekele

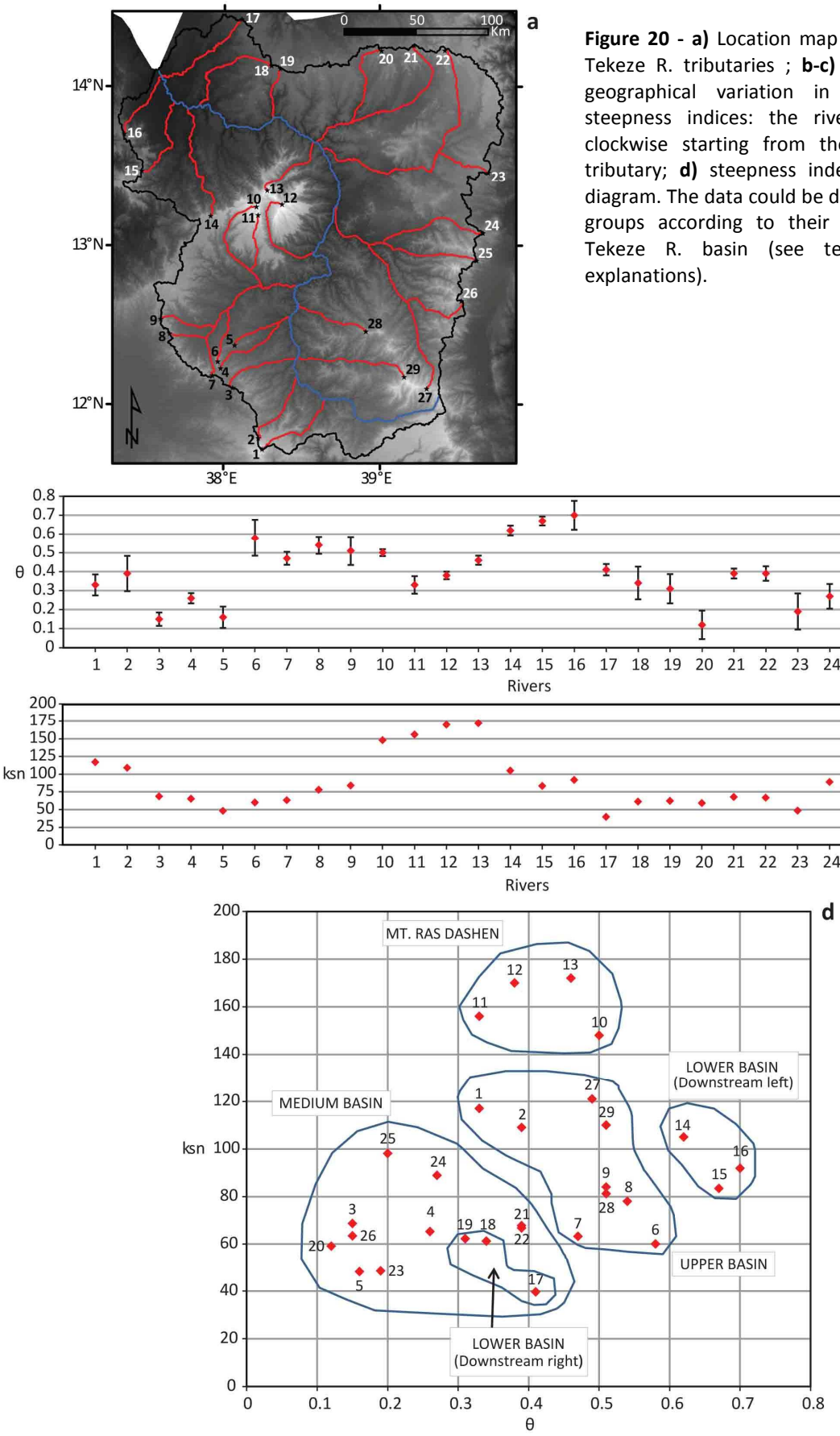

Figure 20 - a) Location map of the analyzed Tekeze R. tributaries ; **b-c)** diagram of the geographical variation in concavity and steepness indices: the rivers are plotted clockwise starting from the southernmost tributary; **d)** steepness index vs. concavity diagram. The data could be divide up into five groups according to their location in the Tekeze R. basin (see text for further explanations).

outlier (rivers 22-23) are less concave (0.39 and 0.19), and less steep (66.8 and 48.5) (**Table 4**).

In the lower basin, rivers form two groups: on the downstream left, rivers rising from the Tana escarpment (>2000 m a.s.l) present high concavity and steepness indices ($0.6<\theta<0.7$, $80<k_{sn}<105$); on the downstream right rivers flow across a low elevated landscape (<1100 m a.s.l.) and are less concave and less steep ($0.3<\theta<0.4$, $40<k_{sn}<65$).

2.4.2.2.3 k_{sn} vs. local relief analysis

In **figure 21** the values of k_{sn} and local relief of both Blue Nile and Tekeze rivers subbasins have been plotted. The relief is a proxy of erosion while the steepness index has been shown to have a linear relationship with the uplift rate (e.g., Snyder et al., 2000; Kirby and Whipple, 2001; Wobus et al., 2006; Kirby et al., 2007). In this respect such plots permit to envise the influence of uplift on the present topographic configuration of the area. Except for the subbasins draining the volcanoes (15-16-17-18 in the Blue Nile R. basin and 5-6-7 in the Tekeze R. basin) in both plots the points characterized by high values of both k_{sn} and local relief (5-6-7-8-9 in the Blue Nile R. basin and 17-19 in the Tekeze R. basin) coincide with the subbasins draining the eastern sector of the Blue Nile and Tekeze rivers basins (rift shoulder). Such subbasins present increasing values of k_{sn} and local relief from north ($2500<relief<3100$; $100<k_{sn}<120$) to south ($2436<relief<3300$; $100<k_{sn}<140$). Exceptions are the subbasins 15 and 16 (Tekeze R. basin) which present low k_{sn} even if they drain the northernmost sector of rift shoulder.

2.4.3 Maps of the along-channel variation in k_{sn}

In order to reveal the general variation in steepness index values along river courses, we extracted the k_{sn} map for both basins (**Fig.22**) by using the Stream Profiler tool (see section 4.2.2). The warm colors (high values of the steepness index) evidence the location of knickpoints and knickzones.

Both maps show a correspondence between high values of k_{sn} and rock type changes, especially along the plateau scarps. Exceptions are two areas: the lower/medium Tekeze R. basin and the lower Blue Nile basin. Both of them correspond with two sector of medium/high values of local relief (**Figs.13e-f**)

Very high values of steepness index are concentrated also in the eastern portions of both basins. In particular the Tekeze basin presents an increase in k_{sn} values from north to south along the rift shoulder.

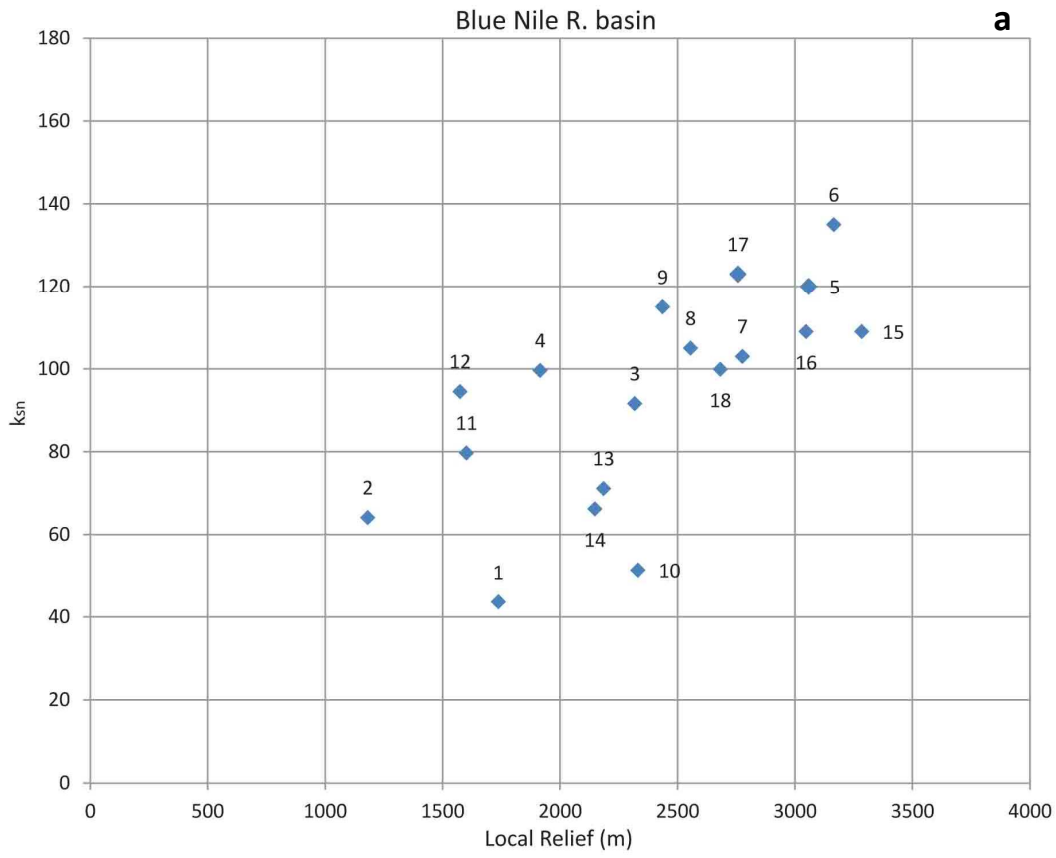

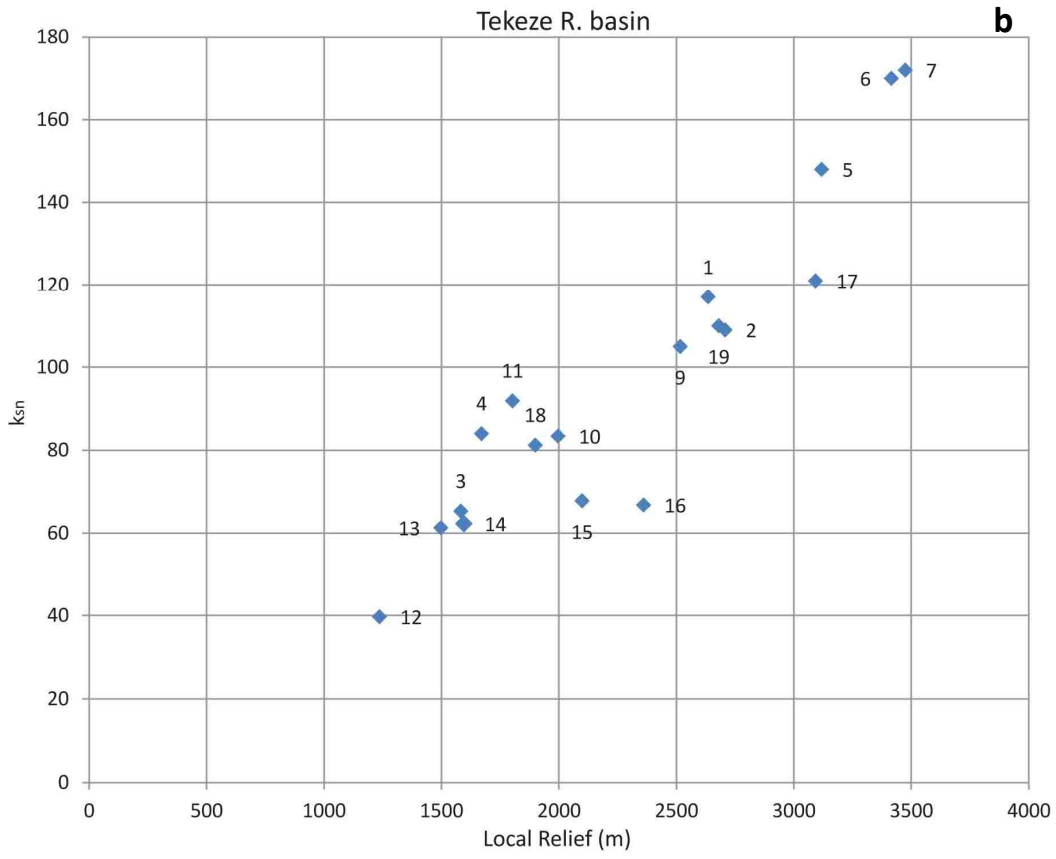

Figure 21 - Correlation between relief and normalized steepness index (*Ksn*) in the Blue Nile (**a**) and Tekeze (**b**) rivers basins. The numbers in the graphs refer to the subbasins of figures 16b and17b

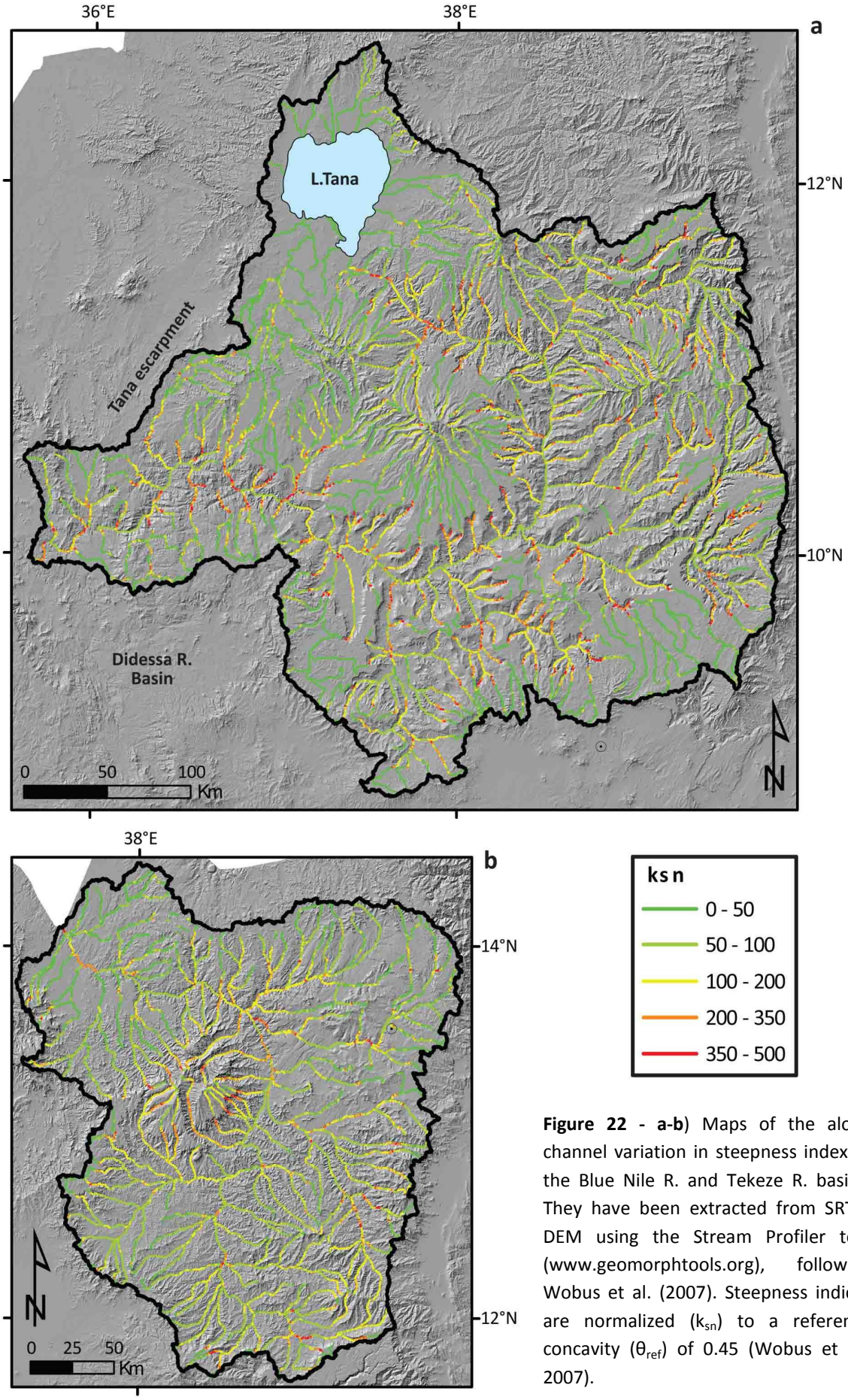

Figure 22 - a-b) Maps of the along channel variation in steepness index of the Blue Nile R. and Tekeze R. basins. They have been extracted from SRTM DEM using the Stream Profiler tool (www.geomorphtools.org), following Wobus et al. (2007). Steepness indices are normalized (k_{sn}) to a reference concavity (θ_{ref}) of 0.45 (Wobus et al., 2007).

2.4.4 Knickpoint celerity model

Rivers respond to a drop in base level by incising their valleys. A base level fall generates a transient knickpoint that works its way through the entire drainage network. The rate of this process and the shape of the knickpoint depend on rock-type, drainage area, amplitude and rate of base level fall.

We used a knickpoint celerity model, based on a simplified solution of the stream power erosion law (Rosenbloom and Anderson, 1994; Crosby and Whipple, 2006; Berlin and Anderson, 2007), to model steady vs unsteady base level fall and to compare incision pattern in the Blue Nile and Tekeze watersheds. The core of this model is the stream power law (see equation 2; Howard and Kerby, 1983; Howard et al., 1994; Whipple and Tucker, 1999). We assumed steady, uniform flow and detachment-limited conditions (in which sediment transport capacity exceeds sediment supply) (Howard and Kerby, 1983).

By assuming that plucking is the dominant erosion process (n = 1 in the equation 2 [Whipple et al., 2000]) is possible to rewrite the equation 2 as:

$$dz/dt = KA^m(dz/dx) \quad (3)$$

$$dx/dt = KA^m \quad (4)$$

where *dx/dt* is the rate of upstream knickpoint migration, *K* is the detachment limited erosion coefficient, *A* is upstream drainage area, and *m* is a non-dimensional constant that depends on basin hydrology, channel geometry, and erosion process (Whipple and Tucker, 1999). This expression describes the upstream propagation speed (or celerity) of a knickpoint not specifying changes in channel width, sediment flux, the effects of stochastic climate events, or the presence of an erosion threshold (Berlin and Anderson, 2007).

We used (4) to model numerically the upstream migration of knickpoints beginning at the confluence with Didessa river (Blue Nile R.) and at the border between Ethiopia and Sudan (Tekeze R.), using the dynamic time step approach described by Crosby and Whipple (2006) and Berlin and Anderson (2007).

To constrain the parameters K (detachment-limited erosion coefficient) and m (exponent on drainage area) in the celerity model, we used a two-parameter search (e.g., Stock and Montgomery, 1999; Crosby and Whipple, 2006; Berlin and Anderson, 2007) to find the best combination of K and m that predicts the knickpoint locations. We extracted for each river the

distance from the outlets (Didessa R. junction for the Blue Nile basin and the Ethiopia/Sudan border for the Tekeze one), the elevation and the drainage area.

On the longitudinal profiles extracted by the Stream Profiler tool (see section 2.4.2.2) we picked the major knickpoints of the Blue Nile and Tekeze tributaries by comparing each profile with its relative slope vs distance from the mouth and slope vs drainage area plots. Then, examining the available geological maps of Ethiopia (scales 1:250.000 [Hailu, 1975; Kazmin, 1976; Garland, 1980; Tsige and Hailu, 2007; Chumburo, 2009; Zenebe and Mariam, 2011] and 1:2.000.000 [Tefera et al., 1990]), we marked knickpoints not related to lithological changes (**Fig.23**).

In the Blue Nile drainage basin we found the recurrence of three non-lithologic knickpoints at about 1100, 2000 and 2500 m a.s.l. (**Fig.23**). The last one seems to be common to the majority of the rivers analyzed with the exception of rivers draining the rift shoulder (11-13). The 2000 m-knickpoint is evident in all the tributaries while the 1100 m-one appears only in the lower Blue Nile basin downstream the Blue Nile gorges.

The Tekeze basin shows a more complex knickpoints pattern: we found two main non-lithologic knickpoints at 1000 and 2500 m a.s.l.

To constrain the knickpoint initiation time in the Blue Nile basin we took as reference the 1100 m-knickpoint present in tributary longitudinal profile 25. We chose this tributary because an undated Quaternary basalt flow, sourced in the Lake Tana area, filled this valley providing a point of relative dating reference for the 1100 m knickpoint. The knickpoint has regressed upstream some 1400 m from the nose of the basalt flow (**Fig.23c**), which means that this segment of the knickpoint retreat cannot be older than 2.5 Ma (base of the Quaternary), and may be significantly younger depending on the age of the flow. For example, if the flow is late Pleistocene, a reasonable assumption given its fresh, dark, relatively unweathered appearance, then the 1400 m of retreat would have been younger than late Pleistocene, requiring that the downstream base level fall at the Didessa R. confluence be older than late Pleistocene. Clearly, the problem is underconstrained, but we proceded on the assumption that the flow is late Pleistocene in age, forcing the downstream base level fall to be older. We chose 1 and 2 Ma as reasonable middle and early Pleistocene guesses for the time of base level fall at the Didessa confluence responsible for the formation of the 1100 m knickpoint. These assumptions are reasonable given the major changes in watershed hydrology and White Nile axial valley adjustments to glacio-eustatic and hydro-climatic changes in the Pleistocene that are likely to lead to base level changes. As we will show below, if we were to choose base level falls greater than 2 Ma in age for the 1100 m

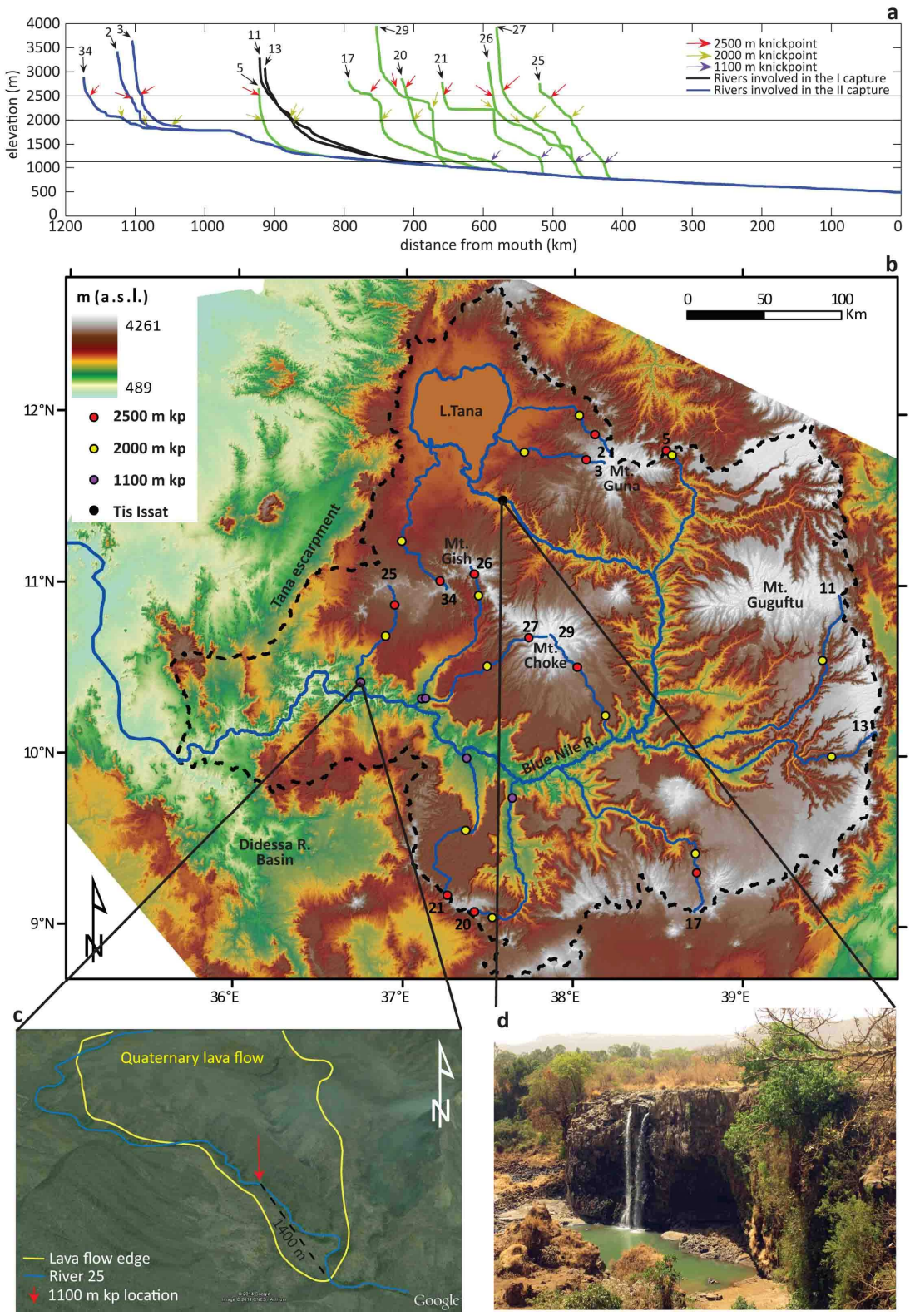

Figure 23 - a) Longitudinal profiles of the Blue Nile R. tributaries, studied in the knickpoint celerity model, plotted on the Blue Nile R. profile. Red, yellow and violet arrows indicate the locations of the major knickpoints used in the knickpoint celerity model; **b)** map showing the location of the analyzed Blue Nile R. tributaries and of their major knickpoints; **c)** 3D satellite image (from Google Earth) showing the location of the 1100 m elevated knickpoint along river 25. The comparison between the present knickpoint location and the most downstream continuation of the Quaternary basaltic flow (solid yellow line) indicates a knickpoint regression of ~1400 m; **d)** image of the Tis Issat waterfall (Blue Nile falls) in the dry season, when most of the flow is taken out for a hydroeletric station. The falls are located 30 km downstream from the Lake Tana and are around 40 m high.

knickpoint, the model ages for the higher, older knicpoints in the Blue Nile drainage become older than the flood basalts and what we know about the geologic formation of the plateau.

No comparable absolute or relative age constraints are present in the Tekeze basin, so we simply extended the assumed knickpoint ages and modeled the parameters derived for the Blue Nile to the Tekeze basin.

The misfit between the modeled and the observed knickpoint locations in the Blue Nile R. basin was minimized with m = 0.58 and K = $6.57 \cdot 10^{-10}$. Choosing 1 Ma as initiation time, we obtained the ages of 1-1.85 Ma, 3.6-6.7 Ma and 8.4-12.2 Ma for 1100, 2000, and 2500 m knickpoints respectively. The ages doubled when we set the initiation time at 2 Ma. Lower 2500 m knickpoint initiation time values resulted for the rivers 13 (6.6 and 13.2 Ma by choosing 1 and 2 Ma respectively) and 17 (4.7 and 9.4 Ma by choosing 1 and 2 Ma respectively) (**Table 5**).

In the Tekeze basin we supposed that the 1000 m and 2500 m knickpoints initiated to migrate at the same time of the 1100 m and 2500 m Blue Nile basin ones. Using the same m and K values we ran four models testing the initiation times of 1 and 2 Ma for the 1000 m knickpoint and the initiation times of 10 and 20 Ma for the 2500 m one (**Tables 6-7**).

In the first model (initiation time 1 Ma) the ages of 1000 m and 2500 m are 0.8-1.2 and 1.3-3.4 Ma (**Table 6**). In the second model (initiation time 2 Ma) the ages range between 0.7-1.0 and 4.6-10.7 Ma (**Table 6**). The third model (Initiation time 10 Ma) shows ages of 1.4-2.1 and 4.6-10.7 Ma (**Table 7**). In the last model (initiation time 20 Ma) the age ranges for the two knickpoints are 2.2-3.3 and 10.8-11.4 respectively (**Table 7**).

Table 5 - Blue Nile R. knickpoint celerity model results. The grey shaded area indicates the tributaries we used to run the model prescribing the 1100 m knickpoint age and solving for the best combination of m and K. We ran two models by choosing the 1100 m knickpoint initiation times of 1 and 2 Ma. For further explanations see the text.

Blue Nile R. basin knickpoint celerity model (Base level 700 m) *						
	1100 m kp		2000 m kp		2500 m kp	
Rivers	Initiation time 1 Ma	Initiation time 2 Ma	Initiation time 1 Ma	Initiation time 2 Ma	Initiation time 1 Ma	Initiation time 2 Ma
25	1 Ma	2 Ma	4.6 Ma	9.2 Ma	12 Ma	24 Ma
26	1 Ma	2 Ma	6.1 Ma	12.2 Ma	10.4 Ma	20.8 Ma
27	1 Ma	2 Ma	3.8 Ma	7.6 Ma	10 Ma	20 Ma
5	1.85 Ma	3.7 Ma	6.7 Ma	13.4 Ma	10 Ma	20 Ma
20	1.5 Ma	3 Ma	4.8 Ma	9.6 Ma	12.2 Ma	24.4 Ma
17	1.8 Ma	3.6 Ma	4.6 Ma	9.2 Ma	4.7 Ma	9.4 Ma
13	1.8 Ma	3.6 Ma	4.5 Ma	9 Ma	6.6 Ma	13.2 Ma
Average	**1.4** +0.45/-0.4 Ma	**2.8** +0.9/-0.8 Ma	**5** +1.7/-1.2 Ma	**10** +3.4/-2.4 Ma	**9.5** +2.7/-4.8 Ma	**19** +5.4/-9.6 Ma

Tekeze R. basin knickpoint celerity model (Base level 700 m) *				
	1000 m kp		2500 m kp	
Rivers	Initiation time 1 Ma	Initiation time 2 Ma	Initiation time 1 Ma	Initiation time 2 Ma
22	1.1 Ma	1 Ma	3.1 Ma	4.9 Ma
21	1.1 Ma	1 Ma	2.7 Ma	6 Ma
19	0.8 Ma	0.7 Ma	X	X
1	1.2 Ma	1 Ma	3.4 Ma	4.8 Ma
Average	**1** ± 0.2 Ma	**0.9** +0.1/-0.3 Ma	**3** +0.4/-0.3 Ma	**5.2** +0.8/-0.4 Ma

Table 6 - Tekeze R. knickpoint celerity model results. We ran two models by choosing the 1000 m knickpoint initiation times of 1 and 2 Ma. For further explanations see the text.

Tekeze R. basin knickpoint celerity model (Base level 700 m) *				
	1000 m kp		2500 m kp	
Rivers	Initiation time 10 Ma	Initiation time 20 Ma	Initiation time 10 Ma	Initiation time 20 Ma
22	1.9 Ma	3 Ma	9.2 Ma	11 Ma
21	2.1 Ma	3.2 Ma	10.7 Ma	10.8 Ma
19	1.4 Ma	2.2 Ma	X	X
1	2.1 Ma	3.3 Ma	9 Ma	11.4 Ma
Average	**1.8** +0.3/-0.4 Ma	**2.9** +0.4/-0.7 Ma	**9.6** +1.1/-0.6 Ma	**11** +0.4/-0.2 Ma

Table 7 - Tekeze R. knickpoint celerity model results. We ran two models by choosing the 2500 m knickpoint initiation times of 10 and 20 Ma. For further explanations see the text.

* The misfit between the modeled and the observed knickpoint locations was minimized with m = 0.58 and K = $6.57 \cdot 10^{-10}$

2.5 Discussion

Our topographic analysis pointed out that the present topographic configuration was determined mainly by a domal-like uplift due to the impinging of hot astenospheric material at the base of East Africa lithosphere. Such trend is very clear in the swath profiles 2 and 3 (**Figs.14c-d**) and in the filtered topography (**Fig.15**) where a topographic high with a maximum elevation of 1500 m has been found in the Addis Ababa region. Several tomographic studies (Lithgow-Bertelloni and Silver, 1998; Davies, 1998; Ebinger and Sleep, 1998; Ritsema et al., 1999; Gurnis et al., 2000; Nyblade et al., 2000; Ritsema and van Heijst, 2000; Montagner et al., 2007; Bastow et al., 2008; 2011; Mucha and Forte, 2011; Nyblade, 2011; Faccenna et al., 2013; Hansen and Nyblade, 2013) show in the same area a huge low velocity anomaly associated to the rise of the Afar plume. The maximum elevation value found in this work (1500 m; see **Fig.15**) is not very far from what has been established in other works (Dainelli, 1943; Mohr, 1967; Menzies et al., 1997; McDougal, 1975; Şengör, 2001; Pik et al., 2003; Gani et al., 2007) which demonstrated that the high standing plateau had experienced up to ~2-km of rock uplift since ~30 Ma. The pattern and the activity of uplift is still subject of debate (Pik et al., 2003; Gani et al., 2007; Ismail and Abdelsalam, 2012).

The western escarpment (Lake Tana escarpment) formed by the erosion of the huge pile of flood basalts (average eroded material thickness ~1000m) since their deposition (~30 Ma). Such process forced the scarp to retreat gradually eastward (Grabham and Black, 1925; Minucci, 1938b; Dainelli, 1943; Camucci, 1950; Jepsen and Athearn, 1961; Mohr, 1967; Hahn et al., 1977; Chorowicz et al., 1998; Gani et al., 2008) and caused, through time, a strong erosional unloading and a consequent flexural uplift in the whole area (see chapter 3 in this thesis). The eastern

escarpment resulted from the tectonic activity of the Afar-MER rift system: the unloading due to estension triggered the flexural uplift on the rift shoulder (Weissel et al., 1995). The flexural rebound on both sides of the plateau is evident in the swath profiles 1 and 2 (**Figs.14b-c**). It prevents the capture of the internal part of the plateau by rivers draining Sudan and Afar lowlands. As a consequence, the escarpments are deeply incised by these rivers as evidenced by the local relief maps (**Figs.13e-f**).

The analysis of longitudinal profiles of the rivers draining the plateau provides some clues on the activity state of both escarpments. Indeed θ values (**Tables 3-4**) of the rivers draining the rift shoulder (rivers 6-7-11-12-13-14; **Fig.19**, **Table 3**) are in the range of 0.4 and 0.6 expected under steady-state conditions (Tarboton et al., 1989; Snyder et al., 2000; Kirby and Whipple, 2001; Lague and Davy, 2003; Whipple, 2004; Wobus et al., 2006; Whipple et al., 2007). Indeed, since early Pleistocene the tectonic activity shifted from the border faults to the axial zone of the rift (Ebinger, 2005). So in around 1 My, the rivers evolved to reach the equilibrium with this local tectonic input. Along the Tana escarpment river 14 (**Fig.20**, **Table 4**) is very concave (0.62±0.026) and is the only one with a steepness index higher than 100 and not draining a volcanic edifice. These values indicate that the river is charcterized by a non-uniform rock uplift, related to the erosional unloading at the base of the escarpment, which keeps the headwater high in elevation. This makes the river 14 steeper and more concave.

The hypsometric analysis of the eastern sectors of Blue Nile and Tekeze basins show strong differences (**Figs.16-17**). The curves of Blue Nile sub-basins (rivers 5-6-7-8; **Fig.16**) have irregular shapes as if each of them is composed by two curves of two different basins now combined together. Indeed, the one at higher elevation is relative to the portion of the present basin located in the plateau and captured by the river originally draining just the downstream portion. On the other hand the hypsometric curves of the Tekeze sub-basins have an almost perfect S-shape. In these basins, the plateau remnants are smaller and the valleys are wider than in the Blue Nile basin. This difference in fluvial erosion is evidenced in the maps of local relief (**Figs.13e-f**): the maximum incision is concentrated in the eastern side of the Blue Nile basin and decreases dramatically northward in the Tekeze basin. It could be related to an increase or a difference in deformation style of the rift tectonic activity that become younger and younger from north to south (Hayward and Ebinger, 1996; Bonini et al., 2005; Keranen and Klemperer, 2008).

Morphometric analysis evidences also a different evolution of the Blue Nile and Tekeze drainage systems. Indeed the concavity index values of the Tekeze R. tributaries (**Table 4**) are closer to the

value relative to an equilibrium profile than the Blue Nile ones (**Table 3**). Similarly the hypsometric curves of Tekeze R. tributaries have an S-shape (**Fig.17**) and low values of the HI, whereas the curves of the Blue Nile tributaries are in general irregular and characterized by high HI. These differences in the river network metrics could be related to topography and erosion patterns of the two basins. Indeed the Blue Nile basin is characterized by a larger number of volcanoes rising from wider plateau remnants. Moreover, here the rivers deeply incise the flat highlands forming valleys with steep flanks and gorges. In the Tekeze basin, rivers erode more laterally shaping wide valleys and progressively reducing the few plateau remnants. This difference in the basin evolution should be related to two main factors: flood basalt thickness and location with respect to the dome center. The Tekeze R. basin, that is located in a marginal sector of the dome (**Fig.15**), is characterized by thinner flood basalts. The Nilo Blue R. cuts across the most elevated portion of the dome (**Fig.15**) and presents thicker basalt deposits (up to 2000 m).

The Lake Tana inflows show θ values close to the reference value (**Fig.19; Table 3)** suggesting they are in equilibrium with the lake as a local base level. Similarly, the hypsometric curves as well as the low values of HI indicate that the rivers are not incising but are widening their valleys (**Fig.16**; **Table 1**). Lake Tana, experienced several desiccation phases related to climate changes (Lamb et al., 2007) and a strong Quaternary volcanic activity (Grabham and Black, 1925; Minucci, 1938b; Jepsen and Athearn, 1961) which caused periodic isolations of the basin. The knickzone 30 km south of the lake (Tis Issat waterfall) demonstrates that although the Blue Nile R. drains the basin, the erosion wave relative to the progressive capture of the uplifted dome landscape does not reach the lake yet. This could be related to the Quaternary volcanic activity south and southeast of Lake Tana, that partially prevented the headward erosion.

The plots k_{sn} vs local relief of both Blue Nile and Tekeze rivers basins (**Fig.21**) show a positive correlation. However the Blue Nile R. basin presents a more scattered points distribution with a flattening in the portion characterized by high k_{sn} and local relief values (subbasins 5-6-7-8-9). Such feature is in disagreement with Montgomery and Brandon (2002) that evidenced a positive hyperbolic correlation between erosion rate and mean local relief. In the case of the Blue Nile R. subbasins this is probably related to the presence of wide plateau remnants at the highest elevation of the subbasins. Here the erosion rate is very low, since the headward migration of the erosion wave relative to the present base level does not affect them yet. On the other hand the more linear correlation evidenced in the Tekeze R. basin plot may be due to a topographic setting characterized by few plateau remnants and a more widely incised landscape.

The maps of the along-channel variation in k_{sn} (**Fig.22**) show a wide area in the medium-lower portion of both Blue Nile and Tekeze basins characterized by high values. In the same locations the medium/high values of local relief indicate an increase in incision. The rivers that drain these areas have the hypsometric curves characterized by a steeper and larger convex segment at lower elevations. Moreover, in both Tekeze and Blue Nile basins, a knickpoint located around 1000-1100 m is present. All these data relative to Tekeze and Blue Nile rivers basins point to a recent base level fall that determined the headward migration of an erosion wave.

The knickpoints analysis permitted us to find three non lithologic knickpoints (at 1100, 2000 and 2500 m a.s.l.) in the Blue Nile R. basin and two (at 1000 and 2500 m a.s.l.) in the Tekeze R. one (**Fig.23**).

In the Blue Nile drainage system the 2500 m knickpoint recurs in all the analyzed tributaries with the exception of rivers 11 and 13. On the other hand the 2000 m knickpoint is common to all the tributaries while the 1100 m knickpoint affects only the lower Blue Nile basin (rivers 20-21-25-26-27 in **Fig.23**). We used these data in the knickpoint celerity model to provide a chronological frame to the evolution of the Ethiopian plateau river network.

According to the age of a lava flow where the 1100 m knickpoint is located in river 25 (**Fig.23**), we assumed an initiation time younger than 2,5 Ma. So we tested the initiation ages of 1 and 2 Ma to calculate the retreat of the knickpoints in Blue Nile R. tributaries (**Table 5**). In the first case the knickpoint celerity model dated the migration of the 2500 m and 2000 m knickpoints at about 10 Ma and 5 Ma respectively. Using 2 Ma as initiation time the ages doubled (**Table 5**).

According to the results of the modeling the migration of the 2500 m knickpoint initiated between 20 and 10 Ma (**Table 5**), after the emplacement of the flood basalts (Baker et al., 1996a; Hofman et al., 1997; Pik et al., 1998; Ukstins et al., 2002; Coulié et al., 2003). The elevation of this knickpoint is similar to the mean altitude of the plateau. For these reasons the 2500 m knickpoint could record the Ethiopian Plateau main capture. A confirmation of that comes from the analysis of the intertrappean beds (Abbate et al., 2014). Such fluvio-lacustrine sediments were deposited in small endorehic basins with an almost flat physiography and mark a period of quiescence in Trap eruption ranging between 29 and 27 Ma (23 Ma in Eritrea; Abbate et al., 2014). This means that the capture of the inner sector of the plateau occurred after 27 Ma. The lack of the 2500 m knickpoint in rivers 11 and 13, draining the rift shoulder, suggests that this area was still internally drained at this time.

The initiation time of the 2000 m knickpoint ranges between 10 and 5 Ma (**Table 5**). Such period coincides with two main events: the formation of the northern and central sectors of the MER (Bonini et al., 2005) and the global climate change at the passage Miocene-Pliocene (Groot, 1991; Cerling et al., 1997; Hodell et al., 2001; Billups, 2002; Vidal et al., 2002; Fortelius et al., 2006; Jimenez-Moreno et al., 2010; Song et al., 2014). While the first event influenced the basin at local scale, the second one may have caused a base level fall downstream, increasing the concavity of the Blue Nile channel and triggering the migration of the 2000 m knickpoint. There are palaeoclimatic data indicating that the Nile catchment experienced an abrupt passage from drier conditions in the Miocene to wetter conditions in the Pliocene (Groot, 1991; Cerling et al., 1997; Hodell et al., 2001; Billups, 2002; Vidal et al., 2002; Fortelius et al., 2006; Jimenez-Moreno et al., 2010; Song et al., 2014). Such climate change coincides with a huge amount of sedimentation rate in the Nile delta (Abdel Aal et al., 1994; Dolson et al., 2001; Gardosh et al., 2009; Kellner et al., 2009) where the most of sediments came from the Ethiopian highlands (Foucault and Stanley, 1989; Woodwart et al., 2007). It is important to note that the knickpoint related to the Messinian base level fall of around 1500 m (Chumakov, 1973; Bini et al., 1978; Finckh, 1978; Rizzini et al., 1978; Rizzini and Dondi,1978; Barber, 1981; Druckman et al.,1995) reached a maximum distance of 2000 km from Nile delta (Loget and Van Den Driessche, 2009), ~1000 km far from the Ethiopian highlands.

The Lake Tana basin rivers (2-3-34 in **Fig.23**) preserved the 2500 and 2000 m knickpoints. This means that the area must have been connected to the main drainage system at least until the end of the 2000 m knickpoint migration. However the morphometric analysis evidences that the Lake Tana tributaries are in equilibrium with the lake as a local base level. For this reason, in a period comprised between the second knickpoint migration and the present, the basin must have been endorheic. The closure of such region has been referred to climate (Lamb et al., 2007) and volcanic (Grabham and Black, 1925; Minucci, 1938b; Jepsen and Athearn, 1961) events which affected the area in the Quaternary time. Probably the Quaternary lava flows prevented the headward erosion of the Blue Nile R. forming the knickzone including the Tis Issat falls (**Figs.18, 23**).

The 1100 m knickpoint has, according to the model, an age comprised between 2 and 1 Ma (**Table 5**), a period characterized by climate changes. Marine sediments sequences demonstrate that subtropical African climate periodically oscillated between markedly wetter and drier conditions, with evidence for step-like (± 0.2 Ma) increases in African climate variability and aridity near 2.8 Ma, 1.7 Ma, and 1.0 Ma, coincident with the onset and intensification of high-latitude glacial cycle

(deMenocal, 2004). Another possible factor may be a local tectonic event that affected the Nile R. far from the Ethiopian highlands. Such events may have caused base level falls downstream the Ethiopian highlands triggering the migration of the 1100 m knickpoint. A base level fall is also indicated by the morphometric analysis (hypsometry, ksn maps and local relief; **Figs.13e-f, 16, 22**) which shows relatively deeper incision and steeper channels in the downstream tributaries of Blue Nile and Tekeze rivers.

Because of the lack of age constraints on Tekeze basin knickpoints, we supposed that the plateau capture in this basin occurred more or less simultaneously with the Blue Nile basin one. We set the initiation ages of the 1000 and 2500 m knickpoints migrations by using the initiation times obtained for the Blue Nile basin (1, 2, 10, and 20 Ma). The results show a general non-convergence except for the 1000 m knickpoint (**Table 6-7**). Indeed using 1 and 10 Ma as initiation times, the 1000 m knickpoint has ages ranging between 0.8-1.18 and 1.4-2.1 Ma respectively that are similar to the ones obtained for the 1100 m Blue Nile basin knickpoint (**Table 5**).

The general non-convergence observed between the knickpoint celerity models of Blue Nile and Tekeze basins, is an additional evidence of the different evolutions experienced by the two basins. However the similar ages of the 1100 m (Blue Nile basin) and 1000 m (Tekeze basin) knickpoints suggest that a recent regional base level fall affected the whole area causing the migration of a erosion wave in both basins. These results evidenced a progressive capture of the Ethiopian Plateau partially enhanced by local or regional processes (tectonics and climate) in constrast with the pulsed uplift evolution model proposed by Gani et al. (2007). This model can not be supported by the geodynamic frame of the region where the topography is the dynamic signature of the Afar plume.

2.6 Conclusions

The study of the topographic configuration of the Ethiopian Plateau and the morphometric analysis of the river network permitted us to develop a conceptual model for the long-term evolution of the plateau drainage system since Oligocene unraveling the influence of deep and tectonic processes on the highland landscape evolution.

The Ethiopian Plateau is mainly underlain by thick and low erodible flood basalts (**Fig.11b**). The landscape of the interior portions is characterized by a poorly incised topography (plateau remnants) only locally deeply incised by rivers (**Figs.13a-b-c-d**). The drainage system is constituted by the Blue Nile and Tekeze rivers which enter into the plateau from southwest and northwest

respectively (**Fig.11a**). Most of the incision concentrates along the downstream portions of the Blue Nile and Tekeze valleys and along the Tana escarpment which borders the plateau to the west (**Figs.13e-f**).

The long wave topography of the study area (**Figs.14-15**) evidences the presence of a bulge whose topography increases from 0 m in the Sudanese and Somalian lowlands up to 1500 m in the Addis Ababa area. Several tomographic studies show in the same area a huge low velocity anomaly associated to the upwelling of hot astenospheric material from the core-mantle boundary (Afar plume; Lithgow-Bertelloni and Silver, 1998; Davies, 1998; Ebinger and Sleep, 1998; Ritsema et al., 1999; Gurnis et al., 2000; Nyblade et al., 2000; Ritsema and van Heijst, 2000; Montagner et al., 2007; Bastow et al., 2008; 2011; Mucha and Forte, 2011; Nyblade, 2011; Faccenna et al., 2013; Hansen and Nyblade, 2013).

The morphometric analysis on drainage basins and stream longitudinal profiles evidences a different evolution of the Blue Nile and Tekeze drainage systems. The shape of longitudinal profiles, quantitatively measured by concavity and steepness indices, indicates that the Tekeze R. tributaries (**Fig.20**, **Table 4**) are closer to equilibrium than the Blue Nile ones (**Fig.19**, **Table 3**). Similarly the hypsometric curves of Tekeze R. tributaries have an S-shape (**Fig.7**) and low values of the HI (**Table 1**), whereas the curves of the Blue Nile tributaries (**Fig.16**) are in general irregular and characterized by high HI (**Table 2**). These results are related to: a) the different location of the two basins with respect to the plume head (Addis Ababa region; **Figs.14-15**): indeed the Tekeze basin, located in the northern peripheral sector of the bulge, has been less affected by the domal uplift; b) the volcanic events concentrated mainly in the Blue Nile basin (**Fig.11a**): such volcanic activity influences the topographic evolution of the Blue Nile drainage system from Oligocene to Quaternary while affected the Tekeze basin only in the early Oligocene; c) the CFB thickness which reaches up to 2000 m in the Blue Nile basin and 1200 m in the Tekeze one (Mohr and Zanettin, 1988). These three factors slowed down erosion in the Blue Nile basin and facilitated the entrance of the Tekeze R. into the Ethiopian Plateau.

The knickpoint celerity model evidences three base level changes in the Blue Nile R. basin (**Fig.23**). The oldest one, initiated between 20 and 10 Ma, is related to the main plateau capture when the endorheic inner part of the plateau (Abbate et al., 2014) has been integrated in the Blue Nile drainage systems. The second event occurs between 10 and 5 Ma and is related to the opening of the Central and North MER and to the Miocene-Pliocene global climate change. The last base level

change is Quaternary in age and is recorded by a knickpoint in the downstream portion of both Blue Nile and Tekeze basins. Such event is probably connected to Quaternary climate changes.

In summary the study of Ethiopian Plateau topographic configuration evidences a dome-shaped topography centered in the Addis Ababa region and associated to the Afar plume bulge. The morphometric analysis of fluvial network shows that the plateau drainage system evolution has been strongly influenced by the principal geological and climatic events which affected the area. The spatial distribution of such events determined a different evolution of the Blue Nile R. and Tekeze R. basins leading the Tekeze R. basin to get closer to equilibrium.

References

Abbate, E., Bruni, P., Ferretti, M.P., Delmer, C., Laurenzi, M.A., Hagos, M., Bedri, O., Rook, L., Sagri, M. and Libsekal, Y. (2014) - "The East Africa Oligocene intertrappean beds: Regional distribution, depositional environments and Afro/Arabian mammal dispersals" - Journal of African Earth Sciences, 99, 463-489.

Abdel Aal, A., El Barkooky, A., Gerrits, M., Meyer, H-J, Schwander, M. and Zaki, H. (2001) - "Tectonic evolution of the Eastern Mediterranean Basin and its significance for the hydrocarbon prospectivity of the Nile Delta deepwater area" - GeoArabia, v. 6/3, p. 363-384.

Baker, B.H., Mohr, P.A. and Williams, L.A.J. (1972) - "Geologyof the EasternRift System of Africa" - Geological Society of America Special Paper, vol. 136. 67 pp., Boulder Colorado.

Baker, J., Snee, L. and Menzies, M. (1996a) – "A brief Oligocene period of flood volcanism in Yemen" - Earth and Planetary Science Letters 138, 39–55.

Ball, J. (1939) – "Contributions to the Geography of Egypt" - Government Press, Cairo, 308 pp.

Barber, P.M. (1981) - "Messinian subaerial erosion of the proto-Nile delta" - Mar. Geol., 44, 253-272.

Barrows, T.T., Williams, M.A.J., Mills, S.C., Duller, G.A.T., Fifield, L.K., Haberlah, D., Tims, S.G. and Williams, F.M. (2014) – "A White Nile megalake during the last interglacial period" – Geology, doi:10.1130/G35238.1.

Bastow, I.D., Nyblade, A.A., Stuart, G.W., Rooney, T.O. and Benoit, M.H. (2008) - "Upper mantle seismic structure beneath the Ethiopian hot spot: rifting at the edge of the African low-velocity anomaly" - Geochemistry, Geophysics, Geosystems 9, Q12022. doi:10.1029/2008GC002107.

Bastow, I.D., Keir, D. and Daly, E. (2011) – "The Ethiopia Afar Geoscientifi c Lithospheric Experiment (EAGLE): Probing the transition from continental rifting to incipient sea floor spreading" - *in* Beccaluva, L., Bianchini, G., and Wilson, M., eds. "Volcanism and Evolution of the African Lithosphere" - Geological Society of America Special Paper 478, p. 51–76, doi:10.1130/2011.2478(04).

Berhe, S.M., Desta, B., Nicoletti, M. and Tefera, M. (1987) – "Geology, geochronology and geodynamic implications of the Cenozoic magmatic province in W and SE Ethiopia" - Journal of the Geological Society of London 144, 213–226.

Berlin, M.M. and Anderson, R.S. (2007) - "Modeling of knickpoint retreat on the Roan Plateau, western Colorado" - J. Geophys. Res., 112, doi:10.1029/2006JF000553.

Beydoun, Z.R. (1960) - "Synopsis of the Geology of East Aden Protectorate" - XXI International Geological Congress, Copenhagen 21, 131–149.

Beyth, M. (1972a) - "To the Geology of Central-Western Tigre" - Ph.D. thesis, Friedrichs Wilhelms Universität, Bonn.

Beyth, M. (1972b) - "Paleozoic–Mesozoic sedimentary basin of Mekelle Outlier, Northern Ethiopia" - AAPG Bull. 56, 2426–2439.

Billups, K. (2002) - "Late Miocene through early Pliocene deep water circulation and climate change viewed from the sub-Antarctic South Atlantic" - Palaeogeography, Palaeoclimatology, Palaeoecology, vol.185, pp.287-307.

Bini, A., Cita, M.B. and Gaetani, M. (1978) - "Southern Alpine lakes - Hypothesis of an erosional origin related to the Messinian entrenchment" - Mar. Geol., 27, 271-288

Blanford, W.T. (1869) - "On the Geology of a portion of Abyssinia" - J.Geol. Soc. Lond. 25, 401−406.

Bonini, M., Souriot, T., Boccaletti, M. and Brun, J.P. (1997) - "Successive orthogonal and oblique extension episodes in a rift zone: laboratory experiments with application to the Ethiopian Rift" - Tectonics 16, 347–362.

Bonini, M., Corti, G., Innocenti, F., and Manetti, P. (2005) – "Evolution of the Main Ethiopian Rift in the frame of Afar and Kenya rifts propagation" - Tectonics, v. 24, doi: 10.1029/2004TC001680.

Bosellini, A., Russo, A., Fantozzi, P.L., Assefa, G. and Tadesse, S. (1997) - "The Mesozoic succession of the Mekelle Outlier (Tigrai Province, Ethiopia)" - Mem. Sci. Geol. 49, 95–116.

Braun, J. (2010) - "The many surface expressions of mantle dynamic" - Nature Geoscience 3, 825–833.

Cerling, T.E., Harris, J.M., MacFadden, B.J., Leakey, M.G., Quade, J., Eisenmann, V. and Ehleringer, J.R. (1997) - "Global vegetation change through the Miocene/Pliocene boundary" - Nature, vol. 389, pp. 153-158.

Chen, Y.-C., Sung, Q. and Cheng, K.-Y. (2003) - " Along-strike variations of morphotectonic features in the Western Foothills of Taiwan: tectonic implications based on stream-gradient and hypsometric analysis" - Geomorphology, 56, 109-137.

Chorowicz, J., Collet, B., Bonavia, F.F., Mohr, P., Parrot, J.-F. and Korme, T. (1998) - "The Tana basin, Ethiopia: intraplateau uplift, rifting and subsidence" - Tectonophysics 295, 351–367.

Chumakov, I.S. (1973) - "Geological history of the Mediterranean at the end of the Miocene - the beginning of the Pliocene according to new data" - In: Initial Reports of the Deep Sea Drilling Project, 13 (Ed. by W.B.F. Ryan, K.J. Hsˇ, W. Nesteroj, G. Pautot,W.C.Wezel, J. Lort, M.B. Cita,W. Mayne, H. Stradner and P. Dumitrica), pp. 1241^1242. U.S. Gov. Printing O⁄ce, Washington, D.C.

Chumburo, F. (2009) – "Geological Map of Debre Markos sheet (NC 37-6)" – EIGS.

Comucci, P. (1950) - "Le vulcaniti del lago Tana (Africa Orientale)" - Accad. Naz. Lincei, Roma, 209 pp.

Corti, G. (2008) - "Control of rift obliquity on the evolution and segmentation of the main Ethiopian rift" - Nature Geoscience 1, 258–262.

Corti, G. (2009) – "Continental rift evolution: From rift initiation to incipient break-up in the Main Ethiopian Rift, East Africa" - Earth-Science Reviews, 96, 1–53.

Coulié, E., Quidelleur, X., Gillot, P.Y., Coutillot, V., Lefevre, J.C. and Chiessa, S. (2003) - "Comparative K–Ar and Ar/Ar dating of Ethiopian and Yemenite Oligocene volcanism: implication for timing and duration of the Ethiopian traps" - EPSL, 206, 477–492, doi:10.1016/S0012-821X(02)01089-0.

Crosby, B. T. and Whipple, K.X. (2006) - "Knickpoints in the Waipaoa River, North Island, New Zealand" - Geomorphology, 82(1–2), 16–38.

D'Agostino, N. and McKenzie, D.P. (1999) - "Convective support of long wavelength topography in the Apennines (Italy)" - Terranova 11 (5), 234–238.

Dainelli, G. and Marinelli, O. (1912) - "Risultati Scientifici Di Un Viaggio Nella Colonia Eritrea" - Firenze.

Dainelli, G. (1943) - "Geologia dell'Africa Orientale (3 vols. text, 1 vol. maps)" - R. Accad. Ital., Roma.

Davidson, A. and Rex, D.C. (1980) – "Age of volcanism and rifting in south-western Ethiopia" - Nature 283, 654–658.

Davies, G. (1998) - "A channelled plume under Africa" - Nature 395, 743.

deMenocal, P.B. (2004) - "African climate change and faunal evolution during the Pliocene-Pleistocene" - EPSL, vol. 220, pp. 3-24.

Dolson, J.C., Shann, M.V., Matbouly, S., Harwood, C., Rashed, R. and Hammouda, H. (2001) - "The petroleum potential of Egypt" - *In* M. Halbouty (Ed.), Petroleum Provinces of the Twenty-first Century, AAPG Memoir 74, p. 453-482.

Dow, D.B., Beyth, M. and Hailu, T. (1971) - "Palaeozoic glacial rocks recently discovered in northern Ethiopia" - Geol. Mag. 108: 53–60.

Druckman, Y., Buchbinder, B., Martinotti, G.M., Siman-Tov, R. and Aharon, P. (1995) - "The buried A¢q Canyon (eastern Mediterranean, Israel), a case study of a Tertiary submarine canyon exposed in Late Messinian times" - Mar.Geol., 123, 167-185.

Ebinger, C.J., Yemane, T.,WoldeGabriel, G., Aronson, J.L. and Walter, R.C. (1993) – "Late Eocene-Recent volcanism and faulting in the southern main Ethiopian rift" - Journal of the Geological Society of London 150, 99–108.

Ebinger, C. and Sleep, N.H. (1998) – "Cenozoic magmatism in central and east Africa resulting from impact of one large plume" - Nature 395, 788–791.

Ebinger, C. (2005) - "Continental breakup: the East African perspective" - Astronomy and Geophysics 46, 2.16–2.21.

Faccenna, C., Molin, P., Orecchio, B., Olivetti, V., Bellier, O., Funiciello, F., Minelli, L., Piromallo, C., Billi, A. (2011) - "Topography of the Calabria subduction zone (southern Italy): clues for the origin of Mt. Etna" - Tectonics 30. doi:10.1029/2010TC002694.

Faccenna, C., Becker, T.W., Jolivet, L. and Keskin, M. (2013) - "Mantle convection in the Middle East: Reconciling Afar upwelling, Arabia indentation and Aegean trench rollback" - EPSL 375, 254-269.

Finckh, P.G. (1978) - "Are southern Alpine lakes former Messinian Canyons? Geophysical evidence for preglacial erosion in the southern Alpine lakes" - Mar. Geol., 27, 289-302.

Flint, J.J. (1974) – "Stream gradient as a function of order, magnitude, and discharge" – Water Resour. Res. 10, 969–973.

Fortelius, M., Eronen, J., Liu, L., Pushkina, D., Tesakov, A., Vislobokova, I. and Zhang, Z. (2006) - "Late Miocene and Pliocene large land mammals and climatic changes in Eurasia" - Palaeogeography, Palaeoclimatology, Palaeoecology, vol. 238, pp.219–227.

Foucault, A. and Stanley, D.J. (1989) - "Late Quaternary paleoclimatic oscillations in east Africa recorded by heavy minerals in the Nile Delta" - Nature, 339, 44–46.

Gani, N.D., Abdelsalam, M.G. and Gani, M.R. (2007) – "Blue Nile incision on the Ethiopian Plateau: pulsed plateau growth, Pliocene uplift, and hominin evolution" - GSA Today 17, 4–11.

Gani, N.D.S., Abdelsalam, M.G., Gera, S. and Gani, M.R. (2008) - "Stratigraphic and structural evolution of the Blue Nile Basin, Northwestern Ethiopian Plateau" - Geological Journal 44, 30–56.

Gardosh, M.A., Druckman, Y. and Buchbinder, B. (2009) - "The Late Tertiary deep-water siliciclastic system of the Levant Margin - an emerging play offshore Israel" - AAPG Search and Discovery Article #10211.

Garland, C.R. (1980) – "Geology of the Adigrat Area" - Ministry of Mines, Addis Ababa Memoir No.1, 51.

George, R., Rogers, N. and Kelley, S. (1998) – "Earliest magmatism in Ethiopia: evidence for two mantle plumes in one flood basalt province" - Geology 26, 923–926.

Grabham, G.W. and Black, R.P. (1925) - "Report of the Mission to Lake Tana 1920–21" - Government Press, Cairo.

Groot, J.J. (1991) - "Palynological evidence for late miocene, pliocene and early pleistocene climate changes in the middle U.S. Atlantic Coastal Plain" - Quaternary Science Reviews, vol.10, Issues 2–3, pp. 147–162.

Gurnis, M., Mitrovica, J.X., Ritsema, J. and van Heijst, H.J. (2000) – "Constraining mantle density structure using geological evidence of surface uplift rates: the case of the African Plume" - Geochemistry, Geophysics, Geosystems 1 1999GC000035.

Hack, J.T. (1957) – "Studies of longitudinal profiles in Virginia and Maryland" - U. S. Geol. Surv. Prof. Pap. 294 (B), 45–97.

Hahn, G.A., Raynolds, R.G.H. and Wood, R.A. (1977) - "The geology of the Angareb Ring Dike complex, northwestern Ethiopia" - Bull. Volcanol. 40, 1–10.

Hailu, T. (1975) - "Geological Map of Adiarkay Sheet (ND 37 -10) 1:250,000" - EIGS.

Hansen, S.E. and Nyblade, A.A. (2013) - "The deep seismic structure of the Ethiopia/Afar hotspot and the African plume" - Geophys. J. Int., doi: 10.1093/gji/ggt116.

Hayward, N.J. and Ebinger, C.J. (1996) - "Variations in the along-axis segmentation of the Afar Rift system" - Tectonics 15, 244–257.

Hodell, D.A., Curtis, J.H., Sierro, F.J., and Raymo, M.E. (2001) - "Correlation of late Miocene to early Pliocene sequences between the Mediterranean and North Atlantic" - Paleoceanography, v. 16, p. 164–178, doi: 10.1029/1999PA000487.

Hofmann, C., Courtillot, V., Feraud, G., Rochette, P., Yirgu, G., Ketefo, E. and Pik, R. (1997) – "Timing of the Ethiopian flood basalt event and implications for plume birth and global change" - Nature 389, 838–841.

Howard, A.D. and Kerby, G. (1983) - "Channel changes in badlands" - Geological Society of America Bulletin 94, 739-752.

Howard, A.D., Dietrich, W.E. and Seidl, M.A. (1994) - "Modeling fluvial erosion on regional to continental scales" - J. Geophys. Res.Solid Earth 99, 13971-13986.

Huang, X. and Niemann, J.D. (2006) - "Modelling the potential impacts of groundwater hydrology on long-term drainage basin evolution" - ESPL, 31, 1802–1823.

Hurtrez, J.E., Sol, C. and Lucazeau, F. (1999) - "Effect of drainage area on hypsometry from an analysis of small-scale drainage basins in the Siwalik Hills (Central Nepal)" - ESPL, 24 (9), 799–808.

Isacks, B.L. (1992) - "Long term land surface processes: Erosion, tectonics and climate history in mountain belts" - In TERRA-1: "Understanding the Terrestrial Environment", Mather, P., Ed.; Taylor and Francis: London, UK, pp. 21–36.

Ismail, E.H. and Abdelsalam, M.G. (2012) - "Morpho-tectonic analysis of the Tekeze River and the Blue Nile drainage systems on the Northwestern Plateau, Ethiopia" - J. Afric. Erth. Sc., 69, 34-47.

Jepsen, D.H. and Athearn, M.J. (1961) - "A general geological map of the Blue Nile River basin, Ethiopia (1:1,000,000)" - Dep. Water Resources, Addis Ababa.

Jimenez-Moreno, G., Fauquette, S. and Suc, J-P (2010) - " Miocene to Pliocene vegetation reconstruction and climate estimates in the Iberian Peninsula from pollen data" - Review of Palaeobotany and Palynology, vol.162, pp. 403-415.

Kazmin, V. (1976) – "Geological Map of Adigrat Sheet (ND 37 -7), 1:250,000" - EIGS.

Keller, E., Pinter, N. (2002) - "Active Tectonics. Earthquakes, Uplift, and Landscape" - Prentice Hall, New Jersey.

Kellner, A., El Khawaga, H., Brink, G., Brink-Larsen, S., Hesham, M., El Saad, H.A., Atef, A., Young, H. and Finlayson, B. (2009) - "Depositional History of the West Nile Delta - Upper Oligocene to Upper Pliocene" - AAPG Search and Discovery Article #30092.

Kendall, J.M., Stuart, G.W., Ebinger, C.J., Bastow, I.D. and Keir, D. (2005) - "Magma assisted rifting in Ethiopia" - Nature 433, 146–148.

Keranen, K. and Klemperer, S.L. (2008) - "Discontinuous and diachronous evolution of the Main Ethiopian Rift: implications for the development of continental rifts" - Earth and Planetary Science Letters 265, 96–111. doi:10.1016/j.epsl.2007.09.038.

Kieffer, B., Arndt, N., Lapierre, H., Bastien, F., Bosch, D., Pecher, A., Yirgu, G., Ayalew, D., Weis, D., Jerram, D.A., Keller, F., and Meugniot, C. (2004) – "Flood and shield basalts from Ethiopia: Magmas from the African Superswell" - Journal of Petrology, v. 45, 793–834.

Kirby, E. and Whipple, K.X. (2001) – "Quantifying differential rock-uplift rates via stream profile analysis" - Geology 29, 415–418.

Kirby, E., Johnson, C., Furlong, K. and Heimsath, A. (2007) – "Transient channel incision along Bolinas Ridge, California: evidence for differential rock uplift adjacent to the San Andreas fault" - J. Geophys. Res. (ISSN: 0148-0227) 112 (F3), 2007. http://dx.doi.org/10.1029/2006JF000559.

Lague, D. and Davy, P. (2003) – "Constraints on the long-term colluvial erosion law by analyzing slope-area relationships at various tectonic uplift rates in the Siwaliks Hills (Nepal)" - J. Geophys. Res. 108 (B2), 2129. http://dx.doi.org/10.1029/2002JB001893.

Lamb, H.F., Bates, C.R., Coombes, P.V., Marshall, M.H., Umer, M., Davies, S.J. and Dejen, E. (2007) - "Late Pleistocene desiccation of Lake Tana, source of the Blue Nile" - Quat. Sc. Rev., 26, 287-299.

Lawson, A. C. (1927) – "The valley of the Nile" - University of California, Chronicle No. 29.

Levitte, D. (1970) - "The Geology of Mekelle. Report on the Geology of the Central Part of Sheet ND 37-11" - Addis Ababa, Ethiopian Institute of Geological Survey.

Lithgow-Bertelloni, C. and P. G. Silver (1998) – "Dynamic topography, plate driving forces and the African superswell" - Nature, 395, 269–272, doi:10.1038/26212.

Lock, J., Kelsey, H., Furlong, K. and Woolace, A. (2006) - "Late Neogene and Quaternary landscape evolution of the Northern California Coast Ranges: evidence for Mendocino triple junction tectonics" - Geological Society of America Bulletin 118, 1232–1246.

Loget, N. and Van Den Driessche, J. (2009) - "Wave train model for knickpoint migration" - Geomorphology, 106, 376–382.

McDougall, I., Morton,W.H. and William, M.A.J. (1975) – "Ages and rates of denudation of trap series basalts at the Blue Nile Gorge, Ethiopia" - Nature 254, 207–209.

Merla, G. and Minucci, E. (1938) - "Missione geologica nel Tigrai" - Roma, Regia Accademia Italiana.

Merla, G., Abbate, E., Canuti, P., Sagri, M. and Tacconi, P. (1979) - "Geological map of Ethiopia and Somalia and comment with a map of major landforms (scale 1:2,000,000)" - Consiglio Nazionale delle Ricerche, Rome. 95.

Minucci, E. (1938b) - "Ricerche geologiche nella regione del Tana" - In: Missione di Studio al Lago Tana. R. Accad. Ital. 1, 19–36.

Moglen, G. and Bras, R.L. (1995) - "The effect of spatial heterogeneities on geomorphic expression in a model of basin evolution" - Water Resour. Res. 31, 2613–2623.

Mohr, P.A. (1962) – "The geology of Ethiopia" - Addis Ababa: Addis Ababa University Press.

Mohr, P.A. (1967) – "The Ethiopian Rift System" - Bulletin of the Geophysical Observatory of Addis Ababa 11, 1–65.

Mohr, P., and Zanettin, B. (1988) – "The Ethiopian Flood Basalt Province" - In McDougall, J.D., ed., Continental Flood Basalts: Dordrecht, Netherlands, Kluwer Academic Publishers, 63–110.

Molin, P., Pazzaglia, F.J. and Dramis, F. (2004) - "Geomorphic expression of active tectonics in a rapidly deforming forearc, Sila Massif, Calabria, southern Italy" - American Journal of Science 304, 559–589.

Molin, P., Fubelli, G., Nocentini, M., Sperini, S., Ignat, P., Grecu, F. and Dramis, F. (2011) - "Interaction of mantle dynamics, crustal tectonics and surface processes in the topography of the Romanian Carpathians: A geomorphological approach" - Glob. Planet. Change, doi:10.1016/j.gloplacha.2011.05.005.

Montagner, J.P., Marty, B., Stutzmann, E., Sicilia, D., Cara, M., Pik, R., Leveque, J.-J., Roult, G., Beucler, E., and Debayle, E. (2007) – "Mantle upwellings and convective instabilities revealed by seismic tomography and helium isotope geochemistry beneath eastern Africa" - Geophysical Research Letters, v. 34, p. L21303, doi:10.1029/2007GL031098.

Montgomery, D.R. and Brandon, M.T. (2002) - "Topographic controls on erosion rates in tectonically active mountain ranges" - EPSL, 201, 481-489.

Moucha, R. and Forte, A.M. (2011) – "Changes in African topography driven by mantle convection" – Nature Geosc. Let. DOI: 10.1038/NGEO1235.

Nyblade, A.A., Owens, T.J., Gurrola, H., Ritsema, J. and Langston, C.A. (2000) - "Seismic evidence for a deep upper mantle thermal anomaly beneath east Africa" - Geology, 28(7), 599-602.

Nyblade, A.A. (2011) - " The upper-mantle low-velocity anomaly beneath Ethiopia, Kenya, and Tanzania: Constraints on the origin of the African superswell in eastern Africa and plate versus plume models of mantle dynamics" - Geol. Soc. Am., Special Paper 478.

Pazzaglia, F.J., Gardner, T.W. and Merritts, D.J. (1998) - "Bedrock fluvial incision and longitudinal profile development over geologic time scales determined by fluvial terraces" - In: Wohl, E., Tinkler, K. (Eds.), River Over Rock: Fluvial Processes in Bedrock Channels. : American Geophysical Union Geophysical Monograph, 107. American Geophysical Union, Washington, DC, pp. 207–235.

Pik, R., Deniel, C., Coulon, C., Yirgu, G., Hofmann, C. and Ayalew, D. (1998) - "The Northwest Ethiopian plateau flood basalts: classification and spatial distribution of magma types" - Journal of Volcanology and Geothermal Research 81, 91–111.

Pik, R., Marty, B., Carignan, J. and Lave, J. (2003) – "Stability of Upper Nile drainage network (Ethiopia) deduces from (U–Th)/He thermochronometry: Implication of uplift and erosion of the Afar plume dome" - Earth and Planetary Science Letters, v. 215, 73–88, doi: 10.1016/S0012-821X(03)00457-6.

Ponza, A., Pazzaglia, F.J. and Picotti, V. (2010) - "Thrust-fold activity at the mountain front of the Northern Apennines (Italy) from quantitative landscape analysis" - Geomorphology, 123, 211–231.

Ritsema, J., H. J. van Heijst and J. H. Woodhouse (1999) – "Complex shear wave velocity structure imaged beneath Africa and Iceland" - Science, 286, 1925–1928, doi:10.1126/science.286.5446.1925.

Ritsema, J. and van Heijst, H.J. (2000) - "New seismic model of the upper mantle beneath Africa" - *Geology,* **28**, 63–66.

Rizzini, A. and Dondi, L. (1978) - "Erosional surface of Messinian age in the subsurface of the Lombardian Plain (Italy)" - Mar.Geol., 27, 303-325.

Rizzini, A., Vezzani, F., Cococcetta, V. and Milad, G. (1978) - "Stratigraphy and sedimentation of a Neogene-Quaternary section in the Nile Delta area" - Mar. Geol., 27, 327-348.

Rosenbloom, N. A. and Anderson, R.S. (1994) - "Hillslope and channel evolution in a marine terraced landscape, Santa Cruz, California" - J. Geophys. Res., 99(B7), 14,013–14,029.

Roy, M., Jordan, T.H. and Pederson, J. (2009) - "Colorado Plateau magmatism and uplift by warming of heterogeneous lithosphere" - Nature 459, 978–982.

Salama, R.B. (1987) – "The evolution of the River Nile, The buried saline rift lakes in Sudan" - J. African Earth Sciences, 6(6), 899-913.

Schwanghart, W. and Kuhn, N.J. (2010) - "TopoToolbox: A set of Matlab functions for topographic analysis" - Environmental Modelling and Software, vol. 25(6), pp. 770-781.

Scotti, V.N., Molin, P., Faccenna, C., Soligo, M. and Casas-Sainz, A. (2013) - "The influence of surface and tectonic processes on landscape evolution of the Iberian Chain (Spain): Quantitative geomorphological analysis and geochronology" - Geomorphology, http://dx.doi.org/10.1016/j.geomorph.2013.09.017.

Şengör, A.M.C. (2001) – "Elevation as indicator of mantle-plume activity" - In Ernst, R.E., and Buchan, K.L., eds., Mantle Plumes: Their identification through time: Geological Society of America Special Paper 352, 183–225.

Snyder, N., Whipple, K.X., Tucker, G.E. and Merritts, D.J. (2000) – "Landscape response to tectonic forcing: digital elevation model analysis of stream profiles in the Mendocino triple junction region, northern California" - Geol. Soc. Am. Bull. 112 (8), 1250–1263.

Song, C., Hu, S., Han, W., Zhang, T., Fang, X., Gao, J. and Wu, F. (2014) - "Middle Miocene to earliest Pliocene sedimentological and geochemical records of climate change in the western Qaidam Basin on the NE Tibetan Plateau" - Palaeogeography, Palaeoclimatology, Palaeoecology, vol. 395, pp. 67-76.

Stern, R.J. (1994) - "Arc assembly and continental collision in the Neoproterozoic East African orogen" - Annual Review of Earth and Planetary Sciences 22, 319–351.

Stock, J. D. and Montgomery, D.R. (1999) - "Geologic constraints on bedrock river incision using the stream power law" - J. Geophys. Res., 104(B3), 4983–4993.

Strahler, A. (1952) - "Hypsometric (area–altitude) analysis of erosional topography" - Geol. Soc. Am. Bull. 63, 1117–1142.

Tarboton, D.G., Bras, R.L. and Rodríguez-Iturbe, I. (1989) - "Scaling and elevation in river networks" - Water Resour. Res. 25, 2037–2051.

Tefera, M, Cherenet, T and Haro, W (1996) – "Geological map of Ethiopia (1:2,000,000)" - Ethiopian Institute of Geological Survey, Addis Ababa, Ethiopia.

Tomkin, J.H., Brandon, M.T., Pazzaglia, F.J., Barbour, J.R. and Willett, S.D. (2003) - "Quantitative testing of bedrock incision models, Clearwater River, NW Washington State" - Journal of Geophysical Research 108 (B6), 2308. doi:10.1029/2001JB000862.

Tsige, L. and Hailu, E. (2007) – "Geological Map of Bure" – EIGS.

Ukstins, I.A., Renne, P.R., Wolfenden, E., Baker, J., Ayalew, D. and Menzies, M. (2002) – “Matching conjugate volcanic rifted margins: 40Ar39Ar chrono-stratigraphy of pre and syn-rift bimodal flood volcanism in Ethiopia and Yemen” - Earth and Planetary Sciences Letters 198, 289–306.

Vidal, L., Bickert, T., Wefer, G., and Rohl, U. (2002) - "Late miocene stable isotope stratigraphy of SE Atlantic ODP Site 1085: Relation to Messinian events" - Marine Geology, v. 180, p. 71–85, doi: 10.1016/S0025-3227(01)00206-7.

Wegmann, K.W. and Pazzaglia, F.J. (2002) - "Holocene strath terraces, climate change, and active tectonics: the Clearwater River basin, Olympic Peninsula, Washington State" - Geological Society of America Bulletin 114, 731–744.

Wegmann, K.W., Zurek, B.D., Regalla, C.A., Bilardello, D., Wollenberg, J.L., Kopczynski, S.E., Ziemann, J.M., Haight, S.L., Apgar, J.D., Zhao, C. and Pazzaglia, F.J. (2007) - "Position of the Snake River watershed divide as an indicator of geodynamic processes in the greater Yellowstone region, western North America" - Geosphere 3 (4), 272–281.

Weissel, J., Pratson, L.F. and Malinverno, A. (1994) - "The length-scaling properties of topography" - J. Geophys. Res. 99 (B7), 13997–14012.

Weissel, J., Malinverno, A. and Harding, D. (1995) – “Erosional development of the Ethiopian Plateau of Northeast Africa from fractal analysis of topography” - In: Barton, C.C., Pointe, P.R. (Eds.) “Fractals in Petroleum Geology and Earth Processes” - Plenum Press, New York, pp. 127–142.

Wells, S.G., Bullard, T.F., Menges, C.M., Drake, P.G., Karas, P.A., Kelson, K.I., Ritter, J.B. and Wesling, J.R. (1988) - "Regional variations in tectonic geomorphology along a segmented convergent plate boundary, Pacific coast of Costa Rica" - Geomorphology 1, 239–265.

Whipple, K.X. and Tucker, G.E. (1999) - "Dynamics of the stream-power river incision model: implications for height limits of mountain ranges, landscape response timescales, and research needs" - Journal of Geophysical Research, vol. 104, 17661-17674.

Whipple, K.X., Hancock, G.S. and Anderson, R.S. (2000) - "River incision into bedrock: mechanics and relative efficacy of plucking, abrasion, and cavitation" - Geological Society of America Bulletin 112, 490-503.

Whipple, K. (2004) - "Bedrock rivers and the geomorphology of active orogens" - Annual Review of Earth and Planetary Sciences, vol. 32, 151-185.

Whipple, K.X., Wobus, C., Crosby, B., Kirby, E. and Sheehan, D. (2007) - "New tools for quantitative geomorphology: extraction and interpretation of stream profiles from digital topographic data" - Geological Society of America Annual Meeting (Short Course Guide: http://www.geomorphtools.org, Denver).

Willgoose, G. and Hancock, G. (1998) - "Revisiting the hypsometric curve as an indicator of form and process in transport-limited catchment" - ESPL, 23, 611–623.

Williams, M.A.J., Adamson, D., Prescott, J.R. and Williams, F.M. (2003) – “New light on the age of the White Nile” - Geology, 31, 1001–1004.

Wobus, C., Whipple, K.X., Kirby, E., Snyder, N., Johnson, J., Spyropolou, K., Crosby, B. and Sheehan, D. (2006) - "Tectonics from topography: procedures, promise, and pitfalls" - In: Willett, S.D., et al. (Ed.), Tectonics, Climate, and Landscape Evolution: Geological Society of America Special Paper, 398, pp. 55–74.

Wolfenden, E., Yirgu, G., Ebinger, C., Deino, A. and Ayalew, D. (2004) – “Evolution of the northern Main Ethiopian rift: Birth of a triple junction” - Earth and Planetary Science Letters, v. 224, 213–228, doi: 10.1016/j.epsl.2004.04.022.

Wolfenden, E., Ebinger, C., Yirgu, G., Renne, P. and Kelley, S.P. (2005) – “Evolution of the southern Red Sea rift: birth of a magmatic margin” - Geological Society of America Bulletin 117, 846–864.

Woodward, J.C., Macklin, M.G., Krom, M.D. and Williams, M.A.J. (2007) – "The Nile: Evolution, Quaternary River Environments and Material Fluxes" – In "Large Rivers: Geomorphology and Management", Edited by A. Gupta, John Wiley and Sons, Ltd.

Zenebe, B. and Mariam, D.H. (2011) – "Geological Map of Yifag area" – EIGS.

CHAPTER 3*

LONG TERM DYNAMIC SUPPORT OF THE ETHIOPIAN SWELL

3.1 Introduction

The surface of the Earth is sculpted by a combination of processes in the crust, in the lithosphere, and at greater depth in the mantle (Molnar and England, 1990; Gurnis, 2001; Wobus et al., 2006; Boschi et al., 2010; Braun, 2010; Burbank and Anderson, 2011; Molin et al., 2011; Braun et al., 2013). Isostasy is considered a main controling process, explaining a large part of the topographic signal in the continents and in the oceanic plates. In addition to this "static" component of topography, another component may arise from density anomalies and resultant flow of the deeper mantle, what is commonly referred to dynamic topography. The long wavelength undulation observed in western (Moucha et al., 2008; Becker et al., 2014) and eastern North America (Rowley et al., 2013), Africa (Lithgow-Bertelloni and Silver, 1998; Moucha and Forte, 2011), Arabia (Daradich et al., 2003; Faccenna et al., 2013) and the small scale topography signal within the Mediterranean (Boschi et al., 2010), for example, have been explained in terms of mantle convection. An outstanding example to study the interaction and feedback between mantle and shallow surface is represented by regions where deep mantle upwellings are associated with large outpourings of volcanism, i.e. flood basalts. Ethiopia has long been recognized as a natural laboratory to study the interaction between mantle dynamics and surface processes because of the presence of the Main Ethiopian Rift (MER), Cenozoic continental flood basalt (CFB) volcanism, and plateau uplift (Ebinger and Casey, 2001; Nyblade and Langston, 2002; Furman et al., 2006; Bastow et al., 2008). Several models proposed that components of the African plate's elevation are related to the effect of dynamic topography (Lithgow-Bertelloni and Silver, 1998; Ritsema et al., 1999; Gurnis et al., 2000; Daradich et al., 2003; Forte et al., 2010; Moucha and Forte, 2011; Becker and Faccenna, 2011; Faccenna et al., 2013). These studies showed the presence of an anomalously high topography region (African Superswell) extending from the southeastern sector of the Atlantic Ocean basin to East Africa with an elevation ranging from few hundreds to almost two thousand meters (Gurnis et al., 2000) that may be related to the effect of a large plume.

*** This chapter will be submitted as: Sembroni, A., Faccenna, C. and Becker, T.W. (2015) - " Long term dynamic support of the Ethiopian Swell".**

The role of mantle plumes to explain Ethiopia's flood basalt and tectonics has been commonly accepted, but the location and number of plumes or mantle upwellings is debated (e.g., Schilling et al., 1992; Burke, 1996; Ebinger and Sleep, 1998; George et al., 1998; Courtillot et al., 1999; Rogers et al., 2000; Furman et al., 2006; Rogers, 2006). Recent works have proposed the existence of one (Ebinger and Sleep, 1998; Furman et al., 2006) or two plumes (George et al., 1998; Rogers et al., 2000) impinging the base of the continental lithosphere. Another source of uncertainty derives from the amount and timing of uplift. The Ethiopian Plateau presents an almost flat physiography with an average elevation of 2500 m a.s.l.. This configuration may have been attained before (Pik et al., 2003) or after (Gani et al., 2007) the flood basalt emplacement.

This study explores the topographic and geological configurations of the Ethiopian Plateau and surrounding areas, quantifying the dynamic and isostatic contributions in order to reconstruct the pre-trap topography and to trace the uplift pattern evolution. Our reconstruction shows that most of the present-day topography was already acquired prior to the emplacement of the flood basalts.

3.2 Geological setting

The Ethiopian Plateau is almost entirely covered with extensive Tertiary (Zumbo et al., 1995; Baker et al., 1996a; Hofmann et al., 1997; Rochette et al., 1998) continental flood basalts (500 - 1500 m in thickness; Minucci, 1938b; Jepsen and Athearn, 1961; Mohr and Zanettin, 1988). Such deposits overlie an alternation of Mesozoic and Tertiary sandstones and limestones unconformably located on a crystalline basement (Kebede, 2013) (**Fig.24b**). Basement rocks are part of the Arabian–Nubian Shield and record folding, compression and metamorphism due to the collision between east and west Gondwana (Stern, 1994). Such collision is marked by north- to east trending sutures (Corti, 2009).

The Trap eruption occurred through fissures (Mohr and Zanettin, 1988) mostly controlled by Precambrian zones of weakness (Mege and Korme, 2004). This event was concomitant with the Red Sea–Gulf of Aden continental rifting (Late Oligocene; Wolfenden et al., 2005), but predates the development of the MER (Middle-Late Miocene; Wolfeden et al., 2004; Bonini et al., 2005). Limited volumes of basalts as old as 45 Ma have been described in southern Ethiopia, separating the MER from the Kenya rift (Davidson and Rex, 1980; Ebinger et al., 1993; George et al., 1998). The location of the fissures system is uncertain. The chemical composition of the flood basalts

supports a magma genesis from a broad region of mantle upwelling, heterogeneous in terms of temperature and composition (Kieffer et al., 2004).

Immediately after the peak of flood basalts emplacement, a number of large shield volcanoes developed from 30 Ma to about 10 Ma on the surface of the basaltic plateau (Kieffer et al., 2004) rising 1000–2000 m above the original plateau surface (Mohr and Zanettin, 1988; Kieffer et al., 2004) (**Fig.24b**).

Since the early Miocene (Hagos et al., 2010; Natali et al., 2013) the northernmost sector of Ethiopia experienced an intense magmatic activity with the formation of huge intrusive bodies (Adwa Plugs and Mekele Dolerite). Since the late Pliocene, magmatic and tectonic activities moved mainly into the axial sector of the rift and in the Afar depression (Ebinger, 2005).

The Ethiopian Plateau is confined on the western and eastern sides by two huge escarpments: Lake Tana and Afar escarpments (**Fig.24a**). Lake Tana is confined to the western portion of the plateau and lies at the convergence of three Mesozoic grabens: the Debre Tabor graben from the east, the Gondar graben from the north-northwest, and the Dengel Ber graben from the south-southwest (Chorowicz et al., 1998). The Tana escarpment develops on the western side of the lake and is considered an erosional feature formed by scarp retreat since the deposition of Trap (Grabham and Black, 1925; Minucci, 1938b; Dainelli, 1943; Comucci, 1950; Jepsen and Athearn, 1961; Mohr, 1967; Hahn et al., 1977; Chorowicz et al., 1998; Gani et al., 2008). The Afar escarpment was formed by the tectonic unloading due to rift extension (Weissel and Karner, 1989; Weissel et al., 1995). The Ethiopian Plateau is drained by two main rivers: the Blue Nile and the Tekeze, respectively from south and north (**Fig.24a**).

The present day topography of the Ethiopian Plateau partly resulted from large spatial extent uplift, but the timing is still uncertain (e.g., Pik et al., 2003; Gani et al., 2007). Early works (e.g., Dainelli, 1943; Beydoun, 1960) suggested uplift to be of Upper Eocene in age and to precede both the flood basalts event and the main rifting episodes (see Mohr, 1962). Later studies (e.g., Mohr, 1967; Merla et al., 1979) argued against major uplift before the flood basalts event and suggested a complex history of uplift and volcanism during the Tertiary (e.g., Baker et al., 1972; McDougall et al., 1975; Berhe et al., 1987). Pik et al. (2003), based on thermochronological and morphological analysis on the Blue Nile drainage system, argued that erosion initiated in the Blue Nile canyon as early as 25–29 Ma ago and the elevated plateau physiography existed since Late Oligocene. More recent analysis based on the incision of the 1.6-km-deep Gorge of the Nile (Gani et al., 2007) suggests that ~2 km uplift occurred episodically in three different phases since ~29 Ma.

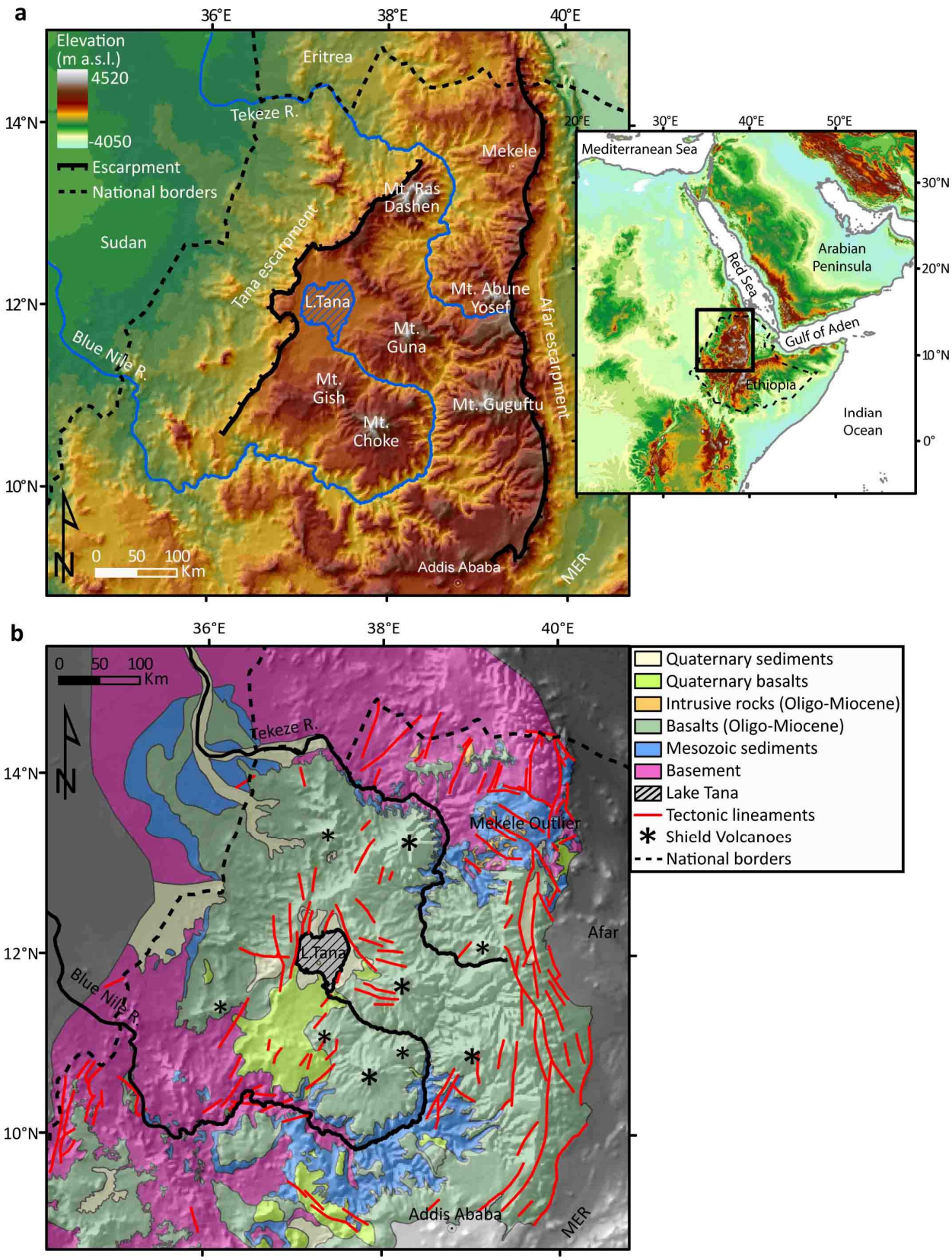

Figure 24 - a) Topography of the Ethiopian Plateau area (ETOPO1 DEM). The black box in the inset indicates the location of the study area and the Ethiopian national boundaries; **b**) geological map of the study area compiled from the 1:2.000.000 (Tefera et al., 1996) and the available 1:250.000 scale maps (Hailu, 1975; Kazmin, 1976; Garland, 1980; Tsige and Hailu, 2007; Chumburo, 2009; Zenebe and Mariam, 2011) of Ethiopia draped over the shaded topography.

3.3 Reconstructing topographic evolution

Topography in the Ethiopian Plateau arises from four major processes: 1) impinging of hot asthenospheric material at the base of lithosphere (Eocene; Ebinger and Sleep, 1998); 2) loading due to deposition of basalts (Late Oligocene; Zumbo et al., 1995; Baker et al., 1996a; Hofmann et al., 1997; Rochette et al., 1998) and formation of shield volcanoes (from Oligocene to Miocene; Kieffer et al., 2004); 3) erosional unloading (since Late Oligocene; Pik et al., 2003; Gani et al., 2007); 4) flexural uplift on the eastern side during the rifting phase (Late Miocene; Wolfeden et al., 2004; Bonini et al., 2005) and on the western side due to the strong erosion of the basalts at the base of Tana escarpment.

We investigated topography at a regional scale by a GIS-based analysis adopting, as digital data source, the ETOPO1 global relief model (downloaded from http://www.ngdc.noaa.gov/), 1 arc-minute in resolution. The aim was to reconstruct the evolution of topography through time by a separation and a quantification of each contribution.

3.3.1 Flexural isostasy

Flexural isostasy is the deflection of Earth's lithosphere under loads that are regionally, rather than locally (Airy) compensated. Flexural lithosphere can be modeled as an elastic layer of finite thickness, typically taken down to the base of the lithospheric mantle, responding to surface loads (Pelletier, 2008). The flexural isostasy model assumes: 1) force balance within the lithosphere achieved not only hydrostatically by density heterogeneities but also by elastic stresses; 2) mechanical interaction between neighboring crustal blocks with shear stresses between vertical columns; 3) compensation of the lithosphere by an elastic plate overlying viscous mantle (Ebinger et al., 1989; D'Agostino et al., 1998).

3.3.1.1 Flexural uplift of the rift shoulder

The displacement occurring along a fault generates mechanical unloading of the lithosphere and a consequent isostatic response (Weissel and Karner, 1989). In a rift system the expression of this process is the flexural uplift of rift shoulders (Buck, 1988; King et al., 1988; Stern and Brink, 1989; Weissel and Karner, 1989; Poulimenos and Doutsos, 1997; D'Agostino et al., 1998; Brown and Phillips, 1999; Mueller et al., 2005; Mueller, 2009; Sachau and Koehn, 2010).

We modeled the uplift of rift flanks as a flexural isostatic response to unloading of the lithosphere due to extension (**Figs.25a**). The vertical displacement *w(x)* due to flexural uplift given by Turcotte and Schubert (1982) for the case of a broken lithosphere is:

$$w(x) = w_0 e^{-x/\alpha} \cos\frac{x}{\alpha} \quad (5)$$

$$w_0 = \frac{V_0 \alpha^3}{4D} \quad (6)$$

$$V_0 = \rho g (x_a + x_b)\frac{h}{2} \quad (7)$$

$$D = \frac{E T_e^3}{12(1-\nu^2)} \quad (8)$$

$$\alpha = \left(\frac{4D}{g(\rho_m - \rho_a)}\right)^{1/4} \quad (9)$$

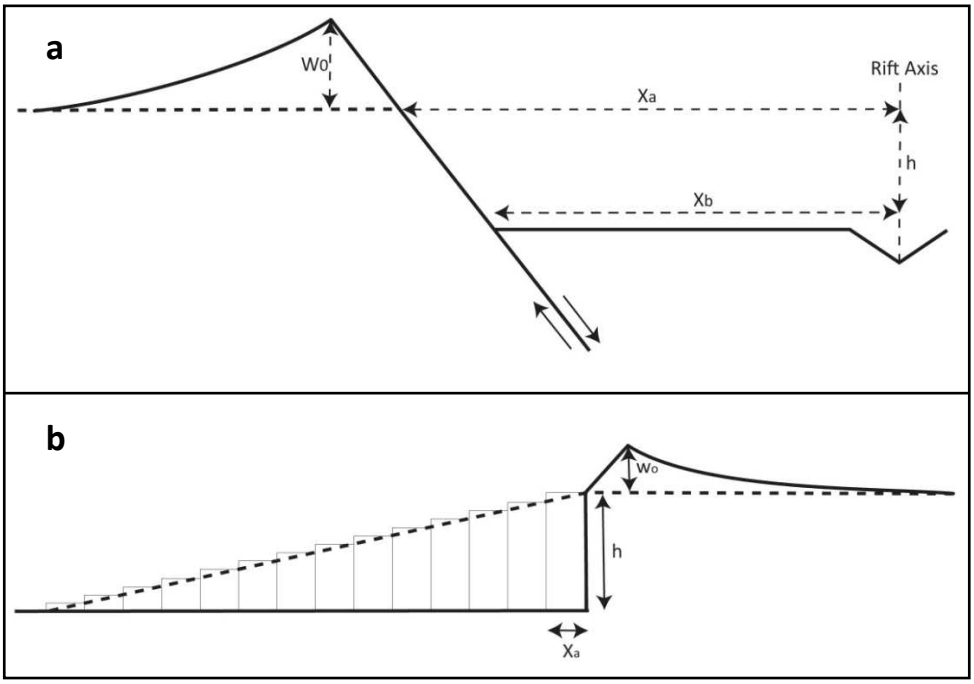

Figure 25 – Geometric schemes adopted in the numerical model of flexural uplift along the rift (**a**) and Tana escarpments (**b**) (see text for further explanations).

where w_0 is the (maximum) vertical displacement caused by the flexure (**Fig.25a**), V_0 is the weight of material displaced by the fault, x_a is the distance between the rift axis and the top of the escarpment (**Fig.25a**), x_b is the distance between the rift axis and the bottom of the escarpment (**Fig.25a**), h is the vertical displacement along the fault (**Fig.25a**), α is the flexural wavelength, D is

the flexural rigidity, T_e is the equivalent elastic thickness of the lithosphere (it corresponds to the

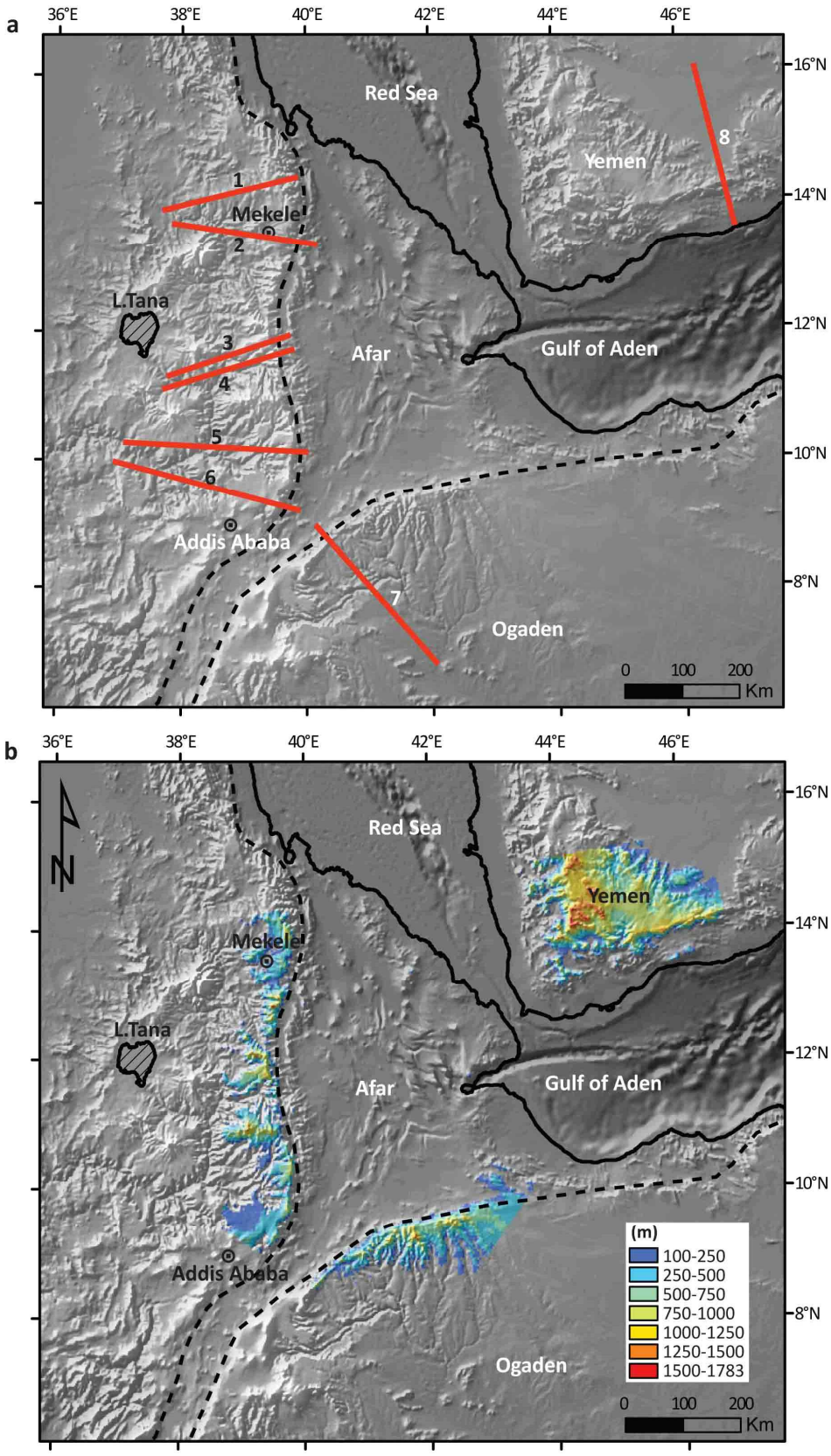

Figure 26 - a) Location map of the eight topographic profiles (Fig.26) used to model the flexural uplift along the rift escarpments (ETOPO1 DEM database). The locations of Lake Tana, the rift borders (dashed black lines) and the coast line (solid black lines) are shown for reference; **b)** map of the areal distribution of flexural uplift.

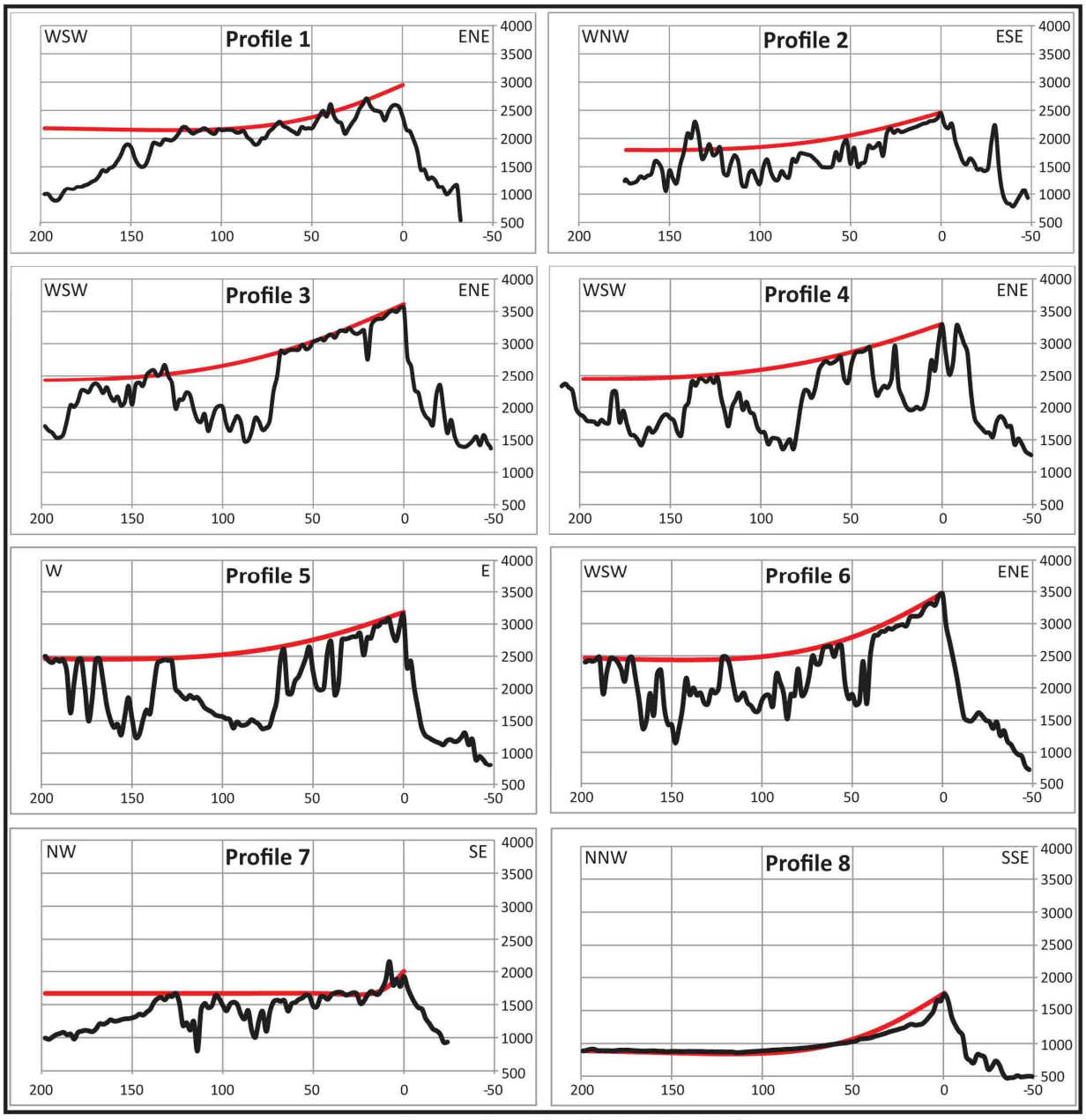

Figure 27 - Comparison between the observed topography (solid black lines) and the curves obtained by the rift escarpments flexural uplift analytical model (solid red lines).

thickness of an idealized elastic beam that would bend similarly to the actual lithosphere under the same applied loads - Watts, 2001), g is the gravity acceleration, ρ_m is the mantle density, ρ_a is the air density.

To be consistent the model curves *w(x)* have to fit the real topography. Such fit can be achieved by comparing curves with residual topography (Brown and Phillips, 1999; Dadarich et al., 2003), observed topography (Stern and Brink, 1989; Weissel and Kerner, 1989; Ten Brink and Stern, 1992; van der Beek, 1997; Basile and Allemand, 2002; Mueller et al., 2005), bathymetric profiles (Bodine

et al., 1981), swath topography (Mueller et al., 2009), maximum topographic envelope (Poulimenos and Doutsos, 1997) or mean topography (Ebinger et al., 1991; Watts et al., 2000).

The widespread presence of plateau remnants flattens the Ethiopian Plateau topography. In such physiography, the mean topography closely approximates the maximum and minimum ones. For this reason we chose to fit model curves with eight topographic profiles orthogonal to rift shoulders using the Monte Carlo method (**Figs.26a-27**). We fixed the ranges of x_a (10 - 150 km)*, h* (1 - 4.5 km) *and* α (20-250 km) and let the other parameters to vary. Each run was made of 100000 iterations. At every step the script calculated the fitting RMS error and chose the combination of values with lowest RMS (**Fig.27**).

3.3.1.2 Flexural uplift of the Tana escarpment

The Tana escarpment is an erosional feature formed by scarp retreat (**Fig.28a**) (Grabham and Black, 1925; Minucci, 1938b; Dainelli, 1943; Comucci, 1950; Jepsen and Athearn, 1961; Mohr, 1967; Hahn et al., 1977; Chorowicz et al., 1998; Gani et al., 2008). We modeled the uplift of Tana escarpment as the flexural isostatic response to unloading of the lithosphere due to erosion. The uplift of the upper part of the escarpment is continuous and migrates as the erosion progresses. According to the present flood basalts outcrops in Sudan, the total Tana escarpment retreat ranges between 150 and 300 km since the deposition of the Traps (~30 Ma; Zumbo et al., 1995; Baker et al., 1996a; Hofmann et al., 1997; Rochette et al., 1998) with an average retreat rate of 5-10 km/Ma. Given this rate we divided the total retreat distance into 30 parts (**Fig.25b**). Each part covers a time interval of 1 Ma and is characterized by an escarpment retreat of 5-10 km. The eroded area in a single step has been approximated in 2D as the area of a rectangle with base varying from 5 to 10 km and height corresponding to the height of the escarpment (**Fig.25b).** The vertical displacement *w(x)* due to flexural uplift is given by Turcotte and Schubert (1982) for the case of a unbroken lithosphere as:

$$w(x) = w_0 e^{-x/\alpha}\left(\cos\frac{x}{\alpha} + \sin\frac{x}{\alpha}\right) \quad (10)$$

$$w_0 = \frac{V_0\alpha^3}{8D} \quad (11)$$

$$V_0 = \rho g(x_a h) \quad (12)$$

where w_0 is the (maximum) vertical displacement caused by the flexure (Fig.25b), V_0 is the weight of the eroded material, x_a corresponds to the retreat distance of the escarpment in 1 Ma (Fig.25b), h is the escarpment height, α is the flexural wavelength, D is the flexural rigidity, g is the gravity acceleration, ρ is the basalt density.

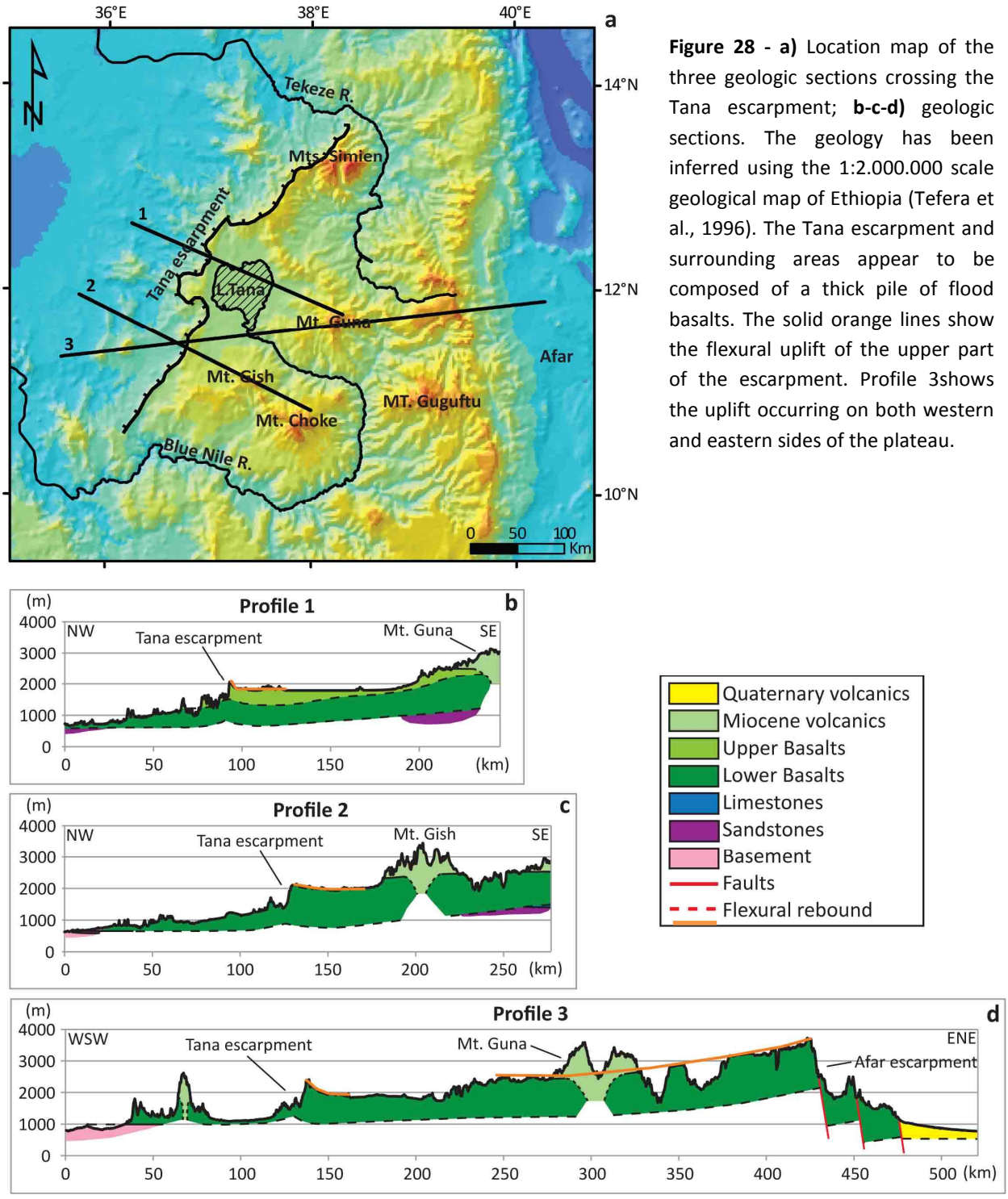

Figure 28 - a) Location map of the three geologic sections crossing the Tana escarpment; **b-c-d)** geologic sections. The geology has been inferred using the 1:2.000.000 scale geological map of Ethiopia (Tefera et al., 1996). The Tana escarpment and surrounding areas appear to be composed of a thick pile of flood basalts. The solid orange lines show the flexural uplift of the upper part of the escarpment. Profile 3shows the uplift occurring on both western and eastern sides of the plateau.

As for the case of rift shoulder uplift we fit the model curves *w(x)* with two topographic profiles (**Fig.28b-c**) using the Monte Carlo method. We fixed the ranges of x_a (5000-10000 m), *h* (100-3000 m) and α (1000-150000 m) and let the other parameters to vary. The results are listed in **Table 8**.

The flexural model of the rift shoulder shows that the process deformed surface up to a distance of 150 km from the rift escarpment in agreement with Weissel et al. (1995) (**Fig.27**). The maximum vertical displacement (w_0) on the Ethiopian Plateau varies from about 700 m up to 1150 m (**Table 8; Figs.26b-27**).

The flexural model of the Tana escarpment caused the warping of basalts up to a distance of 30 km from the escarpment. The flexural uplift ranges between 120 and 260 m (**Table 8**; **Fig.28**).

The Yemen highlands are characterized by anomalous high values of flexural uplift (up to 1700 m) (**Fig.26b**). According to Dadarich et al. (2003) this is related to the combine effect of the flexural uplift of rift shoulders and the dynamically supported tilting of the Arabian plate eastward. The equivalent elastic thickness (T_e) ranges between 22 and 43 km along the rift shoulder and between 51 and 57 km at the Tana escarpment, while the flexural rigidity (*D*), in both cases, is comprised between 10^{22} and 10^{23} Nm (**Table 8**). These data are largely in agreement with the previous studies (Forsyth, 1985; Ebinger et al., 1989; McKenzie and Fairhead, 1997; Pérez-Gussinyé et al., 2009) who estimated effective elastic thickness from Bouguer and free air gravity anomalies all over the East Africa Rift System.

Table 8 – Results of the flexural uplift numerical models for rift and Tana escarpments.

	Vo (N) · 10^{12}	w_o (m)	Xa (m)	Xb (m)	h (m)	D (N) · 10^{22}	Te (m)	α (m)	RMS (m)
Flexural parameters at rift escarpment									
Profile 1	7.08	748.40	132306.28	1440.05	2460.29	5.32	25537.85	54078.79	45.08
Profile 2	9.77	623.31	1593.00	1627.35	3461.65	11.40	31226.10	67361.59	70.26
Profile 3	11.80	1112.49	47770.03	2255.16	3043.02	53.30	43311.28	88902.74	45.65
Profile 4	13.70	801.33	84736.04	1520.75	2818.93	46.70	34607.81	84387.79	12.67
Profile 5	0.92	683.76	5907.66	2283.10	3418.56	39.60	39511.49	70336.75	30.87
Profile 6	6.57	972.69	38745.63	2391.22	3710.90	10.40	26232.68	60544.22	66.00
Profile 7	13.40	331.51	187559.20	728.10	3726.82	2.40	35331.81	10939.36	75.44
Profile 8	14.50	725.26	106862.80	1542.99	1599.30	2.54	22658.93	45342.12	8.06
Flexural parameters at Tana escarpment									
Profile 1	0.14	247.26	9520.55		1530.55	0.41	51132.33	3000.72	46.26
Profile 2	0.03	134.55	8706.66		1812.81	1.46	55659.22	11781.72	32.37

3.3.2 Basalts loading and erosional unloading

Assuming Airy isostasy conditions (no elastic support of loads by crust and mantle) we quantified the unloading due to erosion and loading due to basalt emplacement.

Theoretically, given typical crustal (ρ = 2750 Kg/m^3) and mantle (ρ = 3300 Kg/m^3) densities, crustal thickening drives a rock uplift of roughly 20% of the change in crustal thickness, while the rest results in lowering of the Moho (Molnar and England, 1990; Anderson and Anderson, 2010; Burbank and Anderson, 2011). Conversely, the erosion of a certain amount of material across a broad surface causes the lowering of the valleys and a consequent lowering of the mean topography surface corresponding to 20% of the eroded material thickness; the rest goes into pulling up the base of the Moho (Molnar and England, 1990; Anderson and Anderson, 2010; Burbank and Anderson, 2011).

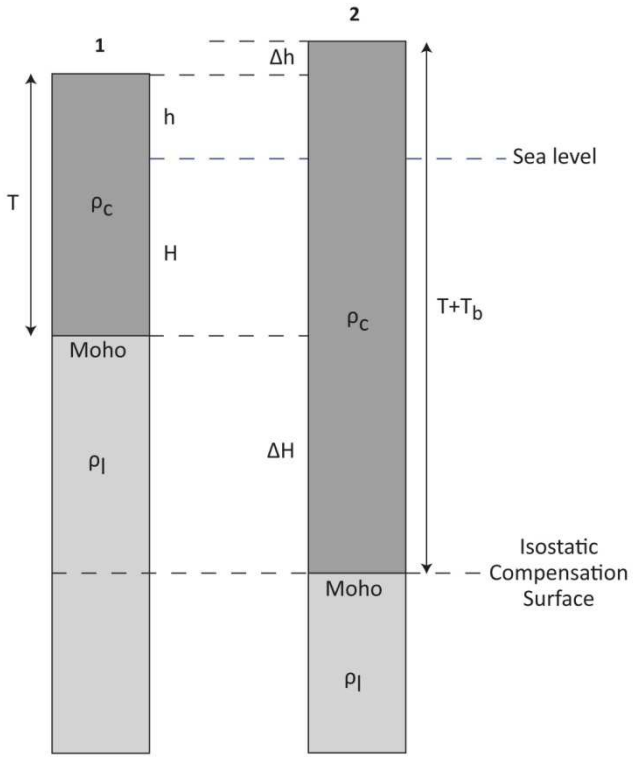

continental flood basalt emplacement. Deepening of the Moho greatly exceeds the increase of the continental elevation above sea level (modified after Anderson and Anderson, 2010).

In this work we used the flood basalts base surface as reference frame for isostatic calculations. The surface has been elaborated by mapping the geologic contacts crystalline basement - basalts and Mesozoic sediments - basalts and correcting the elevation values along the rift shoulder and Tana escarpment by flexural uplift calculated in section 3.3.1 (**Table 8**).

Using a constant lithospheric mantle thickness and using typical basalt (ρ_c = 2800 Kg/m^3) and asthenosphere (ρ_l = 3230 Kg/m^3) densities we calculated the subsidence due to basalts loading and the rock uplift resulted from erosional unloading. In **figure 29** a column of continental crust material of thickness *T* is in isostatic balance (column 1). It floats with a mean elevation *h* above sea level and a depth to the Moho of *H* below sea level. When the huge eruption of continental flood basalts occurred the crust thickened by a value of T_b (basalts thickness) (column 2). The pressure (P) at an arbitrary depth within the mantle beneath the base of the crust must be the same in the two cases:

$$P_1 = P_2 \quad \rightarrow \quad \rho_c T g + \rho_l \Delta H g = \rho_c (T + T_b) g \quad \rightarrow \quad \Delta H = \frac{\rho_c}{\rho_l} T_b \qquad (13)$$

Where ΔH quantifies the lowering of pre-Trap surface after the basalts loading.

Using the density values from above, the term in the brackets becomes 0.87. This means that the thickening of the crust causes a subsidence of the pre-Trap topography equal to 87% of the basalts thickness and an increase in the the final mean topography equal to 13% of the basalts thickness.

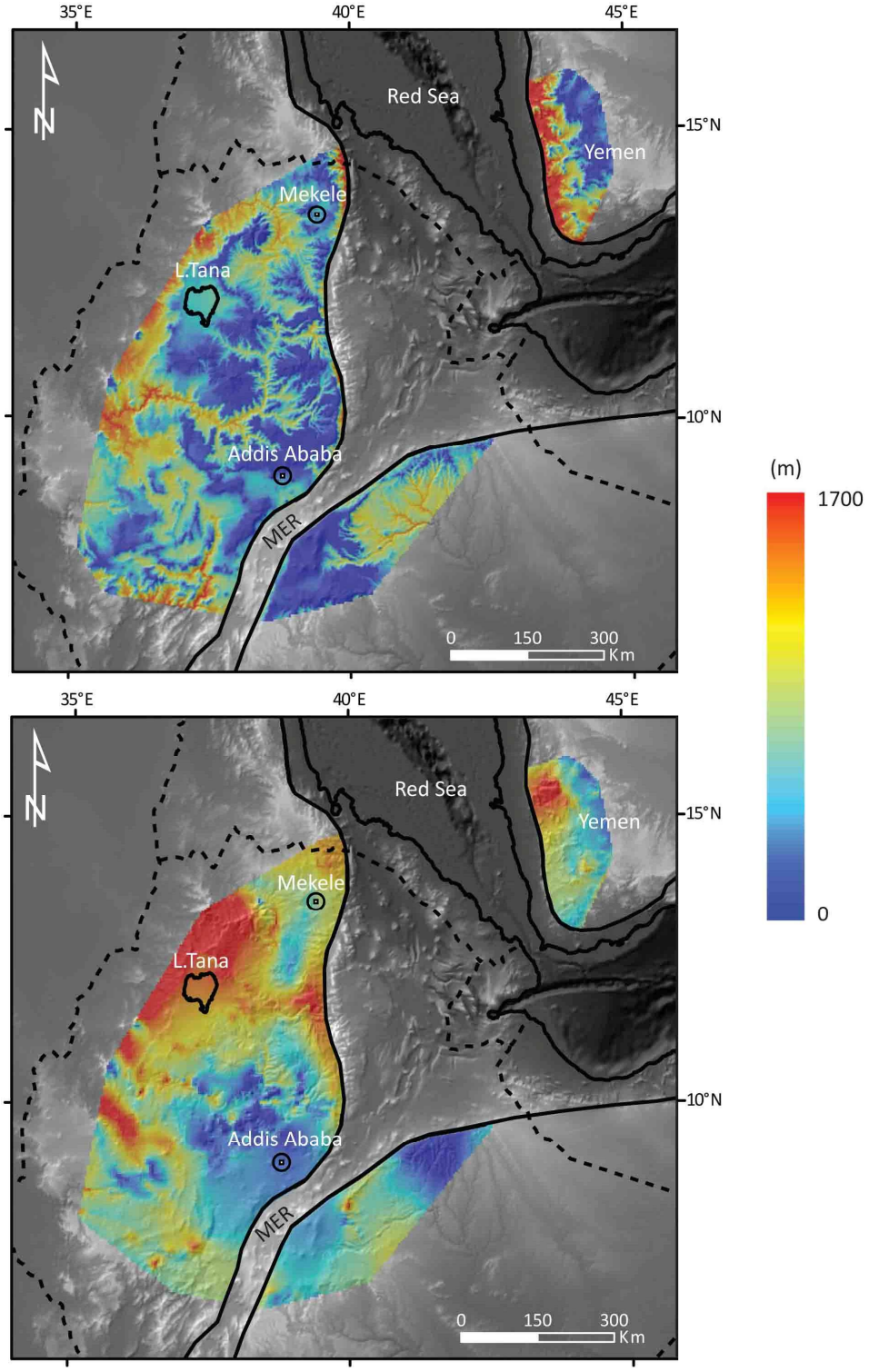

Figure 30 - Maps of the isostatic contributions to topography due to erosional unloading (**a**) and basalts loading (**b**).

In the case of the erosion we used again equations (13) but with $-T_d$ replacing T_b, where T_d is the thickness of the eroded materials. We obtained a rock uplift of the pre-Trap topography

corresponding to 87% of the eroded material thickness ($\Delta h = 87\% T_d$). Consequently the final mean topography results to be 13% of the eroded material thickness lower than the previous one. To quantify such isostatic contributions for the whole study area we used the basalts thickness and erosion maps data elaborated in the chapter 1 of this thesis (**Fig.6**). In particular we calculated the 87% of the value characterizing each pixel of both maps. We obtained the maps of the isostatic contributions of erosional unloading (**Fig.30a**) and Trap loading (**Fig.30b**).

3.3.3 Pre-trap topography

The pre-Trap topography has been restored by subtracting the erosional unloading contribution and adding the loading one from each pixel of the "pre-flexural" Trap base surface. To extract the large–scale signal, we filter the resulted topography by a 50 km in radius circular window (**Fig.31a**). To better understand the geometry of the pre-Trap residual topography with respect to the present flood basalts top and base surfaces, we projected the surfaces into two topographic profiles (**Figs.31b-c**). Such profiles have been extracted from the ETOPO1 DEM and intersect each other at the Addis Ababa area. Profile 1 (**Fig.31b**) has a NW-SE direction and starts from the Sudan lowlands up to the Ogaden basin. Profile 2 presents a NNE-SSW trend and starts from the southern sector of Ethiopia up to Eritrea passing across the Addis Ababa and Mekele cities (**Fig.31c**). The pre-trap topography (**Fig.31a**) presents a 2600 m high bulge elongate in a N-S direction from Addis Ababa to the eastern rift side. Elevation decreases all around up to 700 m a.s.l. at a distance of ~500 km from the Addis Ababa high, giving a net maximum elevation of ~1900 m. The only exception is the Mekele sector which presents elevations comprised between 2000 and 2400 m a.s.l.. The bulge area is characterized by the lowest flood basalts thickness (~300 m). Profile 2 (**Fig.31c**) shows a large depression between the Addis Ababa and Mekele regions. The present bottom of such feature stands at ~1250 m a.s.l. while the pre-Trap elevation is ~1750 m a.s.l. (**Fig.31a**). In correspondence of this area the basalts present the maximum thickness (between 1000 and 1500 m) (**Fig.31c**).

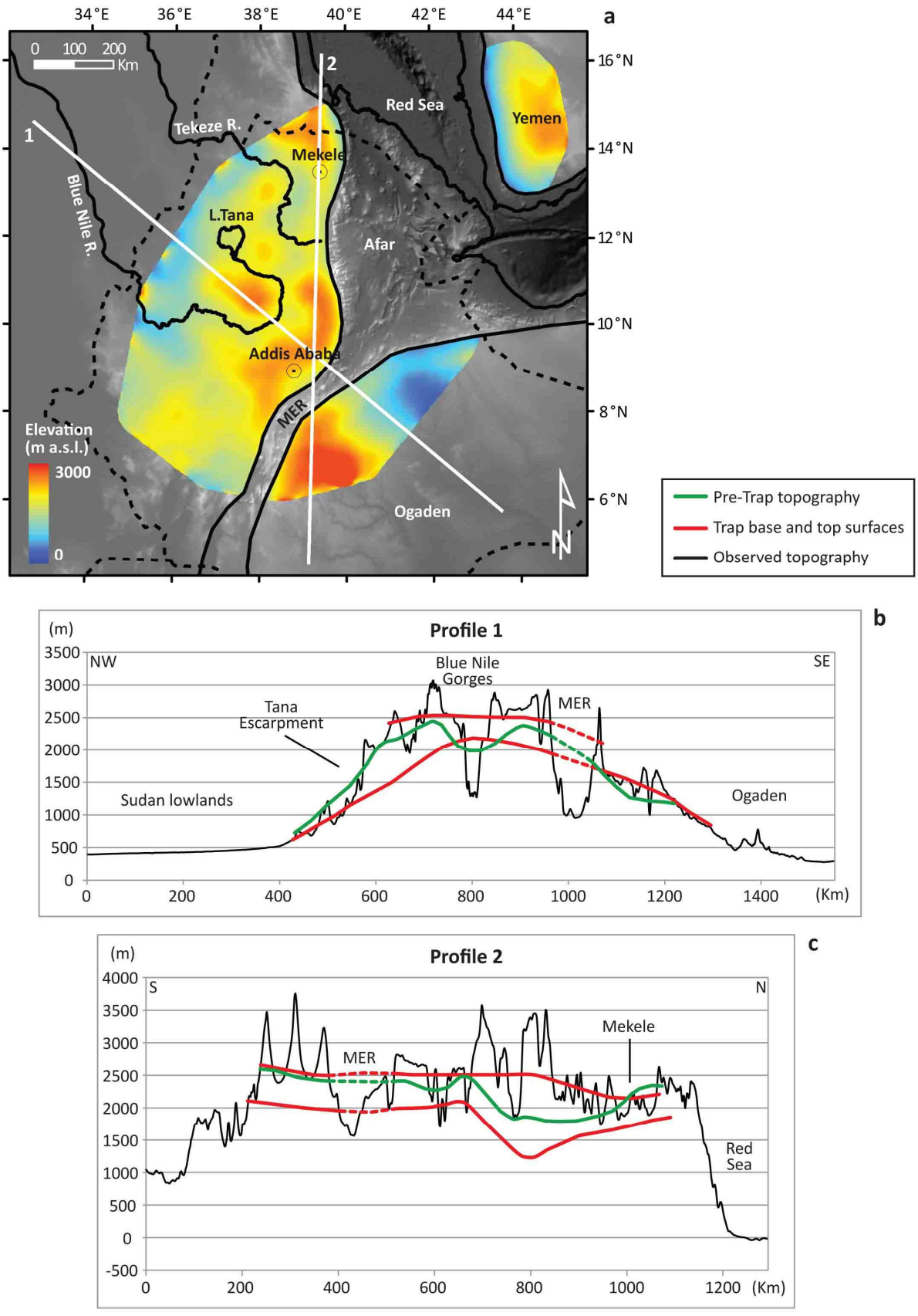

Figure 31 - a) Pre-trap topography map; **b-c)** topographic profiles (solid white lines) with the projections of flood basalts base and top surfaces (red lines) and the pre-trap topography surface (green lines).

The isostatic contributions due to erosional unloading and basalts loading played an important role in changing the pre-Trap topography (**Figs.30a-b**). In particular the erosional unloading is maximized along the Blue Nile and Tekeze rivers major valleys and west of the Tana escarpment (**Fig.30a**). The Trap loading caused up to ~1600 m of subsidence in the area of maximum basalts thickness (**Fig.30b**). The profiles in **figure 31** show that the pre-trap surface (green line in **Figs.31b-c**) is always at higher elevations with respect to the present Trap base surface (red line in **Figs.31b-c**) with the exception of the areas subjected to strong erosion (i.e Blue Nile valley and the eastern shoulder of central MER) where the erosional unloading contribution was much higher than basalt loading one.

3.3.4 Residual topography.

We estimated the residual topography in the area (**Fig.32b**) by subtracting from the actual, smoothed topography (50 km in wavelength circular window) the Airy isostasy predicted topography and the along rift margins flexural isostasy. Crustal thickness is obtained by merging of CRUST 1.0 (Laske et al., 2013) with receiver function Moho depth estimates (Bastow et al., 2011). We also used a 60 km constant lithospheric mantle thickness of density 3250 kgm^{-3}, with a crustal and asthenosphere density of 2831 Kgm^{-3} and 3226 Kgm^{-3}, to minimize residual topography.

The residual topography map (**Fig.32b**) presents high values in Yemen (up to 2000 m, but here crustal thickness is poorly constrained) and in the the Afar (up to 1500 m). On the plateau, we observe a positive residual topography of ~500-600 m with peaks in the Addis Ababa high (up to 1000 m), in the Mekele area (up to 1200 m), along the Somalian rift margins (up to 1400 m).

3.3.5 Dynamic topography

To test the idea that the residual topography is related to the presence of mantle plumes, we estimated the expected dynamic component of topography (z_{dyn}) induced by instantaneous mantle flow due to density anomalies in the mantle, as inferred from *P*-wave seismic tomography models (**Fig.32c**). This deflection may be inferred from the radial tractions acting upon a free-slip surface boundary in an incompressible, Newtonian fluid spherical annulus with only radial viscosity variations (for details, see Becker et al., 2014). The density model was constructed by scaling the seismic velocity structure to temperature (e.g., Ricard et al., 1984, 1993; Hager, 1984; Le Stunff and Ricard, 1995; Panasyuk and Hager, 2000; Becker and Faccenna, 2011).

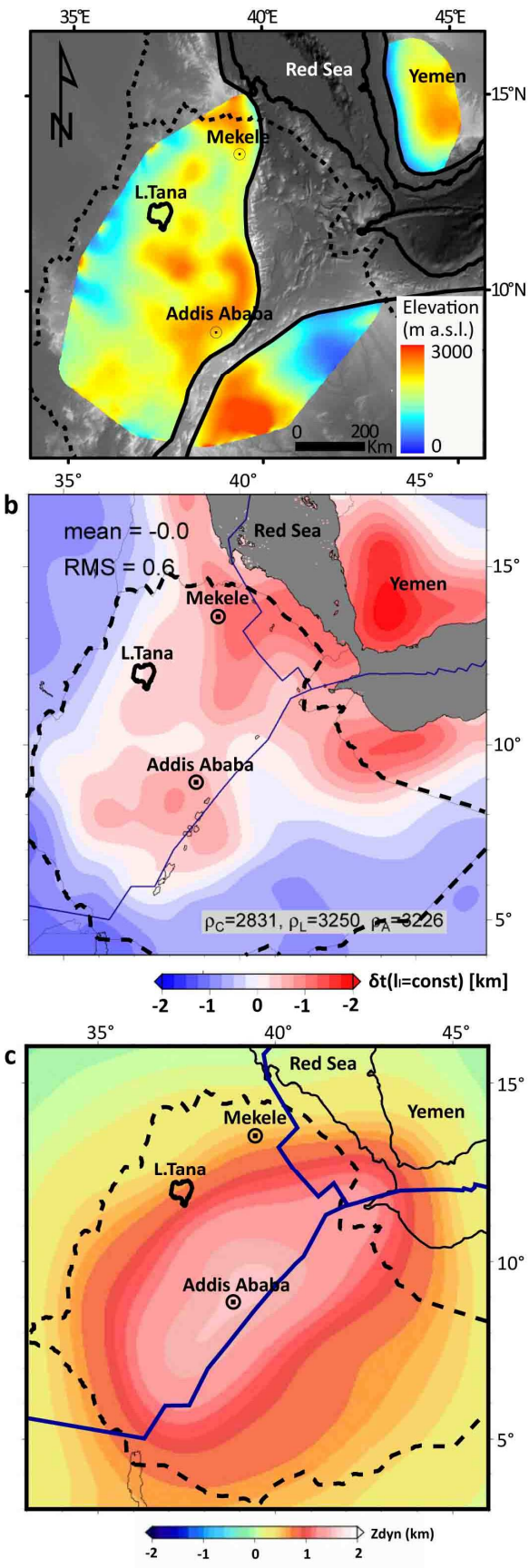

Figure 32 - Comparison between pre-Trap topography (a) and the present residual (b) and dynamic (c) topographies.

All velocity anomalies below 100 km are scaled with a constant velocity to density ratio of $d\ln\rho/d\ln v_{P=}=0.4$ (no anomalies above 100 km). The resulting dynamic topography map (**Fig.32c**) from mantle flow has been obtained by removing long-wavelength (spherical harmonic degree L < 12) signatures to emphasize the regional contributions from upper mantle structure. The tomographic model used is a merger between the HNB12 P-wave tomography (Hansen et al., 2012) and the ETH08 regional tomography (Bastow et al., 2008).

Results show a regional dynamic positive topography, ellipsoidal in shape and centered in Addis Ababa with value of up to 1500 m. Such feature is almost parallel to the MER axis (SW-NE trend) elongating from the southern sector of Ethiopia to the Gulf of Aden. The elevation gradually decreases down to 0 m outside Ethiopian borders.

We compared the dynamic topography obtained with the pre-Trap topography (**Fig.32**) in order to characterize the physiographic evolution of the area since Oligocene and, by so doing, to quantify the rock uplift pattern.

3.4 Discussion

The present topographic configuration of the Ethiopian Plateau is the result of a complex interaction of several geologic processes. The area was characterized in the Late Eocene by the impinging of hot asthenospheric material at the base of the lithosphere (Ebinger and Sleep, 1998; Şengör, 2001). Such event caused a dome-like uplift. Moreover, in two distinct periods (45 Ma [Davidson and Rex, 1980; Ebinger et al., 1993; George et al., 1998] and 30-28 Ma [Zumbo et al., 1995; Baker et al., 1996a; Hofmann et al., 1997; Rochette et al., 1998]), a huge amount of continental flood basalts came out loading the surface. In the same time erosion started determining a general unloading of the surface and the flexural uplift of the western side of the plateau. In the late Miocene the northern and central segments of MER formed (Wolfeden et al., 2004; Bonini et al., 2005) causing the isostatic flexure of the rift shoulders.

The analysis of physiography and geology of the Ethiopian Plateau permitted us to quantify each isostatic contribution in order to delineate the topographic evolution of the area.

The flexural model of rift escarpment demonstrates that the surface deformation reached a maximum distance of 150 km from the rift shoulder (**Fig.27**). The amount of maximum vertical displacement in the Ethiopian Plateau varies between 700 and 1150 m (**Table 6**). The values of equivalent elastic thickness (T_e) and rigidity (D) of the lithosphere obtained from the model (**Table 8**) are in agreement with the previous studies (Forsyth, 1985; Ebinger et al., 1989; McKenzie and Fairhead, 1997; Petit and Ebinger, 2000, Pérez-Gussinyé et al., 2009). In particular T_e ranges between 22 and 43 km with an average of about 33 km. Such values are comprised between rift and internal plateau T_e estimates (21 and 49 km respectively; Ebinger et al., 1989) and are influenced mainly by the combine effect of high regional horizontal stresses, local thermal anomalies, and the presence of preexisting mechanical heterogeneities (Chery et al., 1992).

On the western side of the plateau the Tana escarpment is the result of a combination between erosional processes and flexural response of the lithosphere to the corresponding redistribution of mass across the landscape (Gilchrist et al., 1994; ten Brink and Stern, 1992; van der Beek et al., 2002; Petit et al., 2007). The escarpment evolution is strictly dependent on a number of factors such as initial topography, lithology, interior catchment base-level lowering, climate change and lithospheric rigidity (Beaumont et al., 1992; Gilchrist et al., 1994). The analytical model carried out in this study showed that the erosional unloading at the base of the escarpment deformed the basalts up to a distance of 30 km from the escarpment with flexural uplift values ranging between 100 and 250 m (**Table 8**; **Fig.28**). The erosion started immediately after the deposition of CFB

which in that area flowed up to 300 km far from the present position of the escarpment. The average thickness of the eroded material is ~1000 m with a maximum retreat rate of 10 km/Ma. The lithosphere elastic thickness (T_e) and rigidity (D) values are in agreement with previous works (Ebinger et al., 1989; Pérez-Gussinyé et al., 2009) (**Table 8**).

The flexural uplifts at the Tana escarpment and at the rift shoulder (see **Fig.28d**) may be the cause for the long standing presence of the Lake Tana (5 Ma according to Mohr, 1962) and the Ethiopian Plateau. Indeed the flexure on both sides of the plateau preserved the entire area from erosion inhibiting the capture by the rivers draining Sudan and Afar lowlands.

Figures 30 and **31** show that isostatic contributions strongly influence the topographic configuration of the plateau. In particular the erosional unloading (**Fig.30a**) is maximum along the Tana escarpment and the Blue Nile and Tekeze rivers valleys while is minimum in the inner part of the plateau. The Trap loading (**Fig.30b**) is close to zero in correspondence with Addis Ababa and Mekele where the basalts thickness is minimum and increases up to 1600 m in the Tana region (**Fig.30b-31c**). This area is characterized by the presence of a huge depression beneath the plateau connected with the tectonic structures around the Lake Tana (Chorowicz et al., 1998).

The pre-trap topography (**Fig.31a**), obtained by subtracting all the isostatic contributions from the Trap base surface, shows two topographic highs in the Addis Ababa and Mekele areas. The first one represents the centre of a ~2600 m high bulge with a radius of ~500 km. Several *P* and *S* waves velocity models (Benoit et al., 2006a, b; Bastow et al., 2008, 2011; Hammond et al., 2010; Nyblade, 2011; Hansen and Nyblade, 2013) show in the same region a large, low velocity anomaly interpreted as hot asthenospheric material rising from the core-mantle boundary and impinging the base of the lithosphere (Afar plume). The Mekele topographic high is located at the bulge edge, more than 500 Km far from the centre (**Fig.31a**). For this reason its topography has been poorly influenced by the dynamic processes. The high elevation (between 2000 and 2400 m a.s.l.) may be in part due to the flexural uplift of the Red Sea rift shoulder and in part related to the Early Miocene magmatic activity (Hagos et al., 2010; Natali et al., 2013), characterized by intrusions of basaltic dikes and sills, which thickened the crust and determined an additional uplift of hundreds of meters.

3.4.1 Considerations on pre-Trap topography

The pre-Trap topography (**Fig.31a**) is characterized by a huge depression extending from the Tana basin up to the western rift shoulder. Such a feature has been filled by flood basalts and presents a

pre-Trap elevation ranging between 1750 m (near the bulge centre) and 750 m a.s.l (at the Ethiopia/Sudan border) (**Fig.31a**). The present topography northwest and southeast of the Ethiopian highlands is almost flat and presents a mean elevation of ~500 m a.s.l. (**Fig.24a**). Considering such topography as the original landscape untouched by domal uplift it is possible to suppose that, after the deposition of Trap deposits, the bottom of this depression has been uplifted not more than 1250 m (that is 1750-500 m). On the other hand the present elevation pattern in the study area varies from 4533 m (Mt. Ras Dashen in the northern sector of Ethiopia) to 500 m a.s.l. (eastern and western portions of Ethiopia) with a mean elevation of ~2200 m. Given this value we can approximate the minimum pre-Trap uplift to 950 m (that is 2200-1250 m), in accordance with Şengör (2001).

The pre-Trap and present residual topographies show a similar topographic configuration (**Fig.32**): the elevation is high in coincidence with Mekele and Addis Ababa regions and decrease up to zero at the Ethiopian national borders. This suggests that the topographic pattern remained almost unchanged all over the area since the deposition of CFB (~30 Ma; Zumbo et al., 1995; Baker et al., 1996a; Hofmann et al., 1997; Rochette et al., 1998) as inferred from thermochronological data (Pik et al., 2003). However the comparison reveals a mismatch of ~1000 m. In particular the residual topography is characterized by elevation highs in Mekele and Addis Ababa of ~ 1000 m (**Fig.32b**) while the pre-Trap topography presents in the same areas elevations of 2000 and 2150 m respectively (**Fig.32a**). Such discrepancies may be related to partial isostatic compensation driven by magmatic underplating probably associated with the ~30–28 Ma flood basalts event (Mackenzie et al., 2005; Tiberi et al., 2005). Indeed receiver function, tomography and seismic refraction studies of the Ethiopian Plateau and rift valleys suggest that large volumes of magmatic material have been added to the crust (**Fig.33**; Keranen et al., 2004; Wolfenden et al., 2004; Dugda et al., 2005; Kendall et al., 2005; Mackenzie et al., 2005). Seismic refraction and receiver function data west of 40°E show a 7.4 – 7.7 kms^{-1} layer at ~30 km depth, interpreted as mafic underplate probably accreted during the flood basalts event (**Figs.33b-c**; Mackenzie *et al.* 2005). The existence of thicker crust under the northwestern plateau may have also influenced the evolution of the MER by forcing the migration of hot mantle flow toward thinner crust portions (**Figs.33b-c**).

The elevation pattern of the dynamic topography (**Fig.32c**) demonstrates that part of the topography in Ethiopia may be dynamically sustained in agreement with previous works (Lithgow-Bertelloni and Silver, 1998; Gurnis et al., 2000; Daradich et al., 2003; Forte et al., 2010; Moucha

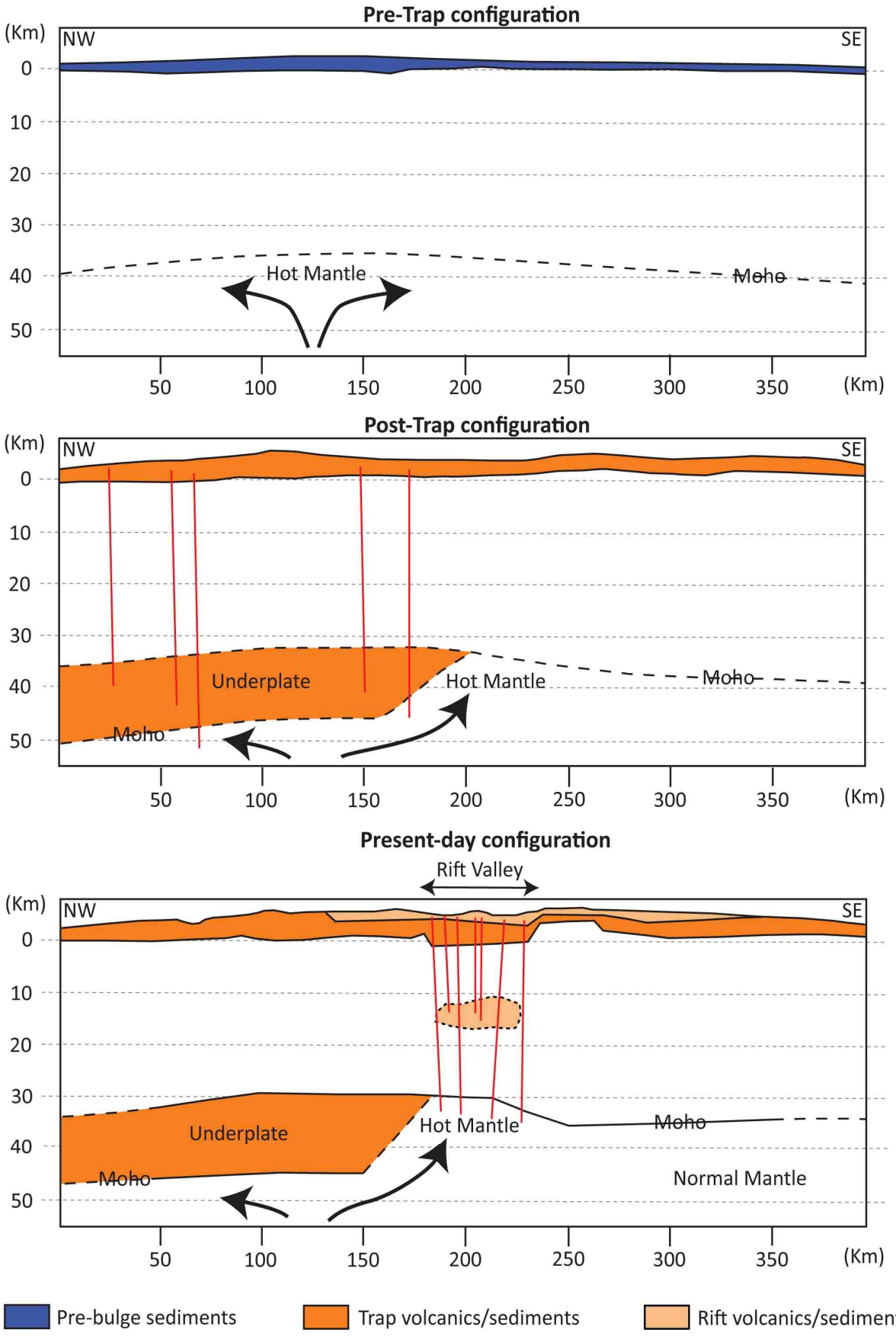

Figure 33 - Three stages cartoon illustrating the crustal evolution of the study area across a NW-SE trending section.

and Forte, 2011; Bagley and Nyblade, 2013; Faccenna et al., 2013). The highest sector coincides with the Addis Ababa topographic high evidenced in the pre-Trap topography (**Fig.32a**) and in the residual topography (**Fig.32b**). Such similarity of patterns may indicate that the deep processes determining the present thermal anomaly shown by several *P* and *S* waves velocity models in the mantle (Benoit et al., 2006a, b; Bastow et al., 2008, 2011; Hammond et al., 2010; Nyblade, 2011; Hansen and Nyblade, 2013) may be the same which shaped the pre-Trap topographic pattern.

3.4.2 Uplift pattern evolution

Uplift associated with the Ethiopian Plateau can be divided into five steps (**Fig.34**); Each step is characterized by an uplift rate calculated by the comparison between the pre-Trap and present topographic configuration (see section 3.4.1).

The pre-bulge topography (**Fig.34a**) was characterized by a low relief landscape with a wide W-E trending depression, related to the Mesozoic rifting event, which streched from the Lake Tana region to the present western rift shoulder. The mean elevation was ~500 m.

At the end of Eocene (**Fig.34b**) (~45 Ma; Ebinger and Sleep, 1998; Şengör, 2001) the Afar plume impinged the base of the lithosphere causing a broad domal uplift of at least 950 m with an uplift rate of 82±19 m/Ma. Such uplift probably reactivated the Mesozoic tectonic lineaments determining a deepening of the depression. The same lineaments may have represented preferential zones of dyke intrusion (Mege and Korme, 2004).

In the Late Oligocene (**Fig.34c**) (30-28 Ma; Zumbo et al., 1995; Baker et al., 1996a; Hofmann et al., 1997; Rochette et al., 1998) a huge eruption of flood basalts covered all the area flatting the landscape. According to the Trap volume calculated by Rochette et al. (1998) the eruption rate has been estimated by 1 km^3/yr. The enormous volume of basalts caused an initial subsidence of the surface directly proportional to the thickness of the Trap. Such an event was accompanied by a large underplating as evidenced by seismic refraction and receiver function data (**Fig.33**; Mackenzie et al. 2005; Tiberi et al., 2005). This process is considered to be an important mechanism for driving regional surface uplift and denudation of large continental areas (White and Lovell, 1997). In the same time (29 Ma; Wolfenden et al., 2005) the onset of continental rifting in the Red Sea–Gulf of Aden systems occurred causing the flexural uplift of the rift shoulders.

Following the eruption of the Ethiopian flood basalts, erosion started to act causing an isostatic rebound which accompanied the still ongoing domal uplift (**Fig.34d**). Such rebound is still active and presents the highest values along the Tana escarpment and in the main valleys; values close to

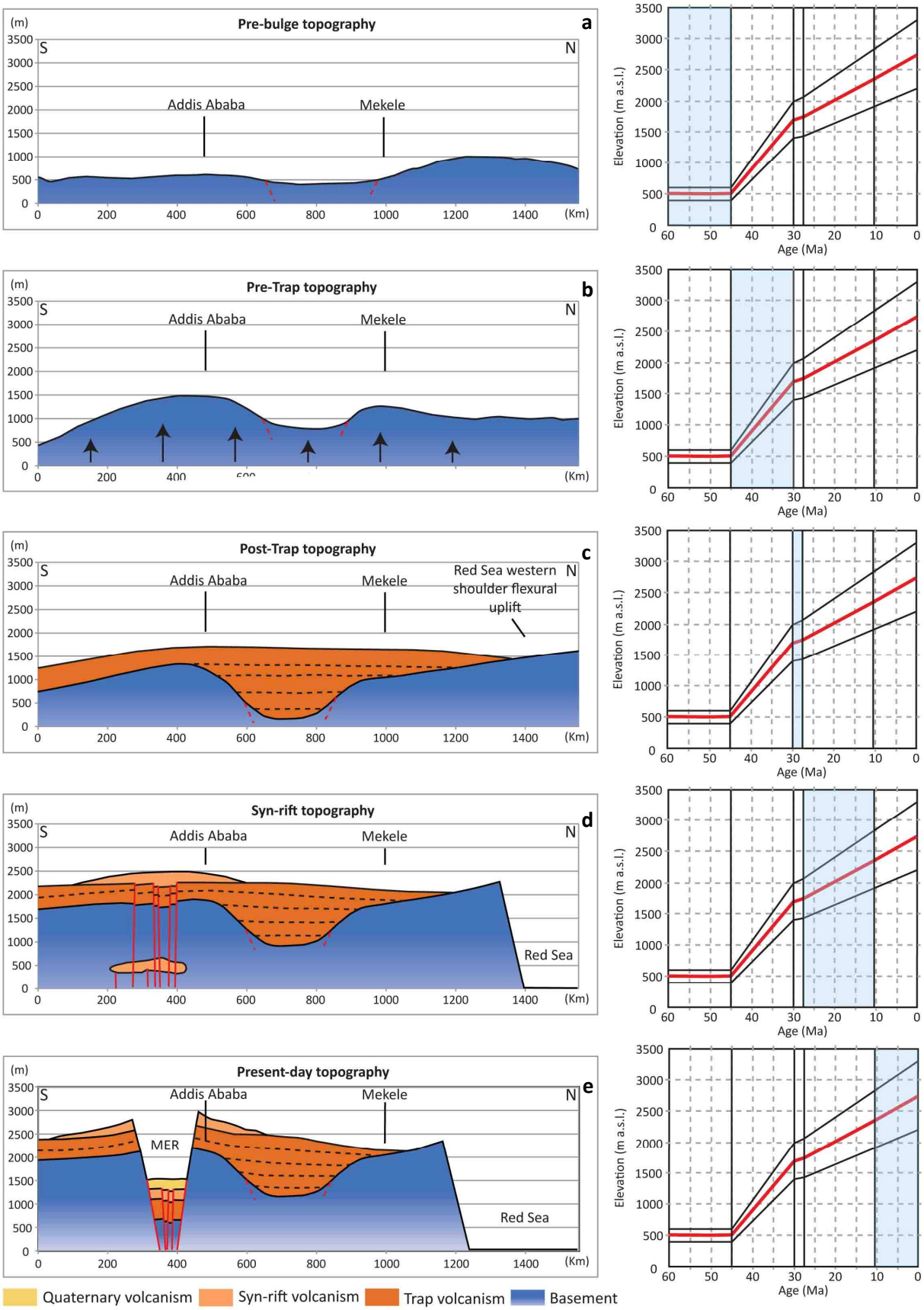

Figure 34 - Schematic cartoon of the uplift pattern evolution of the Ethiopian Plateau based on the contributions to topography analysis realized in the present work (see Figs.30-31). The plots on the right indicate the variation in Ethiopian Plateau uplift rate since 60 Ma. The red solid line indicates the mean uplift rate calculated by the comparison between the pre-Trap and present topographic configuration (see section 3.4.1 for further explanation).

zero characterize the inner portion of the plateau. In the Late Miocene (Bonini et al., 2005) the southern MER started to form determining the flexural uplift along the rift shoulders and a strong eruption event. According to Tiberi et al. (2005) such activity determined an underplating of about 10 km at a depth of 30 km.

As the extension kept going the tectonic activity focalized along the rift axis (**Fig.34e**). The volcanic activity, which in the first rifting phase involved large areas along the rift shoulders, was confined in the inner portion of the rift (Ebinger, 2005; Corti, 2009). The total post-Trap uplift rate estimated is 98±19 m/Ma.

3.5 Conclusions

We analyzed the isostatic and dynamic contributions to topography in the Ethiopian Plateau in order to delineate the topographic evolution of the area since Oligocene. A summary of our results includes the following:

- The flexural isostasy at the rift escarpment deformed the surface up to a maximum distance of 150 km from the rift shoulder (**Fig.27**). The maximum flexural uplift varies between 700 and 1150 m (**Table 8**).

- The Tana escarpment is an erosional feature bordering the western portion of the Ethiopian Plateau and evolved by scarp retreat (**Figs.25b-28a**). The strong erosional unloading at the base of the escarpment determined a flexural rebound of the crust. Such process deformed surface inside the plateau up to 30 km from the escarpment with maximum flexural uplift varying between 120 and 260 m (**Table 8**; **Fig.28**).

- The flexure on both sides of the plateau preserved the Ethiopian Plateau from erosion inhibiting the capture by the rivers draining Sudan and Afar lowlands (**Fig.28d**).

- The isostatic contributions strongly influenced the topographic configuration of the plateau. In particular the erosional unloading (**Fig.30a**) is maximum along the Tana escarpment and the main valleys while is minimum in the inner part of the plateau. The Trap loading (**Fig.30b**) is close to zero in correspondence with Addis Ababa and Mekele where the basalt thickness is minimum and increases up to 1600 m in the Tana region (**Fig.30b-31c**). The area is characterized by the presence of a huge depression beneath the plateau connected with the tectonic structures around the Lake Tana (Chorowicz et al., 1998).

- The pre-Trap topography (**Figs.31a**), obtained subtracting all the isostatic contributions from the Trap base surface, shows two topographic highs in the Addis Ababa and Mekele areas and a huge

depression between the two cities. In particular the Addis Ababa topographic high represents the center of a ~2600 m high bulge with a radius of ~500 km. Several *P* and *S* waves velocity models (Benoit et al., 2006a, b; Bastow et al., 2008, 2011; Hammond et al., 2010; Nyblade, 2011; Hansen and Nyblade, 2013) show in the same region a huge velocity anomaly interpreted as hot asthenospheric material rising from the core-mantle boundary and impinging the base of the lithosphere (Afar plume). The comparison between pre-Trap elevation pattern and present topography permits to calculate a minimum pre-Trap uplift of ~950 m and a maximum post-Trap uplift of ~1250 m.

- The comparison between pre-Trap topography (**Fig.32a**) and present residual topography (**Fig.32b**) shows the same topographic configuration. Indeed the elevation increases in coincidence with the Mekele and Addis Ababa regions and decreases up to zero at the Ethiopian national borders. However a mismatch in the elevation ranges has been found. In particular the present residual topography presents lower elevation values. This may be related to magmatic underplating probably associated with the ~30–28 Ma flood basalts event (**Fig.33**; Mackenzie et al., 2005; Tiberi et al., 2005).

- The pre-Trap topography (**Fig.32a**) and the present dynamic topography (**Fig.32c**) show the same topographic high in the Addis Ababa region. The elevation values are very similar and decreases all around the Addis Ababa high. This suggests that the deep process determining the present thermal anomaly may be the same which shaped the pre-Trap topographic pattern.

References

Anderson, R.S. and Anderson, S.P. (2010) - "Geomorphology: The Mechanics and Chemistry of Landscape" - Cambridge University Press, 640 pp.

As-Saruri, M. (2004) – "Geological map of Yemen" - Ministry of oil and minerals petroleum exploration and production authority.

Bagley, B. and Nyblade, A.A. (2013) - " Seismic anisotropy in eastern Africa, mantle flow, and the African plume" - Geophys. Res. Lett., vol. 40, pp. 1500-1505.

Baker, B.H., Mohr, P.A. and Williams, L.A.J. (1972) - "Geologyof the EasternRift System of Africa" - Geological Society of America Special Paper, vol. 136. 67 pp., Boulder Colorado.

Baker, J., Snee, L. and Menzies, M. (1996a) – "A brief Oligocene period of flood volcanism in Yemen" - Earth and Planetary Science Letters 138, 39–55.

Basile, C. and Allemand, P. (2002) - "Erosion and flexural uplift along transform faults" - Geophys. J. Int., 151, 646-653.

Bastow, I.D., Nyblade, A.A., Stuart, G.W., Rooney, T.O. and Benoit, M.H. (2008) - "Upper mantle seismic structure beneath the Ethiopian hot spot: rifting at the edge of the African low-velocity anomaly" - Geochemistry, Geophysics, Geosystems 9, Q12022. doi:10.1029/2008GC002107.

Bastow, I.D., Keir, D. and Daly, E. (2011) – "The Ethiopia Afar Geoscientifi c Lithospheric Experiment (EAGLE): Probing the transition from continental rifting to incipient sea floor spreading" - *in* Beccaluva, L., Bianchini, G., and Wilson, M., eds. "Volcanism and Evolution of the African Lithosphere" - Geological Society of America Special Paper 478, p. 51–76, doi:10.1130/2011.2478(04).

Beaumont, C., Fullsack, P. & Hamilton, J. (1992) - "Erosional control of active compressional orogens" - In: "Thrust Tectonics" edited by K. R. McClay, pp. 19-31, Chapman and Hall, New York, 1992.

Becker, T.W. and Faccenna, C. (2011) - "Mantle conveyor beneath the Tethyan collisional belt" - EPSL 310, 453-461.

Becker, T.W., Faccenna, C., Humphreys, E.D., Lowry, A.R. and Miller, M.S. (2014) – "Static and dynamic support of western U.S. topography" - Earth Planet. Sci. Lett. 402, 234–246.

Benoit, M.H., Nyblade, A.A. and VanDecar, J.C. (2006a) - "Upper mantle P wave speed variations beneath Ethiopia and the origin of the Afar Hotspot" - Geology 34, 329–332.

Benoit, M.H., Nyblade, A.A., Owens, T.J. and Stuart, G. (2006b) - "Mantle transition zone structure and upper mantle S velocity variations beneath Ethiopia: evidence for a broad, deep-seated thermal anomaly" - Geochemistry, Geophysics, Geosystems 7, Q11013. doi:10.1029/2006GC001398.

Berhe, S.M., Desta, B., Nicoletti, M. and Tefera, M. (1987) – "Geology, geochronology and geodynamic implications of the Cenozoic magmatic province in W and SE Ethiopia" - Journal of the Geological Society of London 144, 213–226.

Beydoun, Z.R. (1960) - "Synopsis of the Geology of East Aden Protectorate" - XXI International Geological Congress, Copenhagen 21, 131–149.

Bodine, J.H., Steckler, M.S. and Watts, A.B. (1981) - "Observations of Flexure and the Rheology of the Oceanic Lithosphere" - J. Geophys. Res., vol. 86, pp. 3695-3707.

Bonini, M., Corti, G., Innocenti, F., and Manetti, P. (2005) – "Evolution of the Main Ethiopian Rift in the frame of Afar and Kenya rifts propagation" - Tectonics, v. 24, doi: 10.1029/2004TC001680.

Boschi, C., Faccenna, C. and Becker, T.W. (2010) - "Mantle structure and dynamic topography in the Mediterranean basin" - Geoph. Res. Let., vol.37,doi:10.1029/2010GL045001.

Braun, J. (2010) - "The many surface expressions of mantle dynamic" - Nature Geoscience 3, 825–833.

Braun, J., Robert, X. and Simon-Labric, T. (2013) – "Eroding dynamic topography" – Geophysical Research Letters, vol.40, 1494-1499.

Brown, C.D. and Phillips, R.J. (1999) – "Flexural rift flank uplift at the Rio Grande rift, New Mexico" – Tectonics, vol.18, pp.1275-1291.

Buck, R.W. (1988) - "Flexural rotation of normal faults" - Tectonics 7, 959–973.

Burbank, D.W. and Anderson, R.S. (2011) – "Tectonic geomorphology" – 2nd edition, Wiley-Blackwell.

Burke, K. (1996) - "The African plate" - S. Afr. J. Geol., 99, 339–409.

Campbell, I.H. and Griffiths, R.W. (1990) - "Implications of mantle plume structure for the evolution of flood basalts" - EPSL, 99, 79-93.

Carey, S.N. (2005) – "Understanding the physical behavior of volcanoes" – In: "Volcanoes and the Environment" – Cambridge University Press.

Comucci, P. (1950) - "Le vulcaniti del lago Tana (Africa Orientale)" - Accad. Naz. Lincei, Roma, 209 pp.

Chery, J., Lucazeau, F., Daignieres, M. and Vilotte, J.P. (1992) - "Large uplift of rift flanks: A genetic link with lithospheric rigidity?" - EPSL, 112, 195-211.

Chorowicz, J., Collet, B., Bonavia, F.F., Mohr, P., Parrot, J.-F. and Korme, T. (1998) - "The Tana basin, Ethiopia: intraplateau uplift, rifting and subsidence" - Tectonophysics 295, 351–367.

Chumburo, F. (2009) – "Geological Map of Debre Markos sheet (NC 37-6)" – EIGS.

Comucci, P. (1950) - "Le vulcaniti del lago Tana (Africa Orientale)" - Accad. Naz. Lincei, Roma, 209 pp.

Corti, G. (2009) – "Continental rift evolution: From rift initiation to incipient break-up in the Main Ethiopian Rift, East Africa" - Earth-Science Reviews, 96, 1–53.

Courtillot, V., Jaupart, C., Manighetti, I., Tapponnier, P. and Besse, J. (1999) - "On causal links between flood basalts and continental breakup" - EPSL 166, 177–195.

D'Agostino, N., Chamot-Rooke, N., Funiciello, R., Jolivet, L. and Speranza, F. (1998) - "The role of pre-existing thrust fault and topography on the styles of extension in the Gran Sasso range (central Italy)" - Tectonophysics, 292, 229-254.

Dainelli, G. (1943) - "Geologia dell'Africa Orientale (3 vols. text, 1 vol. maps)" - R. Accad. Ital., Roma.

Dancan, R.A. and Richards, M.A. (1991) - "Hotspots, mantle plumes, flood basalts, and true polar wander" - Rev. Geophys., 29, 31-50.

Daradich, A., J. X. Mitrovica, R. N. Pysklywec, S. D. Willett and A. M. Forte (2003) – "Mantle flow, dynamic topography, and rift-flank uplift of Arabia" - Geology, 31, 901–904, doi:10.1130/G19661.1.

Davidson, A. and Rex, D.C. (1980) - "Age of volcanism and rifting in south-western Ethiopia"- Nature 283, 654-658.

Davies, G.F. (1994) - "Thermomechanical erosion of the lithosphere by mantle plumes" - J. Geophys. Res., vol. 99, pp. 15,709-15,722.

Ebinger, C. J., T.D. Bechtel, D. W. Forsyth and C. O. Bowin (1989) – "Effective Elastic Thickness beneath the East African and Afar Plateaus and Dynamic compensation for the uplifts" - J. Geophys.Res., 94, 2883-2901.

Ebinger, C.J., Karner, G.D. and Weissel, J.K. (1991) - "Mechanical strength of extended continental lithosphere: constraints from the western rift system, East Africa" - Tectonics, vol. 10, pp. 1239-1256.

Ebinger, C.J., Yemane, T.,WoldeGabriel, G., Aronson, J.L. and Walter, R.C. (1993) – "Late Eocene-Recent volcanism and faulting in the southern main Ethiopian rift" - Journal of the Geological Society of London 150, 99–108.

Ebinger, C. and Sleep, N.H. (1998) – "Cenozoic magmatism in central and east Africa resulting from impact of one large plume" - Nature 395, 788–791.

Ebinger, C.J. and Casey, M. (2001) - "Continental breakup in magmatic provinces: an Ethiopian example" - Geology 29, 527–530.

Ebinger, C. (2005) - "Continental breakup: the East African perspective" - Astronomy and Geophysics 46, 2.16–2.21.

Faccenna, C., Becker, T.W., Jolivet, L. and Keskin, M. (2013) - "Mantle convection in the Middle East: Reconciling Afar upwelling, Arabia indentation and Aegean trench rollback" - EPSL 375, 254-269.

Forsyth, D.W. (1985) - "Subsurface loading and estimates of the flexural rigidity of continental lithosphere" - J. of Geophys. Res., vol.90, 12623-12632-

Forte, A.M., Quere, S., Moucha, R., Simmons, N.A., Grand, S.P., Mitrovica, J.X. and Rowley, D.B. (2010) - " Joint seismic–geodynamic-mineral physical modelling of African geodynamics: A reconciliation of deep-mantle convection with surface geophysical constraints" - EPSL, doi:10.1016/j.epsl.2010.03.017.

Furman, T., Bryce, J., Rooney, T., Hanan, B., Yurgu, G. and Ayalew, D. (2006) - "Heads and tails: 30 million years of the Afar plume" - In: Yirgu, G., Ebinger, C.J., Maguire, P.K.H. (Eds.), The Afar Volcanic Province within the East African Rift System: Geological Society Special Publication, vol. 259, pp. 95–119.

G.M.R.D. (1981) – "Geological map of the Sudan" - Geological and mineral resources department.

Gani, N.D., Abdelsalam, M.G. and Gani, M.R. (2007) – "Blue Nile incision on the Ethiopian Plateau: pulsed plateau growth, Pliocene uplift, and hominin evolution" - GSA Today 17, 4–11.

Gani, N.D.S., Abdelsalam, M.G., Gera, S. and Gani, M.R. (2008) - "Stratigraphic and structural evolution of the Blue Nile Basin, Northwestern Ethiopian Plateau" - Geological Journal 44, 30–56.

Garland, C.R. (1980) – "Geology of the Adigrat Area" - Ministry of Mines, Addis Ababa Memoir No.1, 51.

George, R., Rogers, N. and Kelley, S. (1998) – "Earliest magmatism in Ethiopia: evidence for two mantle plumes in one flood basalt province" - Geology 26, 923–926.

Gilchrist, A.R., Summerfield, M.A. and Cockburn, H.A.P. (1994) - "Landscape dissection, isostatic uplift, and the morphologic development of orogens" - Geology, vol. 22, pp. 963-966.

Grabham, G.W. and Black, R.P. (1925) - "Report of the Mission to Lake Tana 1920–21" - Government Press, Cairo.

Gurnis, M., Mitrovica, J.X., Ritsema, J. and van Heijst, H.J. (2000) – "Constraining mantle density structure using geological evidence of surface uplift rates: the case of the African Plume" - Geochemistry, Geophysics, Geosystems 1 1999GC000035.

Gurnis, M. (2001) – "Sculpting the Earth from inside out" - Sci. Am., 284, 40–47.

Hager, B.H. (1984) – "Subducted slabs and the geoid: constraints on mantle rheology and flow" - J. Geophys. Res. 89, 6003–6015.

Hager, B.H., Clayton, R.W., Richards, M.A., Comer, R.P. and Dziewonski, A.M. (1985) - "Lower mantle heterogeneity, dynamic topography and the geoid" - Nature 313, 541-545.

Hagos, M., Koeberl, C., Kabeto, K. and Koller, F. (2010) – "Geochemical characteristics of the alkaline basalts and the phonolite–trachyte plugs of the Axum area, northern Ethiopia" – Austrian Journal of Earth Sciences, vol. 103/2, 153-170.

Hahn, G.A., Raynolds, R.G.H. and Wood, R.A. (1977) - "The geology of the Angareb Ring Dike complex, northwestern Ethiopia" - Bull. Volcanol. 40, 1–10.

Hailu, T. (1975) - "Geological Map of Adiarkay Sheet (ND 37 -10) 1:250,000" - EIGS.

Hammond, J.O.S., Kendall, J.-M., Angus, D. and Wookey, J. (2010) - "Interpreting spatial variations in anisotropy: insights into the Main Ethiopian Rift from SKS waveform modelling" - Geophys. J. Int., vol. 181, pp 1701-1712.

Hansen, S.E., Nyblade, A.A., Benoit, M.H. (2012) - "Mantle structure beneath Africa and Arabia from adaptively parameterized P-wave tomography: implications for the origin of Cenozoic Afro-Arabian tectonism" - EPSL, 319-320, 23-34.

Hansen, S.E. and Nyblade, A.A. (2013) - "The deep seismic structure of the Ethiopia/Afar hotspot and the African plume" - Geophys. J. Int., doi: 10.1093/gji/ggt116.

Hirt, C., Kuhn, M., Featherstone, W.E. and Gotti, F. (2012) - "Topographic/isostatic evaluation of new-generation GOCE gravity field models" - J. Geophys. Res., vol. 117.

Hofmann, C., Courtillot, V., Feraud, G., Rochette, P., Yirgu, G., Ketefo, E. and Pik, R. (1997) – "Timing of the Ethiopian flood basalt event and implications for plume birth and global change" - Nature 389, 838–841.

Jepsen, D.H. and Athearn, M.J. (1961) - "A general geological map of the Blue Nile River basin, Ethiopia (1:1,000,000)" - Dep. Water Resources, Addis Ababa.

Kazmin, V. (1976) – "Geological Map of Adigrat Sheet (ND 37 -7), 1:250,000" - EIGS.

Kebede, S. (2013) – "Groundwater in Ethiopia – Features, Numbers and Opportunities" – Springer editor.

Kieffer, B., Arndt, N., Lapierre, H., Bastien, F., Bosch, D., Pecher, A., Yirgu, G., Ayalew, D., Weis, D., Jerram, D.A., Keller, F., and Meugniot, C. (2004) – "Flood and shield basalts from Ethiopia: Magmas from the African Superswell" - Journal of Petrology, v. 45, 793–834, doi: 10.1093/petrology/egg112.

King, G.C.P., Stein, R.S. and Rundle, J.B. (1988) – "The growth of geological structures by repeated earthquakes: Conceptual framework" - J. Geophys. Res. 93, 13307–13318.

Laske, G., Masters, G., Ma, Z. and Pasyanos, M. (2013) - "Update on CRUST1.0 - A 1-degree global model of Earth's crust" - Geophys. Res. Abstracts, 15, Abstract EGU2013-2658.

Le Stunff, Y. and Ricard, Y. (1995) – "Topography and geoid due to mass anomalies" - Geo-phys. J. Int. 122, 982–990.

Lithgow-Bertelloni, C. and P. G. Silver (1998) – "Dynamic topography, plate driving forces and the African superswell" - Nature, 395, 269–272, doi:10.1038/26212.

McDougall, I., Morton,W.H. and William, M.A.J. (1975) – "Ages and rates of denudation of trap series basalts at the Blue Nile Gorge, Ethiopia" - Nature 254, 207–209.

McKenzie, D. and Fairhead, D. (1997) - "Estimates of the effective elastic thickness of the continental lithosphere from Bouger and free air gravity anomalies" - J. of Geophys. Res., vol.102, 27523-27552.

Mege, D. and Korme, T. (2004) - "Dyke swarm emplacement in the Ethiopian Large Igneous Province: not only a matter of stress" - Journal of Volcanology and Geothermal Research 132, 283–310.

Merla, G., Abbate, E., Canuti, P., Sagri, M. and Tacconi, P. (1979) - "Geological map of Ethiopia and Somalia and comment with a map of major landforms (scale 1:2,000,000)" - Consiglio Nazionale delle Ricerche, Rome. 95.

Minucci, E. (1938b) - "Ricerche geologiche nella regione del Tana" - In: Missione di Studio al Lago Tana. R. Accad. Ital. 1, 19–36.

Mohr, P.A. (1962) – "The geology of Ethiopia" - Addis Ababa: Addis Ababa University Press.

Mohr, P.A. (1967) – "The Ethiopian Rift System" - Bulletin of the Geophysical Observatory of Addis Ababa 11, 1–65.

Mohr, P. and Zanettin, B. (1988) – "The Ethiopian Flood Basalt Province" - In McDougall, J.D., ed., Continental Flood Basalts: Dordrecht, Netherlands, Kluwer Academic Publishers, 63–110.

Molin, P., Fubelli, G., Nocentini, M., Sperini, S., Ignat, P., Grecu, F. and Dramis, F. (2011) - "Interaction of mantle dynamics, crustal tectonics and surface processes in the topography of the Romanian Carpathians: A geomorphological approach" - Glob. Planet. Change, doi:10.1016/j.gloplacha.2011.05.005

Molnar, P. and England, P. (1990) – “Late Cenozoic uplift of mountain ranges and global climate change: chicken or egg?” - Nature 346, 29 – 34.

Molnar, P. and England, P. and Martinod, J. (1993) – “Mantle dynamics, uplift of the Tibetan Plateau and the Indian Monsoon” – Reviews of Geophysics, 31, 357-396.

Moucha, R., A. M. Forte, J. X. Mitrovica, D. B. Rowley, S. Quere, N. A. Simmons and S. P. Grand (2008) – “Dynamic topography and long-term sea-level variations: There is no such thing as a stable continental platform” - Earth Planet. Sci. Lett., 271, 101–108, doi:10.1016/j.epsl.2008.03.056.

Moucha, R. and Forte, A.M. (2011) – “Changes in African topography driven by mantle convection” – Nature Geosc. Let. DOI: 10.1038/NGEO1235.

Mueller, R.D., Cande, S.C., Stock, J.M. and Keller, W.R. (2005) – “Crustal structure and rift flank uplift of the Adare Trough, Antartica” – Geochem. Geophys. Geosys., Vol.6, n°11.

Mueller, R.D., Kier, G., Rockwell, T. and Craig, H.J. (2009) – “Quaternary rift flank uplift of the Peninsular Ranges in Baja and southern California by removal of mantle lithosphere” – Tectonics, vol.28, doi:10.1029/2007TC002227.

Natali, C., Beccaluva, L., Bianchini, G. and Siena, F. (2013) – “The Axum-Adwa basalt-trachyte complex: a late magmatic activity at the periphery of the Afar plume” – Contrib. Mineral Petrol, 166, 351-370.

Nyblade, A.A. and Langston, C.A. (2002) - "Broadband seismic experiments probe the East African rift" - EOS Transaction on American Geophysical Union 83, 405–408.

Nyblade, A.A. (2011) - "The upper-mantle low-velocity anomaly beneath Ethiopia, Kenya, and Tanzania: Constraints on the origin of the African superswell in eastern Africa and plate versus plume models of mantle dynamics" - Geol. Soc. Am., Special Paper 478.

Panasyuk, S.V. and Hager, B.H. (2000) – “Models of isostatic and dynamic topography, geoid anomalies, and their uncertainties” - J. Geophys. Res. 105, 28199–28209.

Pelletier, J.D. (2008) - "Quantitative Modelling of Earth Surface Processes" - Cambridge University Press.

Perez-Gussinye, M., Metois, M., Fernandez, M., Verges, J. & Lowry, A.R. (2009) – “Effective elastic thickness of Africa and its relationship to other prozie for lithospheric structure and surface tectonics” - Earth Planet. Sci. Lett., 287(1-2), 152-167.

Petit, C., Fournier, M. and Gunnell, Y. (2007) - "Tectonic and climatic controls on rift escarpments: Erosion and flexural rebound of the Dhofar passive margin (Gulf of Aden, Oman)" - J. Geophys. Res., vol. 112.

Pik, R., Marty, B., Carignan, J. and Lave, J. (2003) – “Stability of Upper Nile drainage network (Ethiopia) deduces from (U–Th)/He thermochronometry: Implication of uplift and erosion of the Afar plume dome” - Earth and Planetary Science Letters, v. 215, 73–88, doi: 10.1016/S0012-821X(03)00457-6.

Poulimenos, G. and Doutsos, T. (1997) – “Flexural uplift of rift flanks in central Greece” – Tectonics, vol.16, pp.912-923.

Ricard, Y., Fleitout, L. and Froidevaux, C. (1984) – “Geoid heights and lithospheric stresses for a dynamic Earth” - Ann. Geophys. 2, 267–286.

Ricard, Y., Richards, M.A., Lithgow-Bertelloni, C. and Lestunff, Y. (1993) – “A geodynamic model of mantle mass heterogeneities” - J. Geophys. Res. 98, 21895–21909.

Ritsema, J., H. J. van Heijst and J. H. Woodhouse (1999) – “Complex shear wave velocity structure imaged beneath Africa and Iceland” - Science, 286, 1925–1928, doi:10.1126/science.286.5446.1925.

Roberts, G.G. and White, N. (2010) - "Estimating uplift rate histories from river profiles using African examples" - J. Geophys. Res., vol. 115.

Rochette, P., Tamrat, E., Feraud, G., Pik., R., Courtillot, V., Ketefo, E., Coulon, C., Hoffmann, C., Vandamme, D. and Yirgu, G. (1998) - "Magnetostratigraphy and timing of the Oligocene Ethiopian traps" - EPSL, 164, 497-510.

Rogers, N., Macdonald, R., Fitton, J., George, R., Smith, R. & Barreiro, B. (2000) - "Two mantle plumes beneath the East African rift system: Sr, Nd and Pb isotope evidence from Kenya Rift basalts" - EPSL, 176, 387–400.

Rogers, N.W. (2006) - "Basaltic magmatism and the geodynamics of the East African Rift System" - In: Yirgu, G., Ebinger, C.J., Maguire, P.K.H. (Eds.), The Afar Volcanic Province within the East African Rift System: Geological Society Special Publication, vol. 259, pp. 77–93.

Rowley, D.B., Forte, A.M., Moucha, R., Mitrovica, J.X., Simmons, N.A and Grand, S.P. (2013) – “Dynamic topography change of the eastern United States since 3 million years ago” – Science, 340, 1560-1563.

Sachau, T. and Koehn, D. (2010) – “Faulting of the lithosphere during extension and related rift-flank uplift: a numerical study” - Int J Earth Sci (Geol Rundsch), 99, 1619-1632.

Schilling, J.G., Kingsley, R.H., Hanan, B.B. and McCully, B.L. (1992) – “Nd–Sr–Pb isotopic variations along the Gulf of Aden: evidence for Afar mantle plume-continental lithosphere interaction” - Journal of Geophysical Research B 97 (7), 10,927–10,966.

Şengör, A.M.C. (2001) – “Elevation as indicator of mantle-plume activity” - In Ernst, R.E., and Buchan, K.L., eds., Mantle Plumes: Their identification through time: Geological Society of America Special Paper 352, 183–225.

Simmons, N.A., Forte, A.M., Boschi, L. and Grand, S.P. (2010) – “GyPSuM: a joint tomo-graphic model of mantle density and seismic wave speeds” - J. Geophys. Res. 115, B12310.

Steinberger, B. and Calderwood, A. (2006) – “Models of large-scale viscous flow in the earth’s mantle with constraints from mineral physics and surface observations” - Geophys. J. Int. 167, 1461–1481.

Stern, T.A. and TEN Brink, U.S. (1989) – “Flexural uplift of the Transantartic Mountains” – J. Geophys. Res., Vol.94, pp.315-330.

Stern, R.J. (1994) - "Arc assembly and continental collision in the Neoproterozoic East African orogen" - Annual Review of Earth and Planetary Sciences 22, 319–351.

Ten Brink, U. and Stern, T. (1992) - "Rift flank uplifts and Hinterland Basins: Comparison of the Transantarctic Mountains with the Great Escarpment of southern Africa" - J. Geoph. Res., vol. 97, pp. 569-585.

Tefera, M, Cherenet, T and Haro, W (1996) – “Geological map of Ethiopia (1:2,000,000)” - Ethiopian Institute of Geological Survey, Addis Ababa, Ethiopia.

Tsige, L. and Hailu, E. (2007) – “Geological Map of Bure” – EIGS.

Turcotte, D.L. and Schubert, G. (1982) – “Geodynamics: Applications of Continuum Physics to Geological Problems” - John Wiley and Sons, New York.

van der Beek, P. (1997) - "Flank uplift and topography at the central Baikal Rift (SE Siberia): A test of kinematic models for continental extension" - Tectonics, vol. 16, pp. 122-136.

van der Beek, P., Summerfield, M.A., Braun, J., Brown, R.W. and Fleming, A. (2002) - "Modeling postbreakup landscape development and denudational history across the southeast African (Drakensberg Escarpment) margin" - J. Geophys. Res., vol. 107, pp. 1-18.

Watts, A.B., McKerrow, W.S. and Fielding, E. (2000) - "Lithosphere flexure, uplift, and landscape evolution in south-central England" - J. Geolog. Soc., vol. 157, pp. 1169-1177.

Watts, A.B. (2001) – “Isostasy and flexure of the lithosphere” - Cambridge, Cambridge University Press, p. 458.

Weissel, J. K. and Karner, G.D. (1989) – “Flexural uplift of rift flanks due to mechanical unloading of the lithosphere during extension” - J. Geophys. Res., 94, 13,919– 13,950, doi:10.1029/JB094iB10p13919.

Weissel, J., Malinverno, A. and Harding, D. (1995) – “Erosional development of the Ethiopian Plateau of Northeast Africa from fractal analysis of topography” - In: Barton, C.C., Pointe, P.R. (Eds.) “Fractals in Petroleum Geology and Earth Processes” - Plenum Press, New York, pp. 127–142.

White, N. and Lovell, J.P.B. (1997) - "Measuring the pulse of a plume with the sedimentary record" - Nature, 387, 888-891.

Wobus, C., Whipple, K.X., Kirby, E., Snyder, N., Johnson, J., Spyropolou, K., Crosby, B. and Sheehan, D. (2006) – “Tectonics from topography: procedures, promise, and pitfalls” - In: Willett, S.D., et al. (Ed.) “Tectonics, Climate, and Landscape Evolution” - Geological Society of America Special Paper, 398, pp. 55–74.

Wolfenden, E., Yirgu, G., Ebinger, C., Deino, A. and Ayalew, D. (2004) – “Evolution of the northern Main Ethiopian rift: Birth of a triple junction” - Earth and Planetary Science Letters, v. 224, 213–228, doi: 10.1016/j.epsl.2004.04.022.

Wolfenden, E., Ebinger, C., Yirgu, G., Renne, P. and Kelley, S.P. (2005) – “Evolution of the southern Red Sea rift: birth of a magmatic margin” - Geological Society of America Bulletin 117, 846–864.

Zenebe, B. and Mariam, D.H. (2011) – “Geological Map of Yifag area” – EIGS.

Zumbo, V., Feraud, G., Bertrand, H., and Chazot, G. (1995) - "40Ar/39Ar chronology of the Tertiary magmatic activity in Southern Yemen during the early Red Sea-Aden rifting" - J. Volcanol. Geoth. Res. 65, 265–279.

General conclusions

In this thesis we explored the topographic and geologic configurations of the Ethiopian Plateau in order to characterize the evolution of the region since Oligocene.
Our analysis evidenced that the present physiography of the area is intimately bonded to the interaction between surface and deep processes. A summary of our results includes the following:

1) The Trap base surface is characterized by a rough relief with a wide tectonic depression (extending from Lake Tana to the MER) between the Addis Ababa and Mekele topographic highs and a depression corresponding with the present Blue Nile R. downstream course (**Fig.4b**).

2) The CFB thickness map (**Fig.6a**) shows an asymmetric distribution with respect to the Rift Valley. The thickest deposits (1500-2000 m) are concentrated in the Lake Tana region. The presence of several dike swarms dated at ~30 Ma suggests that Lake Tana was one of the main trap source areas. The CFB flowed from this region filling depressions and slightly covering topographic highs (see geologic sections in **Fig.7**).

3) The morphometric analysis evidenced that, after the main plateau capture, the Tekeze R. was able to get close to equilibrium, whereas the Blue Nile R. is still in a transient state of disequilibrium (**Figs.16-17-18-19-20**; **Tables 1-2-3-4**). This may be related to:
a) the different locations of the two basins with respect to the hypothesized plume head location (Addis Ababa region; **Figs.15-30-31**). The Tekeze basin, located in the northern peripheral sector of the bulge, may have been less affected by dynamic uplift;
b) the volcanoes build up event, concentrated mainly and longer in the Blue Nile basin. Such event influenced the evolution of the Blue Nile drainage system from Oligocene to Pliocene while affected the Tekeze basin only in the early Oligocene;
c) the CFB thickness which reaches up to 2000 m in the Blue Nile basin and 1200 m in the Tekeze one (**Fig.6a**). Such difference slowed down erosion in the Blue Nile basin and facilitated the entrance of the Tekeze R. into the Ethiopian Plateau.

4) The flexural uplift at the rift shoulder deformed the surface up to 150 km from the shoulder itself with uplift values ranging between 700 and 1150 m (**Figs.25-26**; **Table 8**). The equivalent

elastic thickness (T_e) and flexural rigidity (D) ranges are 22-43 km and 10^{22}-10^{23} Nm respectively (**Table 8**), largely in agreement with previous works.

5) The Tana escarpment is an erosion feature boarding the western side of the plateau and retreating since Oligocene. The huge amount of removed material determined an isostatic uplift ranging between 120-260 m (**Fig.27**; **Table 8**).

6) The uplift on western and eastern sides of the Ethiopian Plateau inhibited erosion in the inner portion preserving the paleolandscape (**Fig.27c**). The Lake Tana basin, even if it is part of the Blue Nile drainage system, still conserves the morphometric characteristics of a landscape close to its base level (**Figs.16-19**; **Table 1-3**).

7) The pre-Trap topography (**Figs.30a-31a**), obtained subtracting all the isostatic contributions from the Trap base surface, shows two topographic highs in the Addis Ababa and Mekele areas and a huge depression between the two cities. In particular the Addis Ababa topographic high represents the centre of a ~2600 m high bulge with a radius of ~500 km. Several P and S waves velocity models (Benoit et al., 2006a, b; Bastow et al., 2008, 2011; Hammond et al., 2010; Nyblade, 2011; Hansen and Nyblade, 2013) show in the same region a huge velocity anomaly interpreted as hot asthenospheric material rising from the core-mantle boundary and impinging the base of the lithosphere (Afar plume).

The comparison between pre-Trap topography and present residual topography (**Fig.31**) shows the same topographic configuration. This suggests that the topographic pattern remained almost unchanged all over the area since the deposition of CFB (~30 Ma; Zumbo et al., 1995; Baker et al., 1996a; Hofmann et al., 1997; Rochette et al., 1998) as it is confirmed by thermochronological data (Pik et al., 2003). However a mismatch in the elevation ranges has been found. In particular the present residual topography mean elevation is lower than the pre-Trap one. This may be related to magmatic underplating probably associated with the ~30–28 Ma flood basalts event (**Fig.32**; Mackenzie et al., 2005; Tiberi et al., 2005)

The pre-Trap topography (**Figs.30a-31a**) and the present dynamic topography (**Fig.31c**) show the same topographic high in the Addis Ababa region. The elevation values are very similar and decreases all around the Addis Ababa high. This suggests that the deep process determining the present thermal anomaly may be the same which shaped the pre-Trap topography.

Acknowledgements

I would like to express my very great appreciation to the reviewers of this thesis Prof. F.J. Pazzaglia and Dr. G. Corti for their valuable and constructive suggestions and comments.

I also would like to express my deep gratitude to Prof. C. Faccenna and Dr. P. Molin, my research supervisor and co-supervisors respectively, for their enthusiastic encouragement and useful critiques of this research work.

I thank Prof. B. Thorsten for his contribution in elaborating the residual and dynamic topography of Ethiopia.

I thank Prof. F. Salvini for having disclosed me the mysterious world of elastic flexure and isostasy and for his brilliant suggestions in elaborating the flexural uplift analitical models.

I thank Prof. F. Dramis and Dr G. Fubelli for having made me available their experience and knowledge about Ethiopia.

I thank Dr. M.L. Balestrieri and Dr. V. Olivetti for their collaboration in the thermochronological analysis: I know the results were misery but we tried very hard.

I thank Dr. E. Giachetta for his support for the MatLab Toolbox elaborations and for the discussions about the morphometric analysis data interpretation.

A special thank must go to Prof. B. Abebe for his essential contribution in organizing the two field trips in Ethiopia and for having welcomed me and let my hair down more than 7000 km far from home.

I thank Prof. F.J. Pazzaglia and Prof. C. Ebinger for having hosted me in the USA and for their willingness in discussing my data, you cannot imagine how much I have learned.

I deeply thank Prof. C. Faccenna for his willigness in listening and correcting my PhD oral presentation during the Christmas holidays: it was a very snowy day but it was worth it.

I would like to express my deep gratitude to Dr. P. Molin for having supported me from both academic and humane point of view; thank you for having tolerated my complaints; if I concluded my PhD it's also because of you.

Thanks to my labmates Riccardo Lanari and Gaia Siravo. I know sometimes was not so easy to sit beside me, thank you for your patience and your smiles.

Thanks to all my PhD colleagues for their moral support: you were always there with a steaming cup of tea ready for me! In particular I want to thank a pair of eyes so deep and comfortable which gave me rest from PhD final rush!

As last, but absolutely not the least, I wish to thank my family: my mom for the delicious dishes she prepared me each single evening when I came back from university after 9 (nine) hours of hard work; my father for his suggestions about PC stuff and for having introduced me, since I was a baby, to the world of good music: most of his favorite songs have been the soundtrack of my PhD; my sister for her radiance and her delicious ginger biscuits; my grandmother for her congeniality; my grandfather for his willingness and patience in listening my thesis oral presentation in a language (English) he does not understand!

I can't deny that these three years have been hard and difficult. There have been moments where I was very close to give in. Fortunately I have always found persons who had the right word to lift my spirit. However all these difficulties made me grow day by day until now. If I could I would change nothing of what I have done.

Thanks again to everybody. I wish you all the best.